Department of Civil and Structural Engineering

A novel application of mineral powders in normal strength concrete

Johanna Tikkanen

Aalto University

DOCTORAL DISSERTATIONS

Aalto University publication series
DOCTORAL DISSERTATIONS 182/2013

A novel application of mineral powders in normal strength concrete

Johanna Tikkanen

A doctoral dissertation completed for the degree of Doctor of Science in Technology to be defended, with the permission of the Aalto University School of Engineering, at a public examination held at the lecture hall R2 (Rakentajanaukio 4A) at the Aalto University (Espoo, Finland) on 11 November 2013 at 12 noon.

Aalto University
School of Engineering
Department of Civil and Structural Engineering

Supervising professor
Professor emeritus Vesa Penttala

Preliminary examiners
Professor Ole Mejlhede Jensen, Technical University of Denmark
Doctor of Technology, Tarja Häkkinen, VTT, Finland

Opponent
Professor emeritus Göran Fagerlund, Lund University, Sweden

Aalto University publication series
DOCTORAL DISSERTATIONS 182/2013

ISBN 978-952-60-5423-0
ISBN 978-952-60-5424-7 (pdf)
ISSN-L 1799-4934
ISSN 1799-4934 (printed)
ISSN 1799-4942 (pdf)
http://urn.fi/URN:ISBN:978-952-60-5424-7

Unigrafia Oy
Helsinki 2013

Finland

441 697
Printed matter

Aalto University

Abstract

Aalto University, P.O. Box 11000, FI-00076 Aalto www.aalto.fi

Author
Johanna Tikkanen

Name of the doctoral dissertation
A novel application of mineral powders in normal strength concrete

Publisher School of Engineering

Unit Department of Civil and Sructural Engineering

Series Aalto University publication series DOCTORAL DISSERTATIONS 182/2013

Field of research Building Materials Technology

Manuscript submitted 14 June 2013 **Date of the defence** 22 November 2013

Permission to publish granted (date) 2 October 2013 **Language** English

☒ **Monograph** ☐ **Article dissertation (summary + original articles)**

Abstract

The possibility of using inert mineral powders to replace a part of the cement in concrete and the effects of replacement on the properties of fresh and hardened concrete were studied. In the past, studies of the influence of fillers in concrete have mainly been focused on high strength, self-compacting and high-performance concretes. However, in the current research, the focus was on normal-strength concretes, with adequate to good consistency.

According to the results, mineral powders had a considerable effect on the properties of the cement paste and concrete. The results obtained show that mineral powders can replace cement to a moderate extent, mainly as the result of the reduced water demand of the mineral powder concretes. In concretes with the same amount of cement and similar consistency, mineral powder concretes obtained higher strengths as a result of their lower amount of water. The use of mineral powders had a greater effect on the water demand of concrete than directly on the compressive strength. The direct strength gain, presumably caused by chemical activation of the hydration of cement via heterogeneous nucleation, was, on average, from 0 to 5 MPa. Finally, a statistical model, based on over 70 mix compositions, is proposed for the quantification of the effects of the addition of the powder on the flow and compressive strength of the concrete.

The use of mineral powders in itself was not observed to affect the freeze-thaw resistance, but the consequent binder reduction and strength loss reduced the freeze-thaw resistance. However, it is concluded that the strength loss resulting from the replacement of the cement could be compensated for by reducing the w/c ratio of the mineral powder concretes because of the lowered water requirement.

The use of mineral powders also had an effect on the hydration and microstructure of the concretes. The maturities of the concretes containing mineral additions were continuously higher than that of the reference. In addition, a moderate cement reduction was not observed to have detrimental effects on the microstructure of the concrete.

This work suggests that part of the cement can be replaced by inert powders, which lower the water demand of the concrete and thus allow a partial cement reduction. The advantages of the use of mineral powder in concrete include lower CO_2 emissions and energy consumption in cement and concrete production and the potential to improve the cost-effectiveness of concrete manufacturing.

Keywords Concrete technology, mineral powders, cement replacement, mix design, freeze-thaw durability, hydration, microstucture

ISBN (printed) 978-952-60-5423-0 **ISBN (pdf)** 978-952-60-5424-7

ISSN-L 1799-4934 **ISSN (printed)** 1799-4934 **ISSN (pdf)** 1799-4942

Location of publisher Helsinki **Location of printing** Helsinki **Year** 2013

Pages 198 **urn** http://urn.fi/URN:ISBN:978-952-60-5424-7

Tekijä
Johanna Tikkanen

Väitöskirjan nimi
Mineraalijauheiden uudenlainen käyttö normaalilujuuksisessa betonissa

Julkaisija Insinööritieteiden korkeakoulu

Yksikkö Rakennustekniikan laitos

Sarja Aalto University publication series DOCTORAL DISSERTATIONS 182/2013

Tutkimusala Rakennusmateriaalitekniikka

Käsikirjoituksen pvm 14.06.2013 **Väitöspäivä** 22.11.2013

Julkaisuluvan myöntämispäivä 02.10.2013 **Kieli** Englanti

☒ **Monografia** ☐ **Yhdistelmäväitöskirja (yhteenveto-osa + erillisartikkelit)**

Tiivistelmä

Tutkimuksessa selvitettiin mahdollisuutta korvata osa sementistä inertillä mineraalijauheella sekä sen vaikutuksia tuoreen ja kovettuneen betonin ominaisuuksiin. Aikaisemmat tutkimukset aiheesta ovat pääasiassa keskittyneet korkealujuusbetoneihin, itsetiivistyviin betoneihin sekä muihin erikoisbetoneihin. Kuitenkin tässä tutkimuksessa keskityttiin normaalilujuusbetoneihin, joiden notkeus vaihteli riittävästä hyvään.

Tulosten mukaan, mineraalijauheilla oli merkittävä vaikutus sementtipastojen ja betonien ominaisuuksiin. Saatujen tulosten mukaan kohtuullinen osa sementistä voidaan korvata mineraalijauheilla, pääasiassa pienentyneen vedentarpeen perusteella. Betoneissa, joissa oli sama määrä sementtiä ja vastaavanlainen notkeus, mineraalijauhetta sisältäneet betonit saavuttivat suuremman puristuslujuuden pienentyneen vedentarpeen seurauksena. Mineraalijauheiden käytöllä oli suurempi vaikutus betonien vedentarpeeseen kuin suoraan puristuslujuuteen. Mineraalijauheiden suora lujuusvaikutus oli keskimäärin 0 – 5 MPa; oletettavasti heterogeenisen tiivistymiskeskusten muodostumisen seurauksena. Lopuksi tutkimuksessa muodostettiin yli 70 betonivaluun perustuva tilastollinen malli betonien notkeuden ja puristuslujuuden määrittämiseksi.

Mineraalijauheiden käytön itsessään ei havaittu vaikuttavan betonien pakkasenkestävyyteen, mutta jauheiden käytöstä johtuva sideaineen vähennys ja sitä seurannut lujuuden menetys laski betonien pakkasenkestävyyttä. Kuitenkin voidaan todeta, että sementin vähenemisestä seurannutta puristuslujuuden menetystä voitaisiin kompensoida laskemalla mineraalijauhebetonien vesi-sementtisuhdetta, sillä jauheiden käyttö vähensi näiden betonien vedentarvetta.

Mineraalijauheita sisältäneiden betonien kypsyysasteet olivat yhtäjaksoisesti korkeammat kuin vertailubetonin. Lisäksi, maltillisella sementin korvauksella ei havaittu olevan haitallisia vaikutuksia betonin mikrorakenteeseen. Päinvastoin, pyyhkäisyelektronimikroskoopin kuvat paljastivat mineraalijauhebetonien runkoaineen ja sementtipastan välisten faasirajojen olevan jopa tiiviimpiä.

Tämän tutkimuksen tulosten perusteella, osa sementistä voidaan korvata inerteillä jauheilla, jotka vähentävät betonien vedentarvetta ja siten mahdollistavat sementin osittaisen korvaamisen. Mineraalijauheiden käytön hyötyihin kuuluvat pienemmät CO_2-päästöt ja alhaisempi energiankulutus sementin ja betonin valmistuksessa sekä mahdollisuus parantaa betonin valmistuksen kustannustehokkuutta

Avainsanat Betonitekniikka, mineraalijauheet, sementin korvaaminen, suhteitus, pakkasenkestävyys, hydrataatio, mikrorakenne

ISBN (painettu) 978-952-60-5423-0 **ISBN (pdf)** 978-952-60-5424-7

ISSN-L 1799-4934 **ISSN (painettu)** 1799-4934 **ISSN (pdf)** 1799-4942

Julkaisupaikka Helsinki **Painopaikka** Helsinki **Vuosi** 2013

Sivumäärä 198 **urn** http://urn.fi/URN:ISBN:978-952-60-5424-7

ACKNOWLEDGEMENTS

This research work has been carried out in the laboratory of Building materials technology at Aalto University, School of engineering. The main financial support has been provided by the Academy of Finland, which is gratefully acknowledged. I am also grateful to Rakennusteollisuus, RT for funding this thesis with a grant.

First, I would like to present my gratitude to Professor Vesa Penttala for the supervision of this research work and his valuable advice and criticism. I thank him for urging me to consider becoming a scientist and into doing this dissertation.

I also warmly thank Professor Andrzej Cwirzen for the criticism and comments on the manuscript and for all his useful advice and beneficial conversations on the subject.

I wish to express my gratitude also to M.S(c). Karri Mäkinen for his valuable help during the entire research work. I am grateful that I could always count on his help with all kinds of research related problems – appliance or clerical. I would also like to thank Pertti Alho for helping me with the numerous concrete castings and other laboratory work. In addition, my appreciation goes to M.S(c). Veli-Antti Hakala, especially for his valuable assistance with the data collection and the technology behind it. I would also like to acknowledge WriteIt for revising the language of this thesis.

Finally, I warmly thank my friends and family who have supported me during this entire project.

Johanna Tikkanen

LIST OF ABBREVIATIONS AND SYMBOLS

List of abbreviations

AFm	Monosulphate phase
AFt	Trisulphate phase
ANOVA	Analysis of variance
BSE	Backscattered electron mode
C_3A	Tricalcium aluminate
C_3S	Tricalcium silicate
CH	$Ca(OH)_2$, calcium hydroxide, Portlandite
CIF	Capillary suction, internal damage and freeze-thaw test
CPM	Compressible packing model
C-S-H	Calcium silicate hydrate
DTA	Differential thermal analysis
EDS	Energy dispersive mode
ESEM	Environmental scanning electron microscope
FA	Fly ash
GGBS	Ground-granulated blast furnace slag
HPC	High-performance concrete
ITZ	Interfacial transition zone
LF	Limestone filler/powder
LPDM	Linear Packing Density Model
MO	Consistency test

MP	Mineral powder
OPC	Ordinary Portland cement
PC	Portland cement
PSD	Particle size distribution
RDM	Relative dynamic modulus
SCC	Self-compacting concrete
SF	Silica fume
SP	Superplasticiser
SSM	Solid suspension model
TGA	Thermogravimetric analysis
TSA	Thaumasite form of sulphate attack
XRD	X-ray diffraction

List of symbols

α	Degree of hydration	[-]
β	Hydration parameter	[-]
β_1	Virtual packing density of the large particles	[-]
β_2	Virtual packing density of the small particles	[-]
Γ_m	Relative flow area	[-]
ε_{air}	Air porosity	[dm^3/m^3]
ε_{suc}	Capillary porosity	[dm^3/m^3]
ε_{total}	Total porosity	[dm^3/m^3]
$\zeta(p)$	Efficiency function	[-]
τ	Time constant	[h]
υ	Specific volume	[-]
φ	Packing density	[-]
θ_{ad}	Adiabatic temperature increase	[K]
θ_{HH}	Temperature increase	[K]
θ_s	Temperature increase of the sample	[K]

χ	Volume ratio	[-]
a	Coefficient of temperature loss	[K/h]
A	Air content	[%]
a_{12}	Coefficient for the loosening effect	[-]
b_{21}	Coefficient for the wall effect	[-]
c	Cement content	[kg/m³]
C_{cal}	Apparent heat capacity of the calorimeter	[J/K]
C_s	Heat capacity of the sample	[J/K]
c_{sample}	Cement content in a sample	[mg]
C_T	Total heat capacity	[J/K]
d	Diameter	[µm]
d_{MAX}	Maximum diameter of particles	[µm]
d_{min}	Minimum diameter of particles	[µm]
E	Apparent energy of activation of cement	[J/mol]
F	Mortar flow value	[mm]
F_o	Bottom diameter of flow cone	[mm]
h	Coefficient of heat loss	[J/(h·K)]
H_p	Fineness modulus in weight fraction	[-]
H_v	Fineness modulus in volume fraction	[-]
H_∞	Total heat of hydration of the concrete	[J/m³]
K	Compaction index	[-]
k_t	Temperature factor	[-]
p	Volume fraction of particles	[%]
q	Distribution modulus	[-]
$Q_H(t)$	Rate of heat generation	[W/m³]
R	Universal gas constant (R= 8.314)	[J/(mol·K)]
RH	Relative humidity	[%]
Rm	Relative funnel speed ratio	[1/s]
r	Volume fractions	[-]

t	Time	[s]
T	Temperature	[°C]
t_e	Equivalent age	[-]
W	Water content	[kg/m³]
W_A	Adsorbed water contributing to the Flow	[g]
W_D	Water demand according to Puntke	[g]
W_F	Filling water determining the packing density	[g]
W_i	Mass of the sample after ignition	[mg]
$w_{n,sample}$	Amount of chemically bound water	[mg]
W_s	Mass of a sample prior to ignition	[mg]
wt%	weight per cent	[-]
W_1	Dry weight of the specimen	[g]
W_2	Weight of the specimen after capillary Suction	[g]
W_3	Weight of the specimen after filling with water under pressure	[g]
w^o_n/c	Chemically bound water at complete hydration	[mg]

CONTENTS

APPENDICES

1. Mix design and test results of concretes
2. Calculation of parameters Hp and Hv
3. Mix design of concretes and cement paste used in testing of hydration processes and hydration products.
4. TGA and TGA derivative curves
5. XRD patterns
6. Evaluation of pumpability

1. INTRODUCTION

The purpose of the research project is to study the effects of mineral powders on the properties of fresh and hardened concrete and it aims to investigate the possibility of using a fine powder to replace part of the cement. In this study mineral powders are defined as inert fine powders such as limestone powder and quartz powder, with a particle size distribution close to or finer than that of cement.

1.1 Background

The use of fine material in concrete manufacture has received an increased attention during the last 10 to 20 years. A number of studies have been published on the influence of fillers on special types of concretes, however, the influence of fine material on ordinary concrete is less well examined.

Concrete is the most used building material in the world having an annual production exceeding 5 billion tons. Although a number of investigations have been concentrated on special types of concretes, ordinary Portland cement concrete is the most abundant. Thus, even a small decrease in material cost and an improvement in basic mechanical and durability properties of ordinary Portland cement concrete has a large economical impact and it can have a remarkable effect on the global construction industry.

Nowadays environmental aspects are a key focal point of the cement industry. Each tonne of cement produced requires 60 to 130 kg of fuel oil or its equivalent, depending on the cement variety and the process used, and about 110 KWh of electricity. In addition, the production of one tonne of cement releases about 0.8 to 1.1 tonne of CO_2 into the atmosphere as a consequence of the burning of fuel and calcination of limestone (International Energy Agency 2009, Malhotra 1999). In 2011, the world production of hydraulic cement was 3.6 billion tonnes (Cembureau 2013). Thus the reduction of the ecological impact of concrete would have a significant influence on the global emissions of greenhouse gases.

1.2 Research significance

Mineral powder concretes could offer economic and ecological opportunities for the concrete industry through a reduction of the use of cement. The main benefits of the mineral powder concretes are expected to be the lower material price of the concrete and reduced environmental burden of the concrete because of the lower Portland cement content.

However, so far the research on mineral powders has mainly been focused on self-compacting concretes and high-strength and high-performance concretes, although a significant part of the concrete that is manufactured and used is actually ordinary Portland cement concrete. In this study, the applicability of mineral powders in normal-strength ordinary Portland cement concretes is studied.

In Finland and in the other Nordic countries, all outdoor structures are susceptible to freezing and thawing loads of varying intensity during the winter season. Although a considerable amount of the concrete used is categorised as being exposed only to corrosion caused by carbonation or to no risk of corrosion or chemical attack, the freeze-thaw durability of mineral powder concretes needs to be investigated. In order to be used successfully mineral powder concretes need to possess adequate fresh concrete properties and withstand the cyclic frost attacks of the Nordic climate. Thus, the freeze-thaw durability properties and characteristics affecting the air entrainment of mineral powder concretes are also investigated.

1.3 Objectives

The main objective of this study is to apply different mineral powders in normal strength concretes as a partial replacement of Portland cement and blast-furnace slag-based binders. Only non-pozzolanic and non-hydraulic mineral particles are studied. The effects of the replacement on the properties of fresh and hardened concrete are evaluated with a particular focus on the effect of the mineral powders on concrete consistency, strength, microstructure and frost resistance.

1.4 Defining the research field

The objective of this research was to produce “ordinary” Portland cement concrete with low cement content. Self-compacting, high-strength or otherwise high-performance concretes were excluded from the research goals. This study did not focus on powders possessing pozzolanic or hydraulic properties, such as fly ash, silica fume or natural pozzolans. The mineral powders that were studied were one class of limestone powder and three classes of quartz powder. There are also other mineral powders, such as rock powder, originating from the crushing or drilling of rock, but they are beyond

the scope of this research work. The issue of cost is considered only briefly, in the section titled “Summary” and in the general conclusions. A detailed description of the course of the study is presented in the section titled “Materials and methods – Outline of the research programme”.

This study focuses on the properties of fresh concrete, particularly the consistency of mineral powder concretes and the factors influencing it and also on the hydration process and products of mineral powder concretes and cement pastes. This work also concentrates on the basic properties of hardened concrete, such as its compressive strength and frost durability and the microstructure of hardened concrete. Properties which can also be influenced by mineral powders, such as tensile strength, E-modulus, sulphate resistance and carbonation, were excluded from the study.

As a result of limitations in the laboratory instruments, in some cases experiments were conducted in an unconventional manner, utilising and applying the existing equipment. For example, the heats of hydration were measured semi-adiabatically and the results were converted to correspond to the adiabatic temperature rise. For the same reasons, the porosity was studied using the capillary suction test instead of mercury porosimetry.

In the literature there are several designations used for these powder materials, such as fines, fine filler, microfiller, ultrafine powders, fine-grained particles and mineral fines, to name but a few. In this thesis the term mineral powder is used to identify the powdered fine particles with a particle size distribution close to or finer than that of cement. In addition, the term ultrafine particles is used to refer to the powdered material with a particle size substantially smaller than cement.

2. LITERATURE REVIEW

2.1 General: effects of fine inert particles on concrete

Fillers in concrete come from two sources: they may be within the aggregate, and may vary considerably as a result of differences in the origin and processing of aggregates (crushing etc.), or they may be added separately at the concrete-mixing plants. In the past fine powders were thought to increase the water requirement of the concrete and thus to have an undesirable effect on the concrete. However, now it is known that the addition of certain fillers may actually reduce the water requirement. Recently, the use of different mineral powders in concrete technology has increased as a result of the development of self-compacting concretes and high-performance concretes. Studies of the influence of fillers in concrete have mainly been focused on high-performance, high-strength and self-compacting concretes.

The effects of fine powders (with a particle size distribution close to or finer than that of cement) on the properties of the hardened concrete can be roughly divided into three groups:

I. chemical effects such as hydraulic or pozzolanic effects;
II. the filler effect: a physical effect in which the fine powders fill inter-granular voids between the cement particles and between the cement paste and the coarser aggregate, producing a denser binder matrix. This phenomenon can also be observed in self-compacting concrete (Bentur 1991, Larbi 1993);
III. enhancement of the hydration by acting as nucleation sites for cement particles and thus becoming a part of the binder matrix (Stumm 1992).

The way and extent in which the addition of a filler alters the properties of the concrete depend, among other things, on the amount of filler and whether it is used to replace cement or just increase the amount of fine material in the concrete and, as a result, the w/c ratio, and on the amount of cement. When fillers are used in increased amounts they act as diluents of the cement, resulting in lower compressive strengths than for comparable Portland cement concretes. Factors such as the particle size distribution and particle packing of the mix, the type of cement and the utilisation of

plasticiser also have significance for the properties of the fresh and hardened concrete.

The influence of geometrical factors such as particle size distribution and the particle shape of the aggregates has been studied by, for example, Danielsen and Wallevik (1989), who came to the conclusion that poorer particle shapes – meaning flaky and elongated, of a crushed aggregate compared to a natural aggregate – generally led to a higher air voids ratio and higher water demands. In such a case, the water demand could be reduced by the addition of filler because of the filler filling up the air voids between the coarser particles, thus causing a lubricating effect.

In addition to particle shape, the presence of clays in aggregate contributes to the properties of fresh concrete since clays may adsorb water and expand. The resulting reduction of free water reduces workability (Yool et al. 1998). In addition, if the clays later dry and shrink, the resulting voids reduce strength and permeability (Hudson 2002). Clays may also interfere with admixture performance (Jardine et al. 2002 and Jardine et al. 2003). According to Yool et al. (1998), the effects of clays are a function of their fineness and activity.

The effects on the consistency of concrete – for factors such as shape, angularity, texture and particle size distribution – can be estimated by determining the water demand of the powder materials, such as cement, microfines and other mineral fillers. A short description of the water demand tests used is given in the section titled “Testing water demand”.

2.1.1 Limestone powder in concrete

A great part of the data in the literature regarding the use of inert mineral fillers as a replacement for cement concerns ground limestone. Limestone is not completely inert, as it reacts with the alumina phases of cement to form calcium monocarboaluminate hydrate:

$$C_3A + CaCO_3 + 11H_2O \rightarrow C_3A{\cdot}CaCO_3{\cdot}11H_2O \qquad (1)$$

It has also been suggested that some $CaCO_3$ can be incorporated into the C-S-H formed by C_3S (Ramachandran and Zhang 1986). But since it does not actively form cement gel – as do, for example, ground granulated blast furnace slag or silica fume – it is considered inert in this study.

A number of studies have been carried out on the use of limestone fillers in concrete. At first, the interest was in the substitution of limestone for gypsum as a set regulator (Bobrowski et al. 1977, Negro et al. 1986, Bensted 1980), then to improve the workability and stability of fresh concrete (Ellerbrock et al. 1985, Neto and Campitelli 1990, Sprung and Siebel 1991) and in some instances to improve durability (Soroka and Stern 1976(I)). Adverse effects, such as shrinkage upon drying, have also been observed (Adams et al. 1990).

According to these studies, it appears that the partial substitution of gypsum is possible without harmful side effects. A study by Bobrowski et al. (1977) indicates that false setting is reduced considerably when limestone is used as a partial substitute for gypsum, and that the setting time was not markedly affected. Bensted (1980) and Negro et al. (1986) came to the conclusion that the 25% to 50% replacement of gypsum was possible without deleterious effects on set, shrinkage or compressive strength properties. However, Bensted (1980) concluded that because of differences in their stereochemistry, sulphate ions enter into solid solution more easily than carbonate ions and thus sulphate ions are more effective in controlling setting than carbonate ions. The exact amount of substitution depends on the cement. Ramachandran (1988) found that when both gypsum and limestone are added to Portland cement, the formation of ettringite is accelerated. In his work he detected that the conversion of ettringite to the monosulphate hydrate form is accelerated by the $CaCO_3$.

The easily ground limestone usually has a wide particle size distribution, which allows the limestone particles to fill the gaps between the cement particles, reducing the water demand, improving the stability of fresh concrete and densifying the microstructure of the hardened cement paste. According to Sprung and Siebel (1991), this consolidating effect can lead to increased strengths when the limestone content is less than 10%. They also concluded that the water demand was related to the clay content of the limestone. Neto and Campiteli (1990) studied cements containing up to 15% limestone and discovered that in two-point measurements of the consistency, the yield point values were reduced and the plastic viscosity slightly increased by the presence of limestone, especially for the finer cements.

Sprung and Siebel (1991) studied concretes made with Portland cement and concretes made with Portland limestone cement and found out that those made with Portland limestone cement were less stiff. They concluded that the water requirement is primarily related to interparticle space once the surface forces are counteracted by the chemical admixture. Schmidt (1992) sees the beneficial effect of limestone on the rheology of concrete as a consequence of improved

particle size distribution: the fine particles replace part of the water between the coarser particles, making it available as an additional "internal lubricant". Schmidt et al. (1993) report on concretes made with Portland limestone cements (13% to 17% limestone) that required about 10 l/m^3 less water than plain Portland cement concrete. The w/c ratio was reduced from 0.60 to 0.57 and the strength increased to 8 MPa. Conversely to Schmidt (1992) and Schmidt et al. (1993), Matthews (1994) found out that a 0.01 increase in the w/c ratio was required to achieve the same slump as the addition of 0% to 5% limestone and another 0.01 increase as the addition of 5% to 25%.

2.1.2 Use of fillers in cement manufacture

The European cement standard EN 197-1 defines 5 classes of common cement that comprise Portland cement as a main constituent and of which all classes are allowed to contain up to 5% limestone filler as a minor additive. In addition, class II allows the addition of up to 35% of other single constituents – including limestone filler. In Canada, the CSA standard A5 has allowed up to 5% limestone in Type 10 cement (now Type GU in A3001) since 1983. This was preceded by the presentation of data to show that 5% limestone had no detrimental effect on the concrete properties.

In the United States in 2004 ASTM C150 finally allowed up to 5% limestone to be used in Portland cements. However, many state highway agencies use the American Association of State Highway Officials (AASHTO) standards, rather than ASTM, which did not allow limestone to be added. Finally, in 2007, AASHTO M85 also allowed 5% additions to Types I-V cements. In 2008 CSA A3001 included Portland limestone cement containing 5%-15% limestone and in the US especially the cement industry is striving to adopt the same levels in ASTM C595/M240. Table 1 shows the types of Common Cement in EN 197-1.

Table 1. Types of Common Cement in EN 197-1.

Cement Type	Designation	Notation	Clinker K	G.G.B.S. S	Silica fume D	Pozzolana		Fly ashes		Burnt Shale T	Limestone		Minor Additional constit.
						Natural P	Industrial Q	Silic. V	Calcar W		L	LL	
I	Portland Cement	I	95-100	-	-	-	-	-	-	-	-		0-5
II	Portland Slag Cement	II / A-S	80-94	6-20	-	-	-	-	-	-	-		0-5
		II / B-S	65-79	21-35	-	-	-						0-5
	Portland Silica Fume Cement	II / A-D	90-94	-	6-10	-	-	-	-	-	-		0-5
	Portland Pozzolana Cement	II / A-P	80-94	-	-	6-20	-	-	-	-	-		0-5
		II / B-P	65-79	-	-	21-35	-	-	-	-	-		0-5
		II / A-Q	80-94	-	-	-	6-20	-	-	-	-		0-5
		II / B-Q	65-79	-	-	-	21-35	-	-	-	-		0-5
	Portland Fly Ash Cement	II / A-V	80-94	-	-	-	-	6-20	-	-	-		0-5
		II / B-V	65-79	-	-	-	-	21-35	-	-	-		0-5
		II / A-W	80-94	-	-	-	-	-	6-20	-	-		0-5
		II / B-W	65-79	-	-	-	-	-	21-35	-	-		0-5
	Portland Burnt Shale Cement	II / A-T	80-94	-	-	-	-	-	-	6-20	-		0-5
		II / B-T	65-79	-	-	-	-	-	-	21-35	-		0-5
	Portland Limestone Cement	II / A-L	80-94	-	-	-	-	-	-	-			
		II / B-L	65-79	-	-	-	-	-	-	-	6-20		0-5
		II / A-LL	80-94	-	-	-	-	-	-	-	21-35	6-20	0-5
		II / B-LL	65-79	-	-	-	-	-	-	-		21-35	
	Portland Composite Cement	II / A-M	80-94	<----------6-20---------->									
		II / B-M	65-79	<----------21-35---------->									
III	Blastfurnace Cement	III / A	35-64	35-65	-	-	-	-	-	-	-		0-5
		III / B	20-34	66-80	-	-	-	-	-	-	-		0-5
		III / C	5-19	81-95	-	-	-	-	-	-	-		0-5
IV	Pozzolanic Cement	IV / A	65-89	-	<----------11-35---------->				-	-	-		0-5
		IV / B	45-64	-	<----------36-55---------->				-	-	-		0-5
V	Composite Cement	V / A	40-64	18-30	←----------18-30----------→				-	-	-		0-5
		V / B	20-39	31-50	←----------31-50----------→				-	-	-		0-5

2.1.3 Studies of inert mineral powders used in normal strength concrete

Poijärvi

Poijärvi (1966) studied the influence of various fine powders on the workability, bleeding and air content with and without air-entraining agents, strength properties, shrinkage, water permeability and frost resistance. The concretes were made without plasticisers. Various fine powders, both natural and crushed, were used, and in some of the tests they were replaced by different kinds of mica, two types of clay and bentonite. The amount of fine powders varied from 0 to 24% by weight of the total aggregate. In the mix design the aggregate maximum size was generally 8 mm and the water-cement (w/c) ratios 0.8, 0.6 or 0.4. The w/c ratios and aggregate-cement ratios were maintained at a constant level during the same test series. Some additional tests with a maximum aggregate size of 32 mm were carried out.

The results showed that with 10 to 15% and 5 to 10% of fine powders of aggregate weight in w/c ratios of 0.8 and 0.6 respectively, the fillers improved the workability of the concrete. No effect was detected with a w/c ratio of 0.4. In additional experiments with the 32-mm aggregate a plasticising effect was visually observed, but it could not be measured. Nonetheless, no clear correlation between the workability and surface area, mineralogical composition or grading could be recognised.

Crushed powders diminished the bleeding of the test concretes, depending on their surface area, but no such effect was recognised with the natural fine powders as a result of their small specific surface areas. Different natural powders increased the air content and the crushed powders, particularly the finest (<0.008-mm fraction > 40%) ones, reduced the air content. When air-entraining agents were used, increased dosages of air-entraining agents were needed with an increase in the fineness of the crushed fine powders.

With w/c ratios of 0.8 and 0.6 both natural and crushed fillers improved the compressive strength by 5 to 15% for natural and 9 to 50% for crushed fillers when the use of fillers also improved the workability of the concrete. The more finely divided the crushed fillers were, the more the strength increased. No such correlation was found with the natural fillers. At a w/c ratio of 0.4 the strength effect was negative except with the finest (<0.008-mm fraction > 40%) crushed powders. Poijärvi came to the conclusion that the increase in strength was attributable to improved workability, air content and

the reduced bleeding, as well as possible physical and chemical changes in the bonds between the cement paste and the fine particles and aggregates. The use of fine powders also lowered the water permeability when the workability was improved.

Natural fillers improved the frost resistance of concretes for w/c ratios of 0.8 and 0.6. No improvement was observed when the w/c ratio was 0.4. Crushed powders reduced the frost resistance of non-air-entrained concretes as a result of their reduced air content. According to Poijärvi, the appropriate amount of powders can be estimated by the volume ratio χ = water / (cement + powders). The profitable values of χ vary between 1.2 and 1.5, depending on the desired consistency.

Kronlöf

Kronlöf (1997) studied the effect of different inert mineral powders (MPs) and fly ash on the water requirement of concrete on the basis of particle packing. The work was in general based on stiff/plastic lean mixes (cement content 140-285 kg/m^3) with silica powder and the addition level of powders was up to 19 weight per cent of the total amount of aggregates. The largest MP contents were only examined with the lowest binder content (140 kg/m^3).

In concrete mixes where a superplasticiser was used, the higher the initial consistency was, the more the inert mineral powder lowered the water demand. In the case of round aggregates the reduction in water demand was reported to be in the region of 0-20 l/m^3 and up to 30-40 litres when angular crushed aggregates were used. This leads to a strength increase of about 0-9 MPa in the former case and 6-16 MPa in the latter. The effects of the filler (other than the effect of water reduction) increased the compressive strength by approximately 4 MPa in concretes with both types of aggregate. This increase in strength is due to the improved interaction of the paste and aggregate. Kronlöf describes this as the filler effect, which can be explained by some physical and chemical factors, listed below.

I. Fine particles interfere with the formation and orientation of large crystals at the paste-aggregate interface (also Bentur 1991, Larbi 1993).
II. Large amounts of small particles may alter the rheology, reducing the internal bleeding.
III. The wall effect does not weaken the contact between the paste and fine powder; therefore its function approaches that of the non-reacted cement particle core.
IV. The paste and aggregate are homogeneously mixed, which lowers the stress peaks.

The water requirement of the concrete mixes was estimated with the Linear Packing Density Model (LPDM) (Stovall, de Larrard & Buil 1986). The model was unable to estimate the water requirement needed to convert a mix from compact to workable, but was able to give a coarse estimate for the water volume fraction of a compact mix.

Cyr, Lawrence and Ringot

A project by Cyr, Lawrence and Ringot aimed to develop general mix design rules for concrete containing different kinds of mineral admixtures (Lawrence et al. 2003, Cyr et al. 2005, Lawrence et al. 2005 and Cyr et al. 2006). Replacing up to 75% of the cement with mineral powders was used and the fineness ranged between 180 and 2000 m^2/kg (Blaine). The mineral powders used were crushed quartz, limestone filler and fly ash.

The studies confirmed that the hydration of the cement was enhanced by mineral admixtures and the main effects responsible for the modification of the hydration of the cement were identified. These effects were categorised as the dilution effect and the heterogeneous nucleation effect, which is a physical process resulting in a chemical activation of the hydration of the cement. Heterogeneous nucleation is related to the nucleation of hydrates on foreign mineral particles, which catalyses the nucleation process by reducing the energy barrier. Cyr, Lawrence and Ringot developed an empirical model that included an efficiency function $\zeta(p)$ to quantify the effects of heterogeneous nucleation, since not all of the admixture particles participated in the heterogeneous nucleation process. The efficiency function is independent of fineness, time and of the type of admixture.

The effect of fineness, amount and the type of admixture on strength properties were tested in a series of over 2000 specimens. For hydration between 1 to 2 days the type of mineral powder did not have any considerable effect. During following 6 months, the samples with fly ash presented an increase in strength compared to the other admixtures as a result of pozzolanic activity. Cyr, Lawrence and Ringot concluded that the use of an inert powder to replace cement increased the water/cement ratio and the compressive strength was expected to decrease but with mineral admixtures that had a specific surface area over $100 m^2/kg$ the compressive strength decreased less than expected because of the improved degree of hydration, contradicting popular empirical equations for compressive strength by Féret (1892), Abrams (1918) and Powers & Brownyard (1947).

Kjellsen and Lagerblad

The effect of the mineralogy of fillers on different properties of mortars was studied by Kjellsen and Lagerblad (1995). The minerals used in the study were calcite, quartz, orthoclase, albite, anorthite and wollastonite. The amounts of filler used were up to 45 wt% of the cement. The use of different mineral fillers to replace Portland cement was observed to accelerate the rate of hydration of the cement, especially with the wollastonite and calcite filler, while quartz, orthoclase and albite gave only a slight increase in the hydration rate during the first hours. Kjellsen & Lagerblad presumed that the mineralogy of calcite and wollastonite provides beneficial substrates for the precipitation of CH at lower ion concentrations than other minerals, which may lead to an increase in the hydration rate. The compressive strengths of the mortars were reduced linearly when fillers replaced cement, and no particular effect of mineralogy was observed. A general reduction in flexural strength caused by the replacement of the cement was also observed; however, the fibrous mineral wollastonite was an exception since it was reported to have the ability to enhance the flexural and tensile strength. Mini-slump was used to measure the consistency. The workability of the mortars appeared to be positively influenced by the presence of calcite, wollastonite and anorthite. The presence of the other minerals had little effect on the workability. No plasticisers were used in the experiments.

Moosberg-Bustnes

Moosberg-Bustnes has studied (Moosberg 2000 and Moosberg-Bustnes 2003) the use of inert materials and by-products from the mineral and metallurgical industry as filler in concrete. Some of the fillers had pozzolanic properties and some were inert. A test procedure for screening by-products and to predict their behaviour in concrete was developed by testing several fillers. The screening tests included measurements for rheology, compressive and flexural strength, heat of hydration, shrinkage and x-ray analyses. Some of the by-products affected cement hydration, which was due to metal oxides in the fillers such as ZnO or PbO. In general filler additions caused strength increases, replacement with finest fillers also increased viscosity.

2.2 Mineral powders in high-performance concrete

The term high strength has changed significantly over the years; in the 1950s 40MPa was considered high strength, later 60 MPa and so on. A gradual change in terminology has occurred and the term high-performance concrete (HPC) has been adopted, since it is high durability that is the required property in most cases. High-performance concrete means concrete with high strength and/or low

permeability. What makes concrete “high-performance” is its low water/cement ratio, usually below 0.30, which typically causes a low volume of pores and capillary pore discontinuity.

The study of fillers in concrete has been largely focused on high-performance concretes because of the high amount of cement required, which is an economic and ecological concern for the concrete industry. Because of the very low amount of water, only a part of the cement is hydrated. Consequently, a significant part of the cement functions as an expensive filler, while its full hydraulic potential is not exploited.

In the manufacture of high-performance concretes mineral powders are used, since they improve particle packing in the cementitious system and its rheological and mechanical properties and durability. One of the most successful powders has been silica fume, also known as microsilica, which is a by-product of the production of silica metal or ferrosilicon alloys. It is one of the most widely used supplementary cementitious materials in the production of high-performance concrete since it is so fine-grained that it fills the spaces between the cement particles and between the aggregate and cement particles. In one of the pioneering works, Bache (1981) describes the densely packed binder made of cement and ultra-fine particles, such as silica fume, arranged in the spaces between the cement in an extremely low water content (0.13 - 0.18 by weight of cement + ultra-fine particles). The dense packing is achieved by using a large quantity of superplasticizer. According to Aïtcin (1998), the enhancing effect of silica fume on the mechanical properties and microstructure of the concrete is due to

- pozzolanic reactions
- the filler effect
- creation of nucleation sites

The cost of silica fume has been increasing constantly while availability decreasing. This has motivated to study other alternatives, such as rice husk ash (Mehta 1994, Bui 2001), zeolite (Feng et al. 1990) and inert fillers such as carbon black (Mehta 1987 and Detwiler & Mehta 1989).

2.2.1 Studies of inert mineral admixtures in high-performance concretes

Bentz, Irassar, Brooks, Bucher and Weiss

Bentz and his co-workers (2009(I) and 2009(II)) used the empirical model for the phase distribution of a hardening cement paste by Powers and Brownyard (1947) to analyse the total capillary porosity in limestone-cement pastes and studied durability issues and the effect of limestone fineness in concretes with a low w/c ratio. By using the values from Jensen and Hansen (2001) for non-evaporable water content, chemical shrinkage and cement gel water content, Bentz and his co-workers applied the model for two limiting cases of saturated and sealed curing in order to suggest appropriate replacement levels of limestone filler. The idea of replacement is based on the model's conclusion that at w/c ratios of 0.42 or less, a portion of the cement acts as an inert filler as there is not enough space and/or water for complete hydration to be achieved. Calculations from the model suggested that for a w/c ratio of 0.3 cured under saturated conditions (enough water for complete hydration according to the researchers, however a figure of 0.36 is more common), limestone filler replacement of 15% would be possible. For sealed curing (no additional water) with a w/c ratio of 0.35, a replacement level of about 17 % would be possible. Figure 1 (Bentz et al. 2009(I)) illustrates the calculated capillary porosity with different replacement levels, w/cm (cm = cement and limestone) ratios and curing conditions.

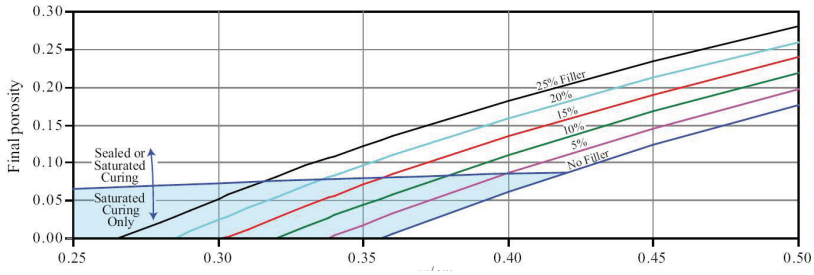

Figure 1. Calculated capillary porosity with different replacement levels with limestone filler, from Bentz et al. 2009(I)

The second part of the report dealt with the effect of limestone fineness on autogenous deformation, the ingress of aggressive ions and hence durability. Basing their conclusions on the results by Bentz et al. (2008) and Bucher (2009), they conclude that in pastes and concretes with a low w/c ratio, the tendency to autogenous deformation and early-age cracking can be reduced by using a limestone powder coarser than cement to replace part of the cement. Bentz et al. (2009 (II)) explain this by the fact that the use of a coarser powder to replace cement reduces capillary stresses and reduces the number of reactive particles. In terms of durability due to ingress of aggressive ions - particularly diffusion of ions, according to Bentz et al. (2009 (b)) in concretes with water/cement + limestone ratios over 0,40 limestone replacement will lead to higher diffusion

rates. On the other hand for lower water/(cement + limestone) ratios diffusion rates were similar to non-limestone filled concretes.

Bonavetti, Donza, Menéndez, Cabrera and Irassar

Bonavetti et al. (2003) investigated the effect of limestone filler on the degree of hydration and compressive strength in low-w/c cement pastes and concretes. The replacement of 10 and 20% of the cement and water/cementitious material ratios of 0.20 and 0.34 (concretes) and 0.25-0.50 (cement pastes) were used. In the pastes with the lowest w/c ratios the highest degree of hydration was obtained when the limestone filler content was increased. The degree of hydration was 14% and 22% lower for pure cement paste than for pastes containing 10% and 20% limestone filler, respectively. For higher-w/c pastes the values of the degree of hydration were similar, since there was sufficient available space for the hydration products to grow. For concretes the results were similar: concretes with limestone filler attained higher degrees of hydration than that of plain Portland cement concretes at all ages. It was calculated that for concrete with a low w/c ratio, more than 35% of the Portland cement remained unhydrated. By using a quadratic statistical model, the optimum limestone filler content was calculated for different w/c ratios. The results also showed that the addition of limestone filler to concrete caused a reduction in compressive strength of 8-12% at 28 days.

Goldman and Bentur

The effect of inert mineral powder on cement hydration and its strengthening effects were also studied by Goldman and Bentur (1993). The purpose of the study was to differentiate the chemical/pozzolanic effect from the mineral powder/physical effect. Three types of carbon black with mean particle sizes of 0.025 μm, 0.073 μm and 0.33 μm were used as an alternative filler to silica fume. As a reference, concretes and pastes (matrices) with and without silica fume and water/binder (w/b) ratios ranging from 0.2 to 0.5 were prepared. The concretes containing carbon black were made only with a w/b ratio of 0.40. The concretes which contained carbon black filler of 0.073 μm or smaller attained greater strength than the concretes without mineral powder or silica powder, while the strength of the paste matrix remained constant. The increased compressive strength of concrete was related to the effect of the inert carbon black filler which was believed to strengthen the interfacial transition zone (ITZ) between the binder matrix and the aggregate i.e. filler effect. The influences on the strength of the concrete were similar with silica fume and carbon black, which indicates that the influence of silica fume on the strength of the concrete is mainly due to the physical filler effect rather than the pozzolanic effect.

Nehdi

Nehdi (1996) studied the optimisation of high-strength limestone filler cement mortars on the basis of a so-called uniform-precision factorial plan in order to limit the number of mortars to be investigated. The two experimental variables were the water/binder ratio (0.3 to 0.4) and the proportion of limestone filler used as a replacement in relation to the volume of cement (0 to 25%). Other factors were kept constant. The same experimental plan was carried out with ordinary Portland cement and a mix with ordinary Portland cement and 10% silica fume replacement. Up to about 10 to 15% by volume the limestone filler replacement did not significantly affect the strength of the mortars at early ages, although higher amounts of limestone caused significant strength losses – especially in the pastes with silica fume. At later ages pastes with only limestone and cement had the lowest compressive strengths, but using a combination of limestone and silica fume to replace part of the cement had a positive effect on strength. Figure 2 shows the compressive strength at a water/binder ratio of 0.33.

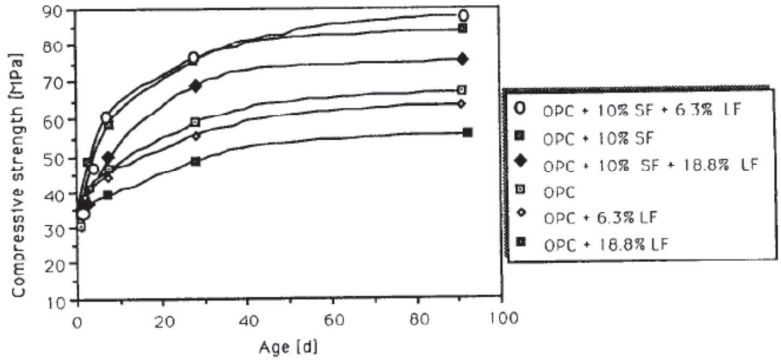

Figure 2. Compressive strength of mortars with different filler contents, from Nehdi (1996). OPC is ordinary Portland cement, LF is limestone filler/powder and SF stands for silica fume.

2.3 Ultrafine particles

Gutteridge and Dalziel (1990) studied the effect of fine inert particles on cement hydration by preparing two series of cement pastes with a water-solids ratio of 0.71, one with an ordinary Portland cement and the other blended by 1/6 by mass with rutile (TiO_2) powder, leading to a slightly higher w/c ratio. The hydration of the two series was studied at time intervals up to 180 days. The amount of Portlandite, together with the degree of hydration of different clinker minerals, was examined. In the series containing fine powder, hydration proceeded faster, as did the amount of Portlandite and chemically bound water. After 14 days the enhancement reached its maximum. The enhancement was expressed by an efficiency factor, which reached its maximum of 0.9 at the age of 3 days and descended to

approximately 0.45 at the age of 100 days. The strength of the specimens was not measured.

Lagerblad and Vogt

Lagerblad and Vogt (2004) studied the effect of several ultrafine (< 10 μm) particles on concrete hydration, strength, shrinkage and paste structure. The fillers used were quartz (three different ones plus wet ground quartz), wollastonite and nepheline. Amounts of filler up to 40% by weight of cement were studied. As the w/c ratio was kept the same as the reference concrete without filler, all the ultrafine particles resulted in increased strength but the mixes required superplasticiser (SP) in order to compensate for the slump loss. This means that cement is in fact replaced by a combination of ultrafine particles and SP.

Lagerblad and Vogt found out that 20% of the cement can be replaced by normal fillers because the increased amount of fillers results in greater strength. However, according to Lagerblad and Vogt, with increased amounts of ultrafine particles it is possible to replace up to 40% of the cement without the strength being substantially affected. The increase in strength was stated to be due to the fineness of the filler, but indications that the fine ground quartz acted as a mild pozzolana were also found. In ESEM (Environmental Scanning Electron Microscope) studies it was observed that the ultrafine particles had become an integrated part of the hydrated cement paste and had generated a more homogeneous interfacial transition zone.

The addition of filler was reported to have a slightly retarding effect on the onset of the acceleration period, except for wollastonite. All of the ultrafine particles accelerated the hydration of the cement and the effect was intensified with increasing fineness.

2.4 Particle packing, rheology and filler effect

The filler effect or particle size effect is defined as the filling of air voids between cement grains by the proper arrangement of small particles, which contributes to an increase in compressive strength without any chemical reaction (Sellevold 1987, Rosenberg and Gaidis 1989 and Goldman and Bentur 1993).

By optimising the composition of the concrete in such a way that the highest possible particle packing is achieved, the particle structure is densified, which leads to fewer voids to be filled with water and, as a

result, the cement content can be lowered. The high packing density leads to a stiff and strong particle structure, which can also have a positive effect on the mechanical properties of the concrete, such as shrinkage and creep. The use of inert material as a fine filler can lead to an increase in strength as a result of an improvement in the particle packing, which is the filling of the voids between the grains of cement.

2.4.1 Particle packing models

Optimal particle size distributions and, consequently, particle packing have been of interest in concrete mix design since the beginning of the last century. In 1907 Fuller and Thompson presented their model in an ideal grading curve, which is still used for the optimisation of concrete and asphalt aggregates:

$$p = \left(\frac{d}{d_{MAX}}\right)^{1/2} \qquad (2)$$

in which p is the volume fraction of particles whose diameter is smaller than d [-]

d is the particle size [mm]

d_{MAX} is the maximum size of the particles [mm].

However, this model does not take sufficient account of the smallest particles. Many models have been derived from the model of Fuller and Thompson (1907), such as the work by Andreasen and Andersen (1930). On the basis of their geometrical considerations and models by Fuller and Thompson (1907) and the work of Furnas (1928), they proposed the following equation for the optimum particle size distribution (PSD), including a constant, q [-], which characterises the degree of curvature of the distribution.

$$p(d) = \left(\frac{d}{d_{MAX}}\right)^{q} \qquad (3)$$

Andreasen and Andersen (1930) concluded from various experiments that the exponent q should be between 1/3 and 1/2 for the densest packing. In various publications afterwards, a distribution coefficient of 1/2 is referred to as the “Fuller curve”.

Funk and his co-authors (1980) modified the particle packing theory of Andreasen and Andersen (1930) by adding a factor of minimum particle size to the equation:

$$p = \frac{d^q - d_{min}^q}{d_{max}^q - d_{min}^q} \qquad (4)$$

in which p is the cumulative sieve passing [%]

d is the particle size [mm]

d_{max} is the maximum particle size of the distribution [mm]

d_{min} is the minimum particle size of the distribution [mm]

q is a distribution modulus [-]

The distribution modulus q influences the ratio between coarse and fine particles. Higher values of the distribution modulus lead to coarser mixtures, whereas smaller values result in mixtures which have a lot of fine particles.

Furnas (1928 and 1931) is often considered as the founder of ideal packing for spherical particles. In his theory the smaller particles could be added into the voids between the large particles. In the model the packing of a mixture consisting of two spherical materials, 1 and 2, with diameters of d_1 and d_2, is considered. The materials have volume fractions of r_1 and r_2 and packing densities of φ_1 and φ_2. With the two size classes present, the following two cases can be observed.

I. The volume fraction r_1 of the small particles is much larger than the volume fraction r_2 of the large particles ($r_1 >> r_2$).

II. The volume fraction r_2 of the large/coarse particles is much larger than the volume fraction r_1 of the small particles ($r_2 >> r_1$).

In the first case the mixture consists of small particles to which discrete larger particles can be added. The smaller particles will have a packing density of φ_1 and contribute to the specific volume of the mixture by r_1/φ_1. If larger particles are added to the matrix of smaller particles, the larger particles fill up the volume they occupy by 100%. Therefore they contribute to the packing density by their partial volume φ_2. In this case the specific volume (υ) and the packing density of the mixture are:

$$\upsilon = \frac{r_1}{\varphi_1} + r_2 \qquad (5)$$

$$\varphi = \frac{1}{\frac{r_1}{\varphi_1} + r_2} \qquad (6)$$

In other words, the packing density in the first case is the volume of the large particles plus the remaining volume filled with the maximum amount of small particles. In the second case small particles can be added into the voids between the large particles and thus the packing density increases. The small particles do not contribute to the overall specific volume of the mixture. The specific volume of the mixture is determined with the specific volume of a monodisperse packing of the large particles. In this second case the specific volume and the packing density of the mixture are:

$$v = \frac{r_2}{\varphi_2} \qquad (7)$$

$$\varphi = \frac{\varphi_2}{r_2} \qquad (8)$$

The packing density is improved in either case compared to the individual components φ_1 and φ_2. However, the model is only valid when $d_1 << d_2$ because the smaller particles must be able to fill the interstices between the larger ones. Additionally, in reality the packing density will be influenced by the wall effect, which is an important factor to be examined when the packing of small particles in the vicinity of large particles is considered. Many particle packing models have been developed since the work of Furnas, such as the models by Aïm and Goff (1968) and Toufar, Born and Klose (1976), and the linear packing density model (LPDM) by Stovall, de Larrard and Build (1986). The solid suspension model (SSM) by de Larrard and Sedran (1994) and the compressible packing model (CPM) by de Larrard (1999) are modified from the LPDM.

The de Larrard models model packing for *n* particle groups (instead of binary packing), and have been used in several (Kronlöf 1997, Jones 2002, Fennis 2011) studies of concrete mix design optimisation. The CPM is the most recent of the models, so only that will be briefly introduced below.

The model introduces the idea of virtual packing density, which can only be achieved if each of the grains in the aggregate mixture is placed grain by grain. The model consists of two parts. In the first part large particles are almost fully packed but as a result of the

loosening effect caused by the small particles, the larger particles are forced apart. The packing density (φ_1) of such a mixture is:

$$\varphi_1 = \frac{\beta_1}{1 - (1 - a_{12}\,\beta_1/\beta_2)x_{v2}} \qquad (9)$$

in which a_{12} is the so-called loosening effect [-]

β_1 and β_2 are virtual packing densities of the large (1) and small (2) particles [-]

x_{v2} is the volume fraction of the small particles in solid phase [-]

In the second part of the model, the small particles are in the interstices of the largest particles, near to their maximum packing density. However, complete packing is not achieved because of the wall effect near the larger aggregate surfaces. The packing density of such a mixture (φ_1) with the coefficient for the wall effect (b_{21}) is:

$$\varphi_2 = \frac{\beta_2}{1 - [1 - \beta_2 + b_{21}\beta_2(1 - 1/\beta_1)]x_{v1}} \qquad (10)$$

in which x_{v1} is the volume fraction of the large particles in a solid phase [-].

The packing density of a mixture is either φ_1 or φ_2, depending on which one is smaller. From the equations, de Larrard (1999) derived an equation that is suitable for several components.

$$\varphi_i = \frac{\beta_i}{1 - \sum_{j=1}^{i=1}\left[1 - \beta_i + b_{ij}\beta_i\left(1 - \frac{1}{\beta_j}\right)\right] - \sum_{j=i+1}^{n}\left[1 - a_{ij}\beta_i/\beta_j\right]x_{vj}} \qquad (11)$$

de Larrard deduced the coefficients for the loosening and wall effect from multiple blends of differently-shaped sands and aggregates. He perceived that it was possible to derive rough equations from the relative size functions of the constituents. The equations for the loosening and wall effect are:

$$a_{ij} = \sqrt{1 - \left(1 - d_j/d_i\right)^{1,02}} \qquad (12)$$

$$b_{ji} = \sqrt{1 - \left(1 - d_i/d_j\right)^{1,50}} \qquad (13)$$

where d_i and d_j are the diameters of the granular classes i and j as defined by sieve sizes [-].

A constant assumed to be characteristic of the placement (compaction) of the mixture, called the parameter *K* or a compaction index, is related to the manner in which the mixture is compacted. The equation for the compaction index is:

$$K = \sum_{j=1}^{n} K_i = \sum_{j=1}^{n} \frac{\frac{x_{vj}}{\beta_i}}{\frac{1}{\phi} - \frac{1}{\rho_i}} \qquad (14)$$

To get a mixture of maximum packing density, one must optimise the above equation for Φ so that Φ is maximised. According to de Larrard (1999), the following values for K can be used, as presented in Table 2.

Table 2. Summary of different K values for different packing methods, from de Larrard (1999)

Type of placement	Simple pouring	Dry-rodding	Vibration	Vibration + compression 10kPa
K-value	4.1	4.5	4.75	9

2.4.2 Testing water demand

The relationship between particle size distribution, packing, strength and water demand is well known. Hunger and Brouwers (2009) studied the packing behaviour and water demand of various powder materials and compared different tests for their evaluation for the production of self-compacting concrete (SCC). The tests used were the spread-flow test, Puntke test, Vicat needle test and modified Marquardt test (Marquardt 2002). The results of Hunger and Brouwers showed that the Puntke and the Marquardt tests always yielded the lowest water demand values, with Puntke being slightly smaller than Marquardt. In all, the spread-flow test and the modified Marquardt method were assessed as being good techniques for

determining water contents for self-compacting concretes. The modified Marquardt method was also expected to give information on the deformability of SCC mixes. Comparisons of the results that were obtained are presented in Figure 3 (Hunger and Brouwers (2009).

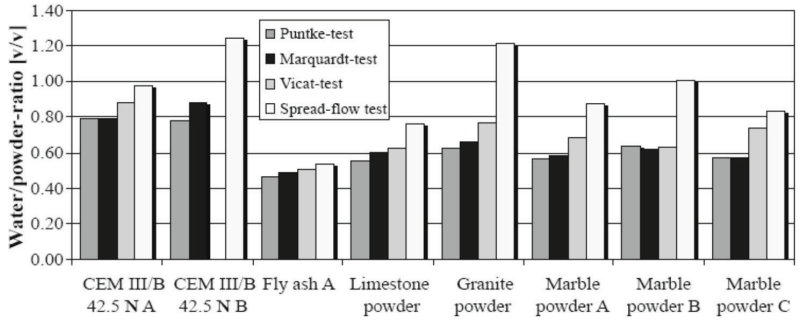

Figure 3. Comparison of volume based water demands derived by different test methods, from Hunger and Brouwers (2009).

The Vicat needle test (SFS-EN 196-3) is the best-known test and the one most used by cement manufacturers (Amziane 2006). Originally used to determine the setting time of cementitious materials, it is based on the penetration of cement paste with a needle with a specific shape and weight, which causes shear strain, and on the idea that stiffening during the set causes a gradual increase in resistance to shear. When the water requirement necessary to obtain a neat cement paste of standard consistency is being determined, the 10-mm Vicat needle should penetrate 34 ±1 mm into the paste.

In the Puntke method (Puntke 2002) the dry materials (50 g for powders, 100 g for sand) are weighed and mixed in a steel vessel and after that, water with superplasticiser is added in small quantities and mixed together with the dry material. Thereafter the beaker is continuously dropped from a constant height until a visible moistening of the surface of the material is obtained. If such wetting does not occur, more water is added and the whole procedure is repeated. The Puntke test will give the water content at the point of saturation, which represents the transition of the mix from a coherent packing to a suspension.

The spread-flow test (Okamura and Ozawa 1995), similarly to the slump flow test, is a classical method for the determination of the water demand in self-compacting concretes. The apparatus for the spread-flow test consists of a mould in the form of a small cone frustum which is filled with the cement paste. Immediately after

filling, the cone is lifted and the paste spreads over the table. From the spread flow of the paste, two diameters perpendicular to each other are determined and their mean is used to calculate the relative spread, which is a measure of the deformability of the mixture.

In the Marquardt method (Marquardt 2002) water is added slowly to a powder mixture in a standard mortar mixer, equipped with a (preferably digital) display showing the power consumption. The basis of this test is the resistance to shear stress of pastes with different moisture contents. When the water is added it forms agglomerates of particles. At less than complete saturation, the strength of the agglomerates increases with the amount of liquid and the surface energy of the liquid. When enough water has been added, the mix liquefies. The power consumption of the mixer will decrease as a result of the increased thickness of the water layers around the particles.

The water demand of a powder can also be determined by the centrifugation of moisturised aggregate fractions (Miller et al. 1996). In the test, a paste is mixed in a three-litre Hobart mixer; first, the dry powders are mixed, after which the water and the superplasticiser are added. The paste is poured into test tubes and the tubes are then centrifuged for ten minutes at 4000 rounds per minute. By determining the mass of the paste in the test tube, the amounts of powder and water in the test tube at the beginning of the test are known. Centrifuging the test tubes causes the particles in the paste to be compacted and less water is necessary to fill the voids in between the compacted particle matrix. As a result, the total sample will have a surplus amount of water, which causes a water layer on top of the centrifuged paste. The water layer is removed with a pipette and measured. By determining the amount of water removed, the amounts of water and particles in the compacted sample are known and thus the water demand of the powder can be calculated. Specific instruments (mixer, centrifuge, test tubes) and specific conditions (mixing and centrifuging times) are necessary for the test.

The single drop test (Bigas et al. 2002) is based on the agglomeration of fine particles by the capillary forces of a drop of water. In the test, a 0.2-ml drop of water is placed on a powder bed, resulting in the formation of an agglomerate. After 20 seconds, the agglomerate is removed from the bed and its mass is determined. The test must be performed 15 times for sufficient precision. The volume of the drop of water (w) and the volume of the agglomerate (f) are determined by the weight and the density of the materials. The water requirement of the blended mixture is characterised by the w/(c + f) ratio, where c is the absolute volume of the cement. Bigas and Gallias (2003) found that the w/f value determined by the single drop test is on average equivalent to 80% of the value obtained by the standard Vicat test.

The Proctor compaction test (SFS-EN 13286-2) is known from soil mechanics but can also be used on fine powders. In the test a powder is mixed thoroughly with a measured amount of water and the mixture is placed in a mould in three layers. After each layer has been placed it is compacted by applying 25 blows of a block-hammer dropped from above the mixture in such a way that the blows are uniformly distributed over the surface of the sample. The excess of the mould is removed and the surface of the compacted mixture is carefully levelled off. The mass of the moist mixture sample is determined and after that the water content w is determined by drying the sample, by which the compacted dry density of the mixture can be calculated for each compacted sample.

For fine powders it is essential to measure the water demand with water and superplasticiser, i.e. in the same fluid as used in the concrete, because of the strong surface forces which influence the packing density.

Gallias, Bigas and Kara-Ali

Gallias, Bigas and Kara-Ali studied (Gallias et al. 2000 and Bigas & Gallias 2002) the effects of fine powders on the packing and water requirement of cement pastes. The first paper dealt with the influence of the granular and morphological characteristics of the powders on the water requirement of a cement paste without superplasticisers. The experimental study consisted of water requirement tests performed with the Vicat apparatus for 14 mineral admixtures and porosity measurements of the pastes. The mineral powders were of natural (e.g. calcite) and industrial (e.g. silica fume) origin and their average particle sizes varied between 0.07 and 60 μm and their BET specific surface areas from 0.3 to 40 m^2/g. The water requirement of the pastes containing mineral powder of a natural origin was observed to increase as the particle size decreased, but powders with industrial origin an opposite trend was noticed. The influence of morphological characteristics was also studied and the results indicated that irregularly-shaped particles required two to four times more water than round or subangularly-shaped powders. In addition, the writers concluded that blended mixtures with increased particle size distributions led to denser packing and optimisation of the water requirement.

The latter study dealt with determination of the main characteristics that influence the water requirement of fine mineral powders and the physical interactions between water and cement affecting the granular packing of cement mixtures. A new test to determine the water requirement and the packing density, called the “single drop” test, was also introduced. The mixtures used were prepared with and

without superplasticisers. Eighteen different mineral powders were used, with the same average particle sizes and BET areas as in the first study, with round, angular and irregular shapes. The water requirement results concerning particle size and shape were similar to those in the previous study. Water requirement studies with the single drop test showed a correlation of $R^2 = 0.91$ with the standard Vicat test. The water requirement value determined with the single drop test was, on average, 80% of the value obtained with the Vicat test. In blended mixtures with a high content of added fine powder (90-98%), the interaction between the cement and powder particles led to increased water dosages. According to the writers, the use of a superplasticiser could diminish this phenomenon, but only in water-saturated mixtures.

2.4.3 Effect of fillers on the rheology of cement paste and concrete

The rheology of concrete is influenced when fine powders are used and the effect on workability depends on the original composition and properties of that mixture. Silica fume, blast furnace slag and fly ash are the most commonly used fillers (Neville, 1995). It is frequently stated that, if the volume concentration of a solid is held constant, the addition of mineral admixtures reduces the workability as a result of the increase in surface area. However, generalising the effects of the addition of fillers to concrete and cement paste is not possible. The type and grading of the aggregate, type and amount of cement, w/c ratio and the type and dosage of the plasticiser influence the rheological properties substantially.

The advance of concretes that have good flowability properties, such as self-compacting concretes, has made the understanding and study of the influence of fillers even more important. Spherical particles such as silica fume and fly ash are assumed to have an enhancing effect on concrete flowability, because of the spherical particles easily rolling over one another (acting as ball bearings) and thus reducing interparticle friction (Ramachandran 2001). A lubricating effect caused by fillers filling up air voids between coarser particles in aggregates with a poorer particle shape has also been described (Danielsen and Wallevik 1989, Kronlöf, 1997).

Various methods are used to measure the rheology of fresh cement paste and concrete and, depending on the technique, various properties are used to describe it. Tattersall and Banfill (1983) distinguished between qualitative parameters, such as workability, consistency, plasticity, compactibility, stability and pumpability, quantitative empirical ones, such as slump and Ve-be, and quantitative fundamental ones, such as viscosity and yield stress.

Packing models have been used to predict the rheology of cement paste and concrete, with varying results. For the most part, those models presented above assume that adding fine powders to a cement-aggregate matrix helps fill up the voids in the particle structure, leaving only minimum space for water. In this way adding fine particles will reduce the water requirement (de Larrard and Sedran 1994, Kronlöf, 1997, Wong and Kwan, 2008(II)).

The usefulness of packing models has been shown in designing self-compacting concrete (SCC). Sedran et al. (1996) applied the solid suspension model successfully in SCC design and concluded that by minimising the void space between the granular skeleton, i.e. improving the packing density, the workability of a mix can be optimised. In 2005 Brouwers and Radix applied packing theories and experiments to SCC and concluded that the packing of all the solids in the mix is of the utmost importance. According to Brouwers and Radix, ideally, the grading curve of all solids should follow the modified Andreasen and Andersen (1930) curve.

As previously mentioned, Kronlöf (1997) used the Linear Packing Density Model (LPDM) (Stovall, de Larrard & Buil 1986) to estimate the water requirement of concrete mixes with fine powders. The packing models were able to give a rough water requirement of a compact mix, but did not estimate the water volume fraction needed to convert a mix from compact to workable. Fennis (2011) also used the LPDM, as well as several other models, to define how particle packing models could be used to calculate the mechanical properties of concrete with a cement content less than 260 kg/m^3, mineral fillers and a strength class within C20/25. Of all the packing models used, Fennis judged the Compressible Packing Model (CPM) to be the most accurate and it was modified to include the influence of interparticle forces on the particle packing density, wall effect and loosening effect. The modified model was shown to predict the strength of a mixture from its packing density calculations and water demand.

However, although there are many favourable results supporting the particle packing theory, various researchers also report the need for an excess amount of water or cement paste to provide sufficient workability. While supporting the particle packing theory, Kwan and Mora (2001) found that maximum particle packing density does not necessarily guarantee a workable concrete mixture. They state that a very dense particle packing comprising too many fine particles produces a coarse concrete mixture. Wong and Kwan (2008 (I)) reviewed the existing methods for measuring the packing density of cementitious materials, and concluded that dry packing methods are beset by agglomeration and are prone to overestimate the voids content and underestimate the packing density of fine particles,

whereas the wet mixing methods – based on determining the water demand as the water content at a certain pre-set consistency – are unsuccessful in proving that the water content attained is actually just enough to fill up the voids. In addition, the air content of the paste in the wet methods is often neglected (Wong and Kwan 2008 (I)). Earlier, Jones et al. (2003) had come to the same conclusion in a study that aimed to produce a minimum voids ratio (or maximum packing density) according to particle packing models. In the experiment, they found that the filler content that gave the lowest water demand, which was thought to be the minimum measured voids ratio in the paste, was lower than the filler content calculated by a packing model to give the minimum voids ratio; see Figure 4.

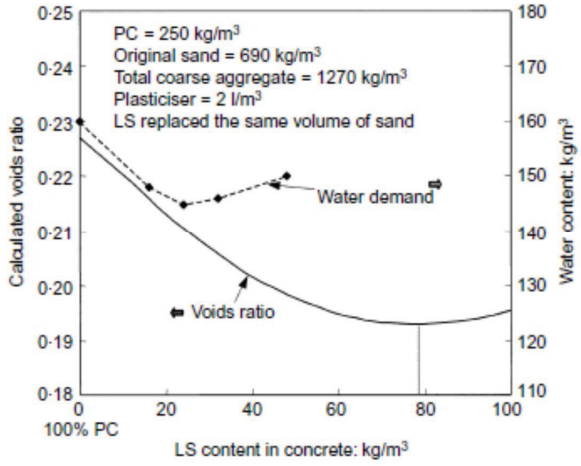

Figure 4. The influence of limestone powder on calculated voids ratio and water demand of concretes, from Jones et al. (2003).

Utilising packing models to predict the rheology of a mixture requires the use of a superplasticiser to break flocculation. Flocculation is the phenomenon in which uncharged particles will attract each other and form larger agglomerates. Electrostatic forces may also cause flocculation, as particles that have opposite charges will attract each other.

Effects of water-reducing admixtures

Water-reducing admixtures are hydrophilic surfactants which, when dissolved in water, de-flocculate and disperse particles of cement and filler. A considerable amount of water reduction can be achieved by using superplasticisers or high-range water-reducing admixtures, which are capable of reducing water contents by 2 or 3 times more than normal plasticisers.

Superplasticisers are ordinarily classified into four main groups: sulphonated melamine-formaldehyde condensates, sulphonated naphthalene-formaldehyde condensates, modified lignosulphonates and others, including sulphonic acid esters, polyacrylates, polystyrene sulphonates, etc. (Ramachandran 2001). Figure 5 illustrates the chemical structures of plasticisers.

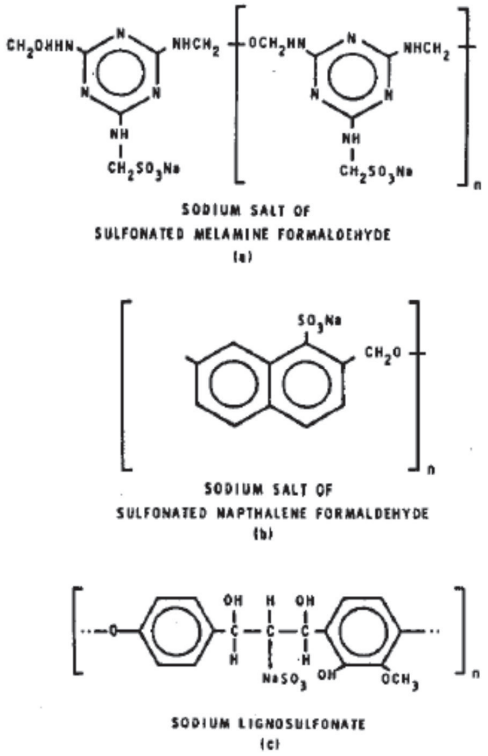

Figure 5. Chemical structures of plasticisers (Ramachandran 2001)

There are, in general, two main mechanisms of particle dispersion in a suspension: electrostatic repulsion and steric hindrance. Basically, the working mechanism of "traditional" superplasticisers such as naphthalene-based plasticisers is said to rely on electrostatic repulsion as the primary mechanism of dispersion, whereas the new generation of synthetic polyacrylates with branched macromolecules were designed to use steric hindrance as the major dispersing mechanism. These mechanisms are demonstrated in Figure 6 and Figure 7.

However, according to Flatt et al. (2000), a clear distinction between these two mechanisms cannot be made and that both electrostatic

and steric repulsion forces should be taken into account in a so-called "electrosteric repulsion", even though steric hindrance may dominate. Once in contact with cement, superplasticiser molecules adsorb on the surface of cement particles, and the saturation dosage depends on the surface area. Once saturated, any further increase in the dosage does not lead to an improvement of the fluidity (Bensted and Barnes 2002).

Nehdi et al. (1998) studied the use of ultra-fine particles of limestone, finely ground silica and silica fume to replace cement and its effects on the rheology of high-performance concrete. They discovered that in order to achieve a slump of 220 ± 20 mm the superplasticiser requirement varied, depending on the replacing ultra-fine particle. Finely ground silica and both of the limestone fillers reduced the superplasticiser requirement; this was so even up to a replacement amount of 20%, while a silica fume replacement of just 5% increased the superplasticiser requirement.

In his later work Nehdi (2000) examined the possible causes of rapid losses of workability in superplasticised mixtures with a low water/cement ratio with sub-micron-level ground carbonate fillers. It was discovered that the magnesium (MgO) content of the carbonate filler had an unfavourable influence on the efficiency of the dispersant and caused rapid losses of workability. According to Nehdi (2000), the possible acceleration of C_3S hydration as a result of calcite and the potential formation of carboaluminates in the hydration of Portland cement can also contribute to rapid losses of workability.

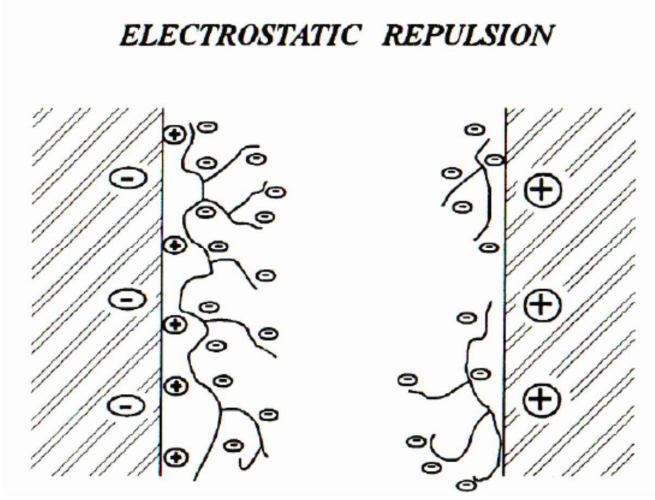

Figure 6. Drawing of how negatively charged polymers may adsorb to both positively and negatively charged areas. From Ramachandran et al. (1998).

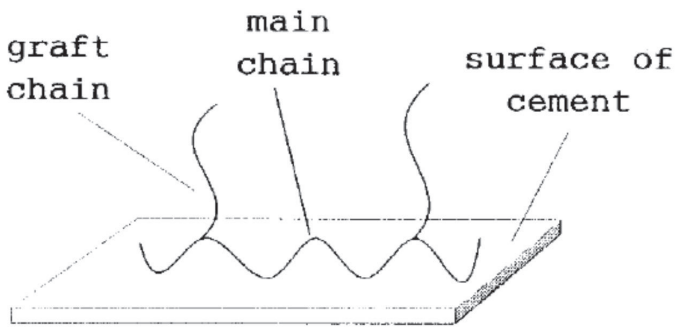

Figure 7. Drawing of grafted polymers adsorbing on the surface of particles, creating steric hindrance which prevents them getting close enough to form agglomerates. From Yoshioka et al. (1997).

Unlike suspensions of inert particles, hydration also contributes to the initial rheology of cement paste. Therefore, there are other mechanisms of how plasticisers can improve the rheology of cement pastes, for example by adsorption to active sites and retardation of the formation of hydration products.

Surface charges are also a significant constituent in cementitious systems. Particles in a cementitious system can obtain a charge either as a result of imperfections in the crystal structure near the surface or through adsorption of specific ions on the surface (Tattersall & Banfill 1983). Particles that are not charged will attract each other and coagulate/flocculate. In addition, electrostatic forces may also cause coagulation and flocculation as oppositely charged particles will attract each other.

Placing charged surfaces in a liquid medium will influence the distribution of the nearby ions in the solution. Ions with opposite charges will attract each other via the Coulomb force and repel ions with the same charge and thus an electrical double layer is formed. The zeta potential is the potential difference between the liquid medium and the layer of fluid attached to the charged surface and it indicates the degree of repulsion between nearby similarly-charged particles in dispersion. Dispersions with high zeta potential are electrically stabilised, while colloids with zeta potentials near zero tend to coagulate or flocculate (Daimon and Roy 1979). Depending on the ions adsorbed on the particle surface, the zeta potential of a particle may be either positive or negative.

Depending on the mineralogy, the z-potential of different fillers may vary considerably. Johansen et al. (1992) measured the zeta potential of various fillers in solutions of pure de-ionised water, CaOH and CaOH water with superplasticiser (lignosulphonate) with a pH of 11. The mineral fillers used were limestone, quartz, soda and potassium feldspars, muscovite, chlorite (20% biotite) and amphibole (15% biotite). The results are shown in Table 3. The addition of a water-reducing admixture had a central effect on the zeta potential: through the adsorption of lignosulphonate on the particle surfaces, all the zeta potentials turned negative.

Table 3. Zeta potentials of different fillers according to Johansen et al. (1992).

	H_2O	$Ca(OH)_2$	$Ca(OH)_2$ + 0.5% SP
Limestone	+12	+26	-15
Quartz	-23	-1	-26
K-feldspar	-23	0	-19
Plagioclase feldspar	-40	0	-28
Muscovite	-39	+3	-20
Chorite	-19	-2	-15
Amphibole	-31	+9	-11

In contrast to the results by Johansen et al. (1992), the aforementioned study by Kjellsen and Lagerblad (1995) measured zeta potentials of about -3 mV, which were independent of the filler type and time. Kjellsen and Lagerblad came to the conclusion that the reason for the contradictory results must lie in the pore solution pH, which in their study was a more realistic 12.2. Thus, the significance of zeta potentials may be minor, or at least the results should be treated with caution. In addition, with superplasticisers designed to have dispersing mechanisms that are mainly based on steric hindrance, the relevance of the zeta potential is probably lower.

2.4.4 Filler effect: influence on the interfacial transition zone

Concrete is generally considered as a composite material, consisting of aggregates and cement paste. The interfacial transition zone (ITZ) describes the area surrounding the larger aggregate particles, where, on average, there are more pores, calcium hydroxide and ettringite needles and fewer cement particles than in the “bulk” paste regions further away from the aggregate. The presence of an ITZ was reported for the first time by Farran (1956). Since this, many theories on the origin and special features of the ITZ have been presented.

Barnes et al. (1978) studied the contact zone between glass slide “aggregates”, quartz and cement pastes using SEM and EDS. They introduced a geometrical model for the ITZ and detected a duplex

film that was typically 1 to 1.5 μm thick. The inner part, which is formed in direct contact with the aggregates/glass surface, is Portlandite and the outer part is C-S-H gel. Models of the ITZ introduced by Barnes et al. (1978), Ollivier and Grandet (1982), Zimbelmann (1985) and Monteiro and Mehta (1986) are presented in Figure 8.

The so-called wall effect, a packing phenomenon in fresh concrete, has been widely presented to explain the formation of the ITZ in, for example, Maso (1980) and Scrivener and Pratt (1986)). It is a phenomenon which occurs when aggregate particles create a "wall" for the extensively smaller cement grains, which disrupts their packing, resulting in loose arrangement of the cement grains and consequently a higher local w/c ratio and porosity near the aggregate surface. In addition to the wall effect, the difference in porosity between the transition zone and the rest of the paste leads to ionic diffusion at a faster rate than in the rest of the paste, and as a result the ITZ is abundant in hydration products formed with the most mobile ions, such as ettringite and portlandite (Maso (1980), Breton et al. (1993)).

Because of the wall effect, the area closest to the aggregate contains predominately small grains, while larger grains are found further away from the aggregate. Consequently, the ITZ can be modified by altering the particle size distribution of the cementitious materials. Bentz et al. (1999) found out that at conventional w/c ratios, coarser cement results in an ITZ microstructure characterised by a higher porosity and larger pores. This means that the size of the ITZ is comparable with the size of the cement or (micro)filler grains. At low (0.3) w/c ratios, this effect became less significant (Bentz et al. 1999).

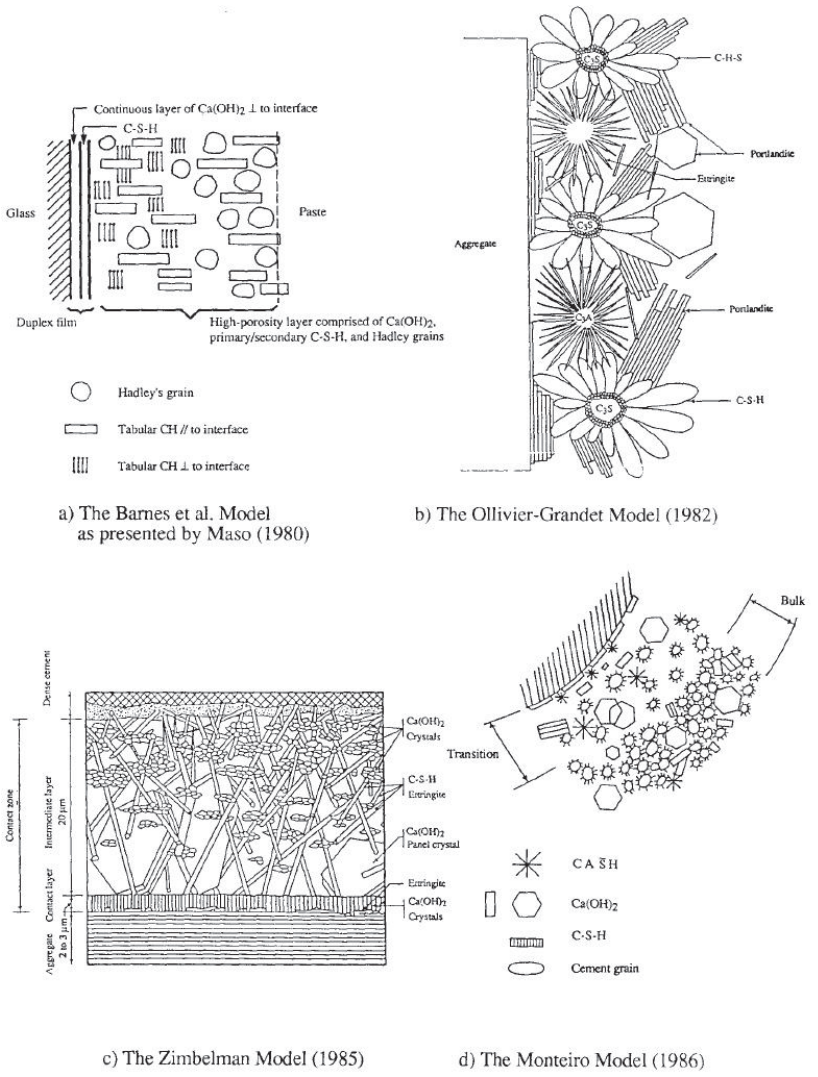

Figure 8. ITZ models from Breton et al. (1993).

Another explanation to describe the formation of the ITZ was proposed by Goldman and Bentur (1992): during the vibration of concrete and before setting, microbleeding leads to an accumulation of water under the aggregate particles, which causes the ITZ. These results were confirmed by Hoshino (1988), who observed, on the basis of experiments using a 1% solution of red aniline dye on cut surfaces, that the w/c ratio was partially increased near the lower surface of coarse aggregate in concrete. He concluded that a considerable increase in the w/c ratio occurs under the aggregate before hardening. There is no distinct borderline in the ITZ region, since the change from the ITZ to bulk paste takes place progressively and is most significant in the first 15-20 µm closest to the aggregate (Scrivener et al. 2004). Figure 9 describes the gradual transition of the ITZ and the particle size distribution near the aggregate surface.

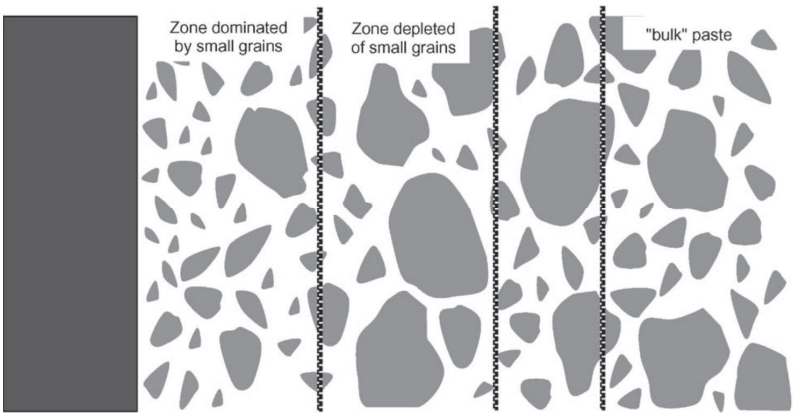

Figure 9. A schematic representation of the gradual transition of the ITZ, from Scrivener et al. (2004).

The strengthening effect of chemically inert fillers, i.e. particles with no pozzolanic or hydraulic properties, is based on their ability to alter the pore structure either by filling the empty spaces in the cement paste or by modifying the hydration reaction by acting as nucleation sites for the precipitation of hydration products, thus forming a stronger and more dense cement gel. Both of these processes contribute simultaneously to the development of the microstructure in the ITZ. For instance, Goldman and Bentur (1993) and Nehdi (1998) illustrated the effects of mineral powders on the microstructure of the ITZ. Their results show that fillers such as silica fume and very fine ground limestone filler reduce the porosity of the ITZ and the w/c gradient (Figure 10).

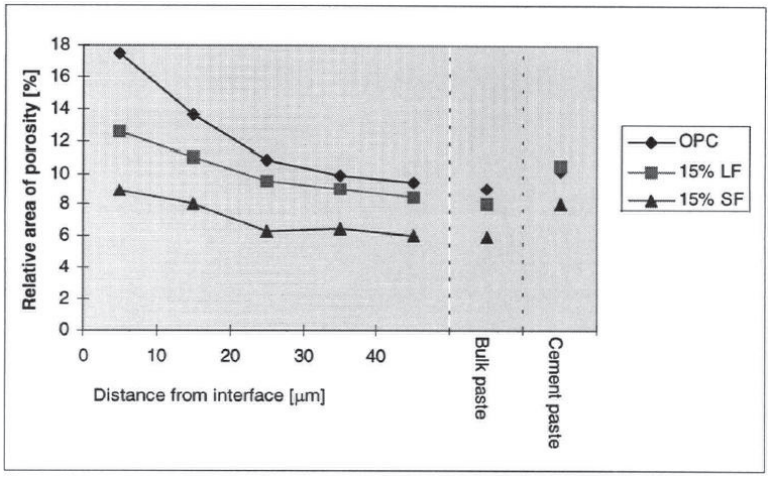

Figure 10. Filler effect of silica fume (SF) and very fine ground limestone filler (LF) on the relative area of porosity in the transition zone (w/b = 0.33 28d). From Nehdi (1998)

The influence on the ITZ of powders with a similar particle size to that of the cement is inferior to that of the ultrafine particles since the wall effect is not affected. However, these powders, such as fly ash and granulated blast furnace slag, can reduce the ITZ by means of some phenomena: creating nucleation sites for crystallisation, which would help the formation of smaller crystals of CH, by lowering the permeability of fresh concrete and thereby lessening the accumulation of bleed water at the aggregate surface and the pozzolanic reaction with CH, which densifies the cement paste. The size and type of the aggregates also affects the transition properties, as presented by Ping et al. (1991). Their research showed that in concretes containing smaller limestone aggregates the transition zone was denser than in similar concretes containing quartz aggregate, possibly as a result of chemical interaction between the limestone and Portland cement paste.

2.5 Durability issues

The effects of chemically inert fillers on the durability of concretes, such as permeability, freeze-thaw resistance, carbonation and the capability to resist aggressive compounds, have been studied relatively little, especially, if one makes a comparison with the studies of mineral additives such as fly ash, ground-granulated blast furnace slag or silica powder.

The durability of a porous material, such as concrete or mortar, depends greatly on its permeability. Deterioration mechanisms are usually associated with the ingress of harmful agents such as water, chlorides, sulphates, acids etc. Permeability and diffusivity are related to the total porosity and the size and continuity of the voids in the concrete. By improving the pore structure of the concrete, permeability and diffusivity can be reduced.

The addition of fine powders can help to reduce the volume of pores, the sizes of the pores and the connectivity of the pores in the paste and reduce the porosity of the transition zone. Permeability and diffusivity can also be reduced by increasing the hydration, which, in the case of inert fillers, is done by creating nucleation sites for the hydrating cement particles. Sellevold et al. (1982) reported an improvement in pore structure, which they attributed to the nucleation effect of the fine particles of $CaCO_3$, which was due to the refinement of the pore structure, which reduced its connectivity.

In a recent study Uysal et al. (2012) showed that the chloride ion permeability of self-compacting concretes was reduced when the amount of mineral admixtures was increased, regardless of the admixture type. The mineral admixtures used were fly ash,

granulated blast furnace slag, limestone powder, basalt powder and marble powder.

Tsivilis et al. (2003) studied the effect of the limestone content on the gas permeability, water permeability, sorptivity and porosity of concrete. The Portland limestone cement used was produced by intergrinding clinker, 0-35 weight-% limestone and 5% gypsum. Compared to the plain Portland cement concretes, the Portland limestone cement concretes possessed higher gas permeability values but the use of limestone as a replacement had a positive effect on the water permeability and the sorptivity of the concrete, although the compressive strength results were lower than that of the control. In addition, Tsivilis et al. (2003) reported that the addition of limestone up to 15% did not change the porosity.

2.5.1 Carbonation

Carbonation is the reaction between the calcium from calcium hydroxide ($Ca(OH)_2$) and calcium silicate hydrate (C-S-H) with CO_2 dissolved in the concrete pore fluid to form calcite ($CaCO_3$) or its other forms, vaterite or aragonite. In reality, the process of carbonation is more complex but it will not be discussed further here.

One of the most important factors controlling carbonation is the diffusivity of the hardened cement paste, which can be influenced by the type of cement, water/cement ratio, degree of hydration and curing conditions. The addition of mineral powders affects the carbonation indirectly, through the reduced water/cement ratio, according to Kronlöf (1997). That is, when the packing density is improved by adding inert filler, the water/cement ratio can be lowered and thus the carbonation rate is slowed down.

Katz and Baum (2006) presented data on the carbonation of concretes with powders derived from crushed stone and with median particle sizes ranging from 8 to 28 μm at levels of up to 227 kg/m^3. A distinct reduction in the carbonation rate was observed with concretes made with the coarser powders at moderate contents but when the smaller powders were used, the carbonation rate increased considerably. The results of the carbonation tests are presented in Figure 11. Most of the concretes exhibited improvement in their compressive strengths as a result of the addition of filler, but this did not seem to correlate with the carbonation rate.

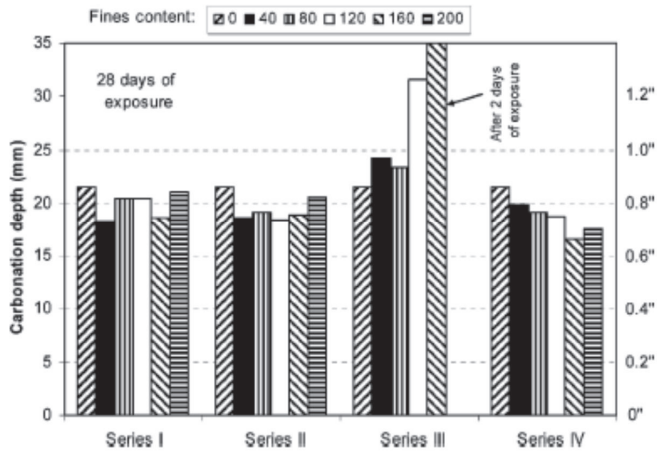

Figure 11. Carbonation depth of concretes with crushed stone powders after 28 days of exposure to accelerated carbonation conditions, from Katz and Baum (2006).

2.5.2 Freeze-thaw resistance

Sprung and Siebel (1991) found that concretes made with Portland limestone cement containing 15% limestone showed reduced resistance to frost damage in comparison with those made with Portland cements, even when the strengths were the same. The cement contents of the concretes were 300 kg/m^3 and the water/cement ratios 0.60. However, Sprung and Siebel concluded that it is possible to make concretes from Portland limestone cement that are as frost-resistant as comparable concretes made with Portland cement, provided that the limestone content does not exceed 20% by mass of the cement, and equal concrete strengths are reached. They also discovered that in general concretes made with Portland limestone cement showed increased rates of carbonation in comparison with those made with regular Portland cements, even when the strengths were the same.

Kronlöf (1997) also studied the effects of fine cement additions on the long-term durability of concretes. The concrete mixes were made with three reference and three rock powder concretes with cement contents varying from 170 to 450 kg/m^3. One of each was air-entrained, all of the concretes contained superplasticiser and the amount of rock powder was about 5% of the weight of the aggregates. The freeze-thaw durability of the rock powder concretes was found to be related to the same aspects as in normal concretes: protective pore ratio and water/cement ratio.

2.5.3 Sulphate resistance

There has been some controversy with respect to the effect of fillers – especially calcareous ones, on the sulphate resistance of Portland cement. In 1949 Daniels claimed that a specific calcite improved

concrete strength and its resistance to sea water. These claims were later rejected, since no evidence was found that calcite improved the strength or resistance to sulphates any better than other fillers. Later, however, studies of the sulphate resistance of calcareous additions to cement seemed to indicate that the addition of $CaCO_3$ improved the sulphate resistance of mortars.

For example, tests conducted by Chatterji and Jeffery (1967) and Soroka and Stern (1976(I)) showed that the sulphate resistance of mortars increased with the addition of $CaCO_3$. Soroka and Stern added 10, 20, 30 and 40 per cent CaF_2 or $CaCO_3$ filler, replacing sand in a mortar mixture, and measured increased sulphate resistance in the mortars containing $CaCO_3$. The onset of cracking in the CaF_2 and in the reference block made of Portland cement was apparent after 6 days. The mortar block containing $CaCO_3$ began cracking in 10-16 weeks. This improved sulphate resistance is demonstrated in Figure 12. According to Soroka and Stern, the improved sulphate resistance of the mortars containing $CaCO_3$ was possibly due to the formation of calcium carboaluminate, since both mortars with the addition of filler exhibited similar strengths and higher degrees of hydration. The positive effect of limestone filler on sulphate resistance was so definite that in 1972 a German patent was even issued for sulphate-resistant Portland cement containing finely ground limestone (Portland-Zementwerke Heidelberg, A.-G., 1972).

.

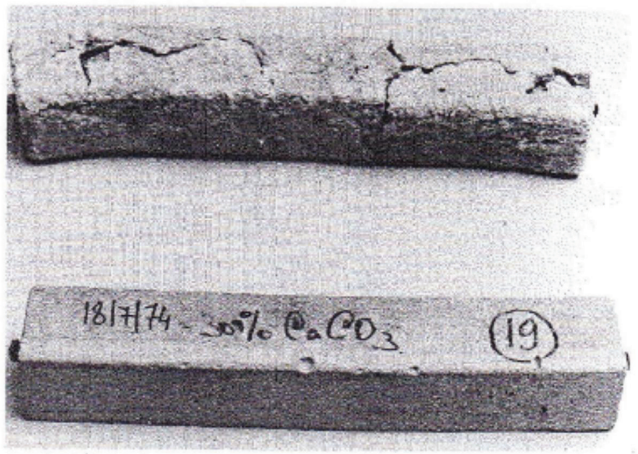

Figure 12. Mortar bars after 150 days of immersion in 5% Na_2SO_4 solution. The upper bar is the reference; the lower bar contains 30% $CaCO_3$. Picture from Soroka and Stern (Setter) (1976(I)).

The minerals most commonly seen as a product of sulphate attack are gypsum ($CaSO_4 \cdot 2H_2O$) and ettringite ($3CaO \cdot Al_2O_3 \cdot 3CaSO_4 \cdot 32H_2O$).

Ettringite has been considered to be the main mineral responsible for expansion and deterioration in concretes and mortars experiencing sulphate attack. However, during the last 40 years, another mineral – thaumasite – has increasingly been found in cement-based materials which have been exposed to sulphates.

Thaumasite form of sulphate attack

Thaumasite is a naturally occurring mineral of the type $CaSiO_3 \cdot CaSO_4 \cdot CaCO_3 \cdot 15H_2O$ and it is similar to ettringite in its crystal structure and morphology. The first reports of the thaumasite form of sulphate attack (TSA) are from the '60s and '70s (Erlin and Stark 1966, Fiskaa et al. 1971). Contrary to the well-known sulphate attack, where portlandite ($Ca(OH)_2$) transforms to gypsum and calcium aluminate hydrate to ettringite, in the thaumasite form of sulphate attack calcium silicate hydrates (C-S-H) react to form the mineral thaumasite, provided that a constant source of sulphates and carbonate ions are available. It is assumed to form in wet and cold environments. Generally, four risk factors are named, which, without the possibility of the occurrence of TSA, are thought to be negligible:

- the presence of a source of sulphate and/or sulphide
- the presence of mobile (ground)water
- the presence of carbonate, usually in the concrete aggregate
- low temperature; preferably 0-5 °C and generally less than 15°C

However, Sims and Huntley (2004) presented a series of TSA cases where the four primary risk factors are not all present, and in other studies too, evidence of TSA has been presented at temperatures above 15 °C (Brown and Doerr 2000 and Brown and Hooton 2002, Irassar et al. 2005).

As thaumasite is formed, the C-S-H is targeted for reaction and as a result of the chemical reactions it loses its binding ability and the concrete or mortar is converted to a brittle material often described as "mush", with a distinguishing white colouration. According to Taylor (1997), just as an ordinary sulphate attack is limited by the amount of aluminium in the concrete, the formation of thaumasite does not involve aluminium; given an adequate supply of SO_4^{2-} and a source of CO_2 or CO_3^{2-} ions, thaumasite can continue to form until the calcium silicate hydrate is completely exploited. Thus, sulphate-resistant Portland cement does not offer protection against TSA.

As described earlier, European Portland cements are permitted to contain up to 5% limestone filler as a minor addition that can be

ground into cements. This source of carbonate in the Portland cement has raised concern about the risk of TSA. In 1999 the UK Thaumasite Expert Group (Clark 1999) advised that this amount of carbonate was rather low, and that it would not adversely affect the performance of the Portland cement. However, Hartshorn et al. (2001) and Torres et al. (2002) showed experimentally that TSA can occur in Portland cement pastes containing only 5% fine limestone.

The beginning of deterioration in susceptible structures ranges from a few months (Hartshorn et al. 2001) to as long as years (Bensted 1999). According to some researchers, TSA can be minimised by utilising water/cement ratios that are as low as practicable to minimise the transport of water and ions such as Ca^{2+}, CO_3^{2-} and SO_4^{2-} (Bensted 1999). Another way of protecting concrete against the formation of thaumasite, according to Crammond and Halliwell (1997), is by using blast furnace slag. They found that slag improved the resistance to TSA of limestone-filled mortars at low temperatures but fly ash did not. However, according to Vuk et al. (2002), only the addition of silica fume to limestone cement improved its resistance to sulphates, while the utilisation of blast furnace slag and fly ash gave poorer results.

More recent results by Bellmann and Stark (2007) indicate that an adequate amount of a pozzolanic or latently hydraulic admixture such as silica fume, fly ash or blast furnace slag is a sufficient way of protecting against TSA. Their research showed that if the calcium/silicon ratio of the C-S-H phases were lowered to about 1.1 with pozzolanic or latently hydraulic admixtures, these phases could resist much higher sulphate concentrations without yielding to thaumasite.

2.6 Summary of the literature review

There are a vast number of studies concerning the effects of filler addition to concrete. Currently most of them have been focused on high-strength, self-compacting and high-performance concretes. The performed studies have shown that a part of the binder can be replaced with mineral powders, especially in low-w/c cement pastes and concretes. Because of the very low amount of water, only a part of the cement is hydrated and consequently, a substantial part of the cement functions as an expensive filler, while its full hydraulic potential is not exploited.

To a great extent, reductions in cement content have been made by optimising the composition of the concrete in such a way that the highest possible particle packing is achieved. For this purpose many different packing models have been presented, ranging from as early as 1907 with the Fuller and Thompson model to more modern models by de Larrard (1999). The de Larrard models have been used in several (Kronlöf 1997, Jones 2002, Fennis 2011) studies of concrete mix design optimisation with varying results. In general, packing models estimate the water requirement of compact mixes by optimising the composition of the concrete in such a way that the highest possible particle packing is achieved and the particle structure is densified, which leads to fewer voids to be filled with water. The particle packing behaviour can also be studied by water demand tests.

Favourable results have been obtained with replacing cement with ultrafine particles i.e. fillers with a particle size substantially smaller than cement. They have been found to enhance hydration (Gutteridge and Dalziel (1990)), increase compressive strength (Lagerblad and Vogt (2004)) and improve the structure of the ITZ (Goldman and Bentur (1993) and Nehdi (1998)). In addition, reports of possible retarding effects on hydration (Lagerblad and Vogt (2004)) and effects on superplasticiser dosages (Nehdi et al. (1998)) have been reported.

The effects of chemically inert fillers on the durability of concretes, such as permeability, freeze-thaw resistance, carbonation and the capability to resist aggressive compounds, have been studied relatively little. According to the studies, the addition of fine fillers may improve the durability and pore structure, which can be mainly attributed to the nucleation effect. However, in concrete containing carbonate, the thaumasite form of sulphate attack has increasingly been reported.

3. MATERIALS AND METHODS

3.1 Outline of the research programme

This research work was divided into three parts. According to the literature review, cement can be replaced by inert powders, especially in low w/c ratio mixes. However, there are no well-defined limits for the replacement. It is clear however, that packing of the particles plays an important role in the optimization of the composition of the concrete. For this reason, the first part of the research, titled "Initial laboratory studies of cement paste", contains tests performed to clarify the effects of different mineral powders on cement pastes and their interaction with cements coupled with different superplasticisers. The particle size distribution of the mineral powders was adjusted with the particle size distribution of the normal hydraulic binders so that the water demand of the mix could be minimised and the need for plasticising admixture was kept low. The optimisation included the determination of the minimum water demand, which corresponds to the maximum packing density.

The results of the preliminary laboratory studies were used in the second part of the research, which focused on the mix design optimisation of mineral powder concretes. This part was more extensive; rheology and mechanical properties were determined for over 70 mix compositions with different mineral powders and superplasticisers. Based on the results from the preliminary laboratory studies and the literature review, the effect of mineral powder addition on consistency is evaluated at first. The optimisation also included the formulation of a statistical model which incorporated the most significant variables affecting the workability and strength of mineral powder concretes.

The second part also included the development of a test method for evaluating the pumpability of concrete. The results and discussion of this study are, however, presented at the end of this report in the appendices, in a separate section titled "Evaluation of pumpability".

The third part of the research focused on studies defining the possible changes mineral powders make to basic concrete properties:

- microstructure
- hydration process
- frost durability

In addition a study on hydration products was carried out.

According on the literature review, freeze-thaw resistance of mineral powder concretes has been studied relatively little. In Finland and in the other Nordic countries, all outdoor structures are susceptible to freezing and thawing loads of varying intensity during the winter season. In order to be used successfully, mineral powder concretes need to possess adequate fresh concrete properties and withstand the cyclic frost attacks of the Nordic climate. In this study, the freeze-thaw durability properties and characteristics affecting the air entrainment of inert mineral powder concretes were investigated. Furthermore, in the third group of tests the incorporation of ground granulated blast furnace slag at levels of 50% and 70% with mineral powders was studied.

3.2 Materials

This chapter presents the materials used in this research project. Most of the data is given according to the information received from the producers.

3.2.1 Binders

The cements used were CEM I 52.5 R and CEM II/ A-M(S-LL) 42.5 N, produced by a local company, Finnsementti Oy. The apparent energies of activation of the cements according to the producer were 33.5 kJ/mol and 39.00 kJ/mol, respectively. A summary of cement properties is presented in Table 4.

Table 4. Chemical composition of the cements, according to the producer.

Component	CEM II / A-M (S-LL) 42.5 N [%] *	CEM I 52.5 R [%]
CaO	65.1	61.4
SiO	20.9	19.7
Al_2O_3	5.2	4.7
Fe_2O3	3.4	2.5
MgO	2.8	3.0
Na_2O	0.8	0.8
K_2O	0.9	0.8
SO_3	0.7	4.0

*The CEM II/ A-M(S-LL) 42.5 contains 8 % limestone and 3 % GGBS as additives.

The slag used was ground granulated blast furnace slag, also produced by the Finnish Finnsementti Oy. According to the producer, the slag was ground to a specific surface of 400m²/kg. The particle size distributions of the binders, determined with a Coulter LS 13320 laser analyser, are presented in Table 5 and Figure 13.

Table 5. Cumulative particle sizes of binders.

	0.001	0.002	0.004	0.008	0.016	0.031	0.063	0.125
	[mm]							
CEM I 52.5 R	10.4	17.2	26.4	41.0	66.7	92.0	100	100
CEM II / A-M(S-LL) 42.5 N	5.7	12.1	22.7	38.5	58.5	79.9	95.6	99.8
Slag, KJ400	5.5	11.9	23.4	40.0	60.0	79.3	98.0	99.6

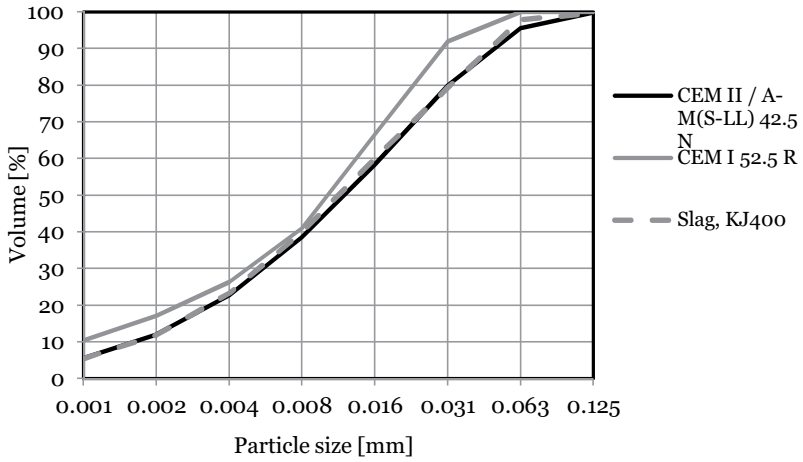

Figure 13. Cumulative particle size distributions of the binders.

3.2.2 Mineral powders

Two types of mineral powders were used in this research. The first group consisted of three types of crushed quartz powders and the second of one limestone powder. A summary of the properties of the powders is given in Table 6 and Table 7.

Table 6. Chemical composition and physical properties of quartz, according to the producer.

Component	Nilsiä/EHK [%]	Kemiö [%]
SiO_2	99.4	98.6
Al_2O_3	0.3	0.7
K_2O	0.06	0.12
Fe_2O3	0.03	0.028
Density [g/cm^3]	2.65	2.59
Bulk density [t/m^3]	1.1	1.4
pH (10% w/w)	5.5	8.3

Table 7. Chemical composition and physical properties of limestone powder, according to the producer.

Component	Limestone [%]
CaO	40
SiO_2	9.2
TiO_2	0.06
Al_2O_3	1.9
Fe_2O_3	0.87
MgO	9.1
K_2O	0.43
Na_2O	0.18
MnO	0.03
P_2O_5	0.02
$CaCO_3$	71.3
Density [g/cm^3]	2.6
Bulk density [t/m^3]	12.5

Nilsiä quartz is a crushed, ground and sorted rock powder originating from the Nilsiä quartzite deposit, which is milled using an iron-free ball mill. EHK quartz is produced by the additional grinding of Nilsiä quartz. Kemiö quartz is quarried on Kemiö Island. It is produced from pegmatite ore using a flotation technique and it is cleaned and ground. The limestone powder that was used comes from Sipoo and is produced by Nordkalk. It is ground calcium carbonate that originates from a natural limestone deposit.

The determination of the particle size distributions for the powders was performed with a Coulter LS 13320 laser granulometer capable of measuring from 0.04 to 2000 μm. The cumulative particle size distributions are presented in Table 8 and Figure 14

Table 8. Cumulative particle sizes of powders.

	0.001	0.002	0.004	0.008	0.016	0.031	0.063	0.125
				[mm]				
Limestone powder	4.6	10.0	16.4	25.3	35.6	50.8	74.0	96.5
Quartz Nilsiä	1.7	6.4	14.0	23.1	33.5	49.0	71.9	92.0
Quartz Kemiö	8.3	12.5	30.8	46.0	62.0	84.0	99.4	100
Quartz EHK	13.2	24.3	57.4	86.0	100	100	100	100

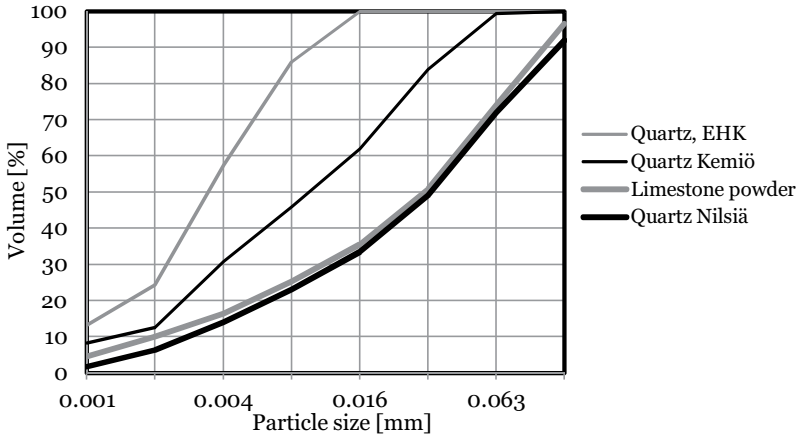

Figure 14. Cumulative particle size distributions of powders.

The particle shapes of the two different quartzes and limestone powder were determined with an environmental scanning electron microscope (ESEM). No additional conductive coating was applied. All the images were taken in the energy-dispersive mode (EDS), and are presented in the section titled "Results of the particle analysis".

3.2.3 Aggregates

The aggregate used was a combination of 5 different fractions, one of which was crushed (the 5-16-mm fraction). The maximum aggregate size in the mixes was 16 mm. The cumulative particle size distribution curves of the aggregate are shown in Figure 15. The particle size distributions for the aggregate were determined by sieving.

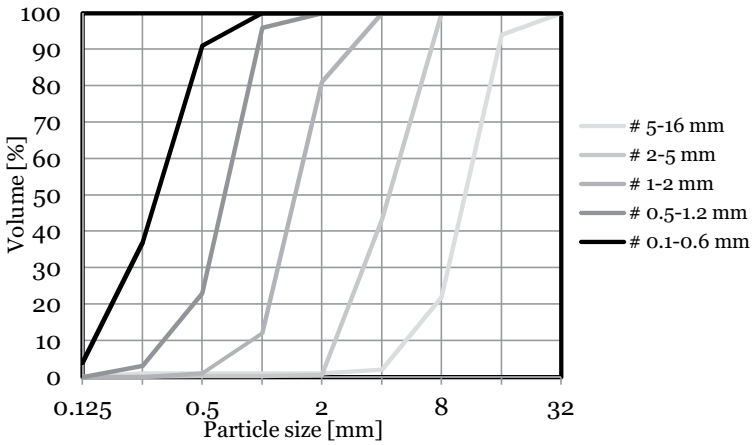

Figure 15. Cumulative particle size distribution curves of aggregate.

In addition to the mineral powders and coarse aggregate, fine sand was used. In the mix design calculations fine sand was calculated as a part of the aggregate. The particle size distribution curve for the fine sand is presented in Figure 16.

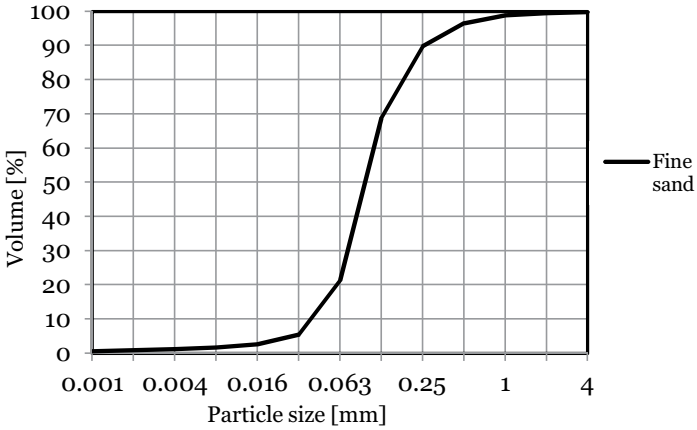

Figure 16. Particle size distribution curve of fine sand.

3.2.4 Superplasticizers

Two types of superplasticisers were used in this research. In the preliminary studies, and at the beginning of the mix design optimisation, their efficiency was evaluated and eventually only one was chosen for the third part of the work. Table 9 summarises their technical information.

Kolloment GE

Kolloment GE is a new-generation high-range water-reducing admixture, distributed in Finland by Conjust Oy. It is a modified polycarboxylate ether type of superplasticiser and, according to the producer, it causes an accelerated hydration reaction.

Glenium 51

Produced by BASF, Construction Chemicals Finland, this is a new-generation superplasticising admixture based on chains of modified polycarboxylate ether. The product has primarily been developed for use in the precast concrete industry.

Table 9. Technical information of the superplasticisers.

	Kolloment GE	Glenium 51
Form	Viscous liquid	Viscous liquid
Colour	Brown	Brown
Viscosity (20 °C)	350 - 650 mPas	128 ± 30 mPas
Density (20 °C)	1060 ± 20 kg/m^3	1100 ± 50 kg/m^3
Dry content	30 %	35 ± 1 %
pH (20 °C)	5.5 – 7.5	6-7
Chloride content	< 0.10 wt.-%	< 0.01%

3.2.5 Air-entraining agents

The air-entraining agent Ilma-Parmix, an aqueous solution of tall oil fatty acid and distilled tall oil soap, produced by Finnsementti Oy, was used for the concretes tested for freeze-thaw resistance.

3.3 Methods

3.3.1 Testing water demand

In order to test the packing density of the mixes, to find out the optimum powder amount in the concrete mix design and to determine the water requirement, a simple, slightly modified Puntke test (Puntke 2002) was used to compare the effects of the powders. In the experiment, a steel beaker with a planar base and a volume of 120 ml was filled and weighed with a mixture of cement and powder. In the next step water with superplasticiser was added to the mix in very small quantities with a pipette. After each addition of liquid, the mixture was neatly blended by hand with a small metal spatula until a uniform mix was obtained. Instead of the beaker being tapped, as in the original Puntke test, the sample was placed on a vibration table for 15 seconds, in order to expose it to a defined amplitude. This

makes the procedure more reproducible since the placed compaction energy is always the same. If the sample surface did not show a visible moistening, more liquid was added and the whole procedure was repeated until a shining surface was obtained on the water-powder mixture. The required quantity of water was determined by weighing. A mixture of ordinary tap water and a polycarboxylic ether-based superplasticiser, Glenium 51, produced by BASF Construction Chemicals Finland, was employed for the test.

3.3.2 Production and curing

The production of the test specimens was divided into two parts: initial studies of cement paste and the main tests on concrete.

The cement paste was produced using a Hobart-type mixer with a maximum capacity of 5 litres. The amount of 4.5 litres of cement paste was always produced in order to create similar mixing conditions. On the basis of earlier tests, the following mixing procedure was adopted in order to get a uniform paste:

- mixing of all dry components for 1 minute in a separate mixer;
- adding 3/4 of the water and the superplasticiser to a mixer and starting the mixer at a low speed;
- once the mixer was turned on, dry components were uniformly and continuously added to the mixer during a 2-minutes period;
- when all of the dry material had been added, the rest of the liquids were poured into the mixer and mixed for an additional 2 minutes at high speed.

The cement paste specimens were cast in steel moulds of 160x40x40 mm^3, vibrated and cured at 20 °C and ≥ 95% humidity until the testing.

The main laboratory studies of the concrete included the production of 30-dm^3 batches of concrete using a Zyklos 75 pan mixer. The total mixing time varied from 4 to 5 minutes. The mixing procedure was the following:

- adding all of the dry material and ¾ of the water and mixing for 1 minute;
- addition of the air-entraining agent when needed and mixing for 1 minute;
- addition of the rest of the water mixed with the superplasticiser and continuing mixing for 3 minutes.

The test concretes were cast in 100-mm steel cube moulds and vibrated on a vibrating table. The moulds were cured under plastic

sheets and at the age of 24 hours the specimens were de-moulded and stored at 20 °C and ≥ 95% relative humidity.

3.3.3 Fresh concrete properties

Rheology of cement pastes

The rheological properties of the cement pastes were evaluated using two methods. The first was a so-called mini cone, which is normally used to measure the flow of cement paste and mortar. Figure 17 illustrates the apparatus used. No dropping of the table was used. For the purpose of this research, a second technique, illustrated in Sugamata et al. (2001), was used. The test method consists of a V-shaped funnel (Figure 18) with a hatch on the bottom that is filled with cement paste. The relative funnel speed is obtained from the funnel discharging time once the hatch is opened and the paste can discharge without restriction.

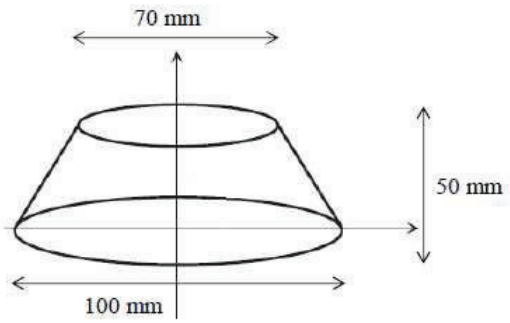

Figure 17. Dimensions of the mini cone.

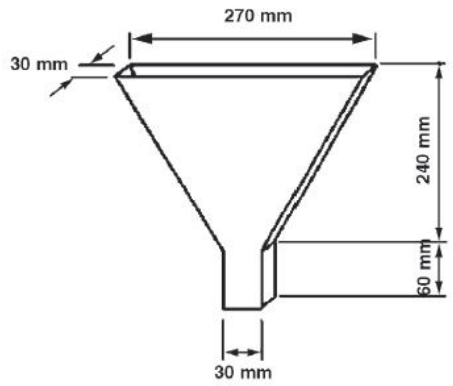

Figure 18. Dimensions of the funnel apparatus, adapted from Sugamata et al. (2001).

For all the concrete mixes, a flow table test (Finnish standard SFS-EN 12350-5) was performed to determine the consistency of the fresh concretes. Since factors such as hydration and admixture incompatibility can alter the consistency of concrete in time, the flow test was performed 15 and 45 minutes after the addition of water to the mix. The air content of the concretes was determined according to the Finnish standard SFS-EN 12350-7.

3.3.4 Mechanical tests

The compressive strength of the cement paste was measured according to the European standard SFS-EN 196-1 “Methods of testing cement. Part 1: Determination of strength”, using 160x40x40-mm^3 prisms. The tests were performed at the ages of 1, 2, 7 and 28 days. All the specimens were stored at 20 °C and ≥ 95% relative humidity until the test.

The compressive strength of the concrete was evaluated in accordance with SFS-EN 12390-3 “Testing hardened concrete. Part 3: Compressive strength of test specimens". For each measurement 3 100x100x100-mm^3 specimens were used. The tests were performed at the ages of 1, 2, 7, 28 and 56 days, depending on the specimens. The cubes were measured and weighed before the test. All the specimens were stored at 20 °C and ≥ 95% relative humidity until the test.

3.3.5 Microstructure

The influence of the mineral powders on the microstructure of the hardened concrete was investigated using environmental scanning electron microscopy (ESEM). At the age of 28 days, the specimens for the ESEM investigation were cut into slices approximately 10x10x2 mm thick from the 100x100x100-mm^3 concrete cubes with a diamond saw and using alcohol as the lubricating and cooling liquid. The specimens were dried using an alcohol exchange method (Cwirzen 2004) and impregnated with resin under a vacuum. Finally, the impregnated samples were ground and polished using diamond spray (9, 4, 1 and 0.25 μm). No additional conductive coating was applied. All the images were taken in backscattered electron mode (BSE). The images were taken at a magnification of 250-1000X. The main magnifications used for studying the results of air entrainment were mainly 250X and 500X.

Since the contrast in BSE images is produced by the variation in the average atomic number, it is possible to identify different phases, such as unhydrated cement and porosity, according to the method first presented by Scrivener and Pratt (1987) and later revised by Scrivener (2004), in which images are separated into phases using

grey-level histograms. A typical histogram of cement paste is presented in Figure 19.

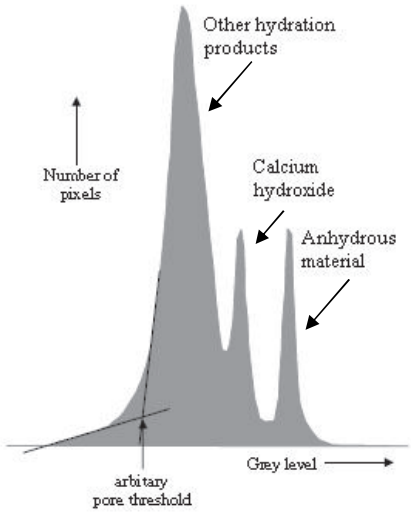

Figure 19. A typical grey-level histogram for hardened cement paste, presented by Scrivener (2004).

In most cases the porosity does not show an explicit peak. The upper level of porosity can be approximated by finding the point where the tangent to the upper portion of the hydration products intersects with the initial tangent on the grey-level histogram. In this study the threshold values were defined manually by approximating the threshold values corresponding to the porosity directly on the graph. The GNU Image Manipulation Program (GIMP) was used for the analysis of the ESEM/BSE digital images.

3.3.6 Hydration process and hydration products

Many test methods are available for evaluating the hydration process and hydration products of cement and concrete. For this study semi-adiabatic calorimetry, thermogravimetric analysis (TGA) combined with differential thermal analysis (DTA) and X-ray diffraction (XRD) were used to study the effects of varying amounts of mineral powders on hydration.

Semi-adiabatic calorimetry

Semi-adiabatic calorimetry tests were performed on 14 different concrete mixture proportions using cylinder-shaped, insulated containers produced from expanded polystyrene. The cylinder was equipped with a thermo sensor linked to a data logger to determine the temperature development inside the cylinder. The cylinders had a

radius of 7.5 cm and a height of 20 cm and the thickness of the insulating layer was 3 cm at the sides and 5 cm at the top and bottom. Before the tests with the concrete, the calorimeter was filled with hot water (+50 °C) to measure the heat loss and thermal capacity of the calorimeter.

Figure 20 illustrates the expanded polystyrene cylinder. The concrete specimens were placed in the containers and the lids were sealed and data collection commenced right after mixing. Data was collected every 60 seconds for a total of 28 days.

Figure 20. Expanded polystyrene cylinder

During the testing a small heat loss occurs in the semi-adiabatic calorimeter and thus the temperature increase does not correspond to the adiabatic temperature rise. Because of this, the measured heat evolution is transformed to correspond to the adiabatic temperature rise by specifying the heat loss of the thermo vessel. For this purpose the heat loss and thermal capacity of the calorimeter are identified and thus the heat evolution in a semi-adiabatic calorimeter can be calculated using the following equations from Rilem TC 119-TCE (1997) and Schindler and Folliard (2003). The heat capacities of the samples are assumed to be similar.

$$\theta_{HH} = \left(1 + \frac{C_{cal}}{C_s}\right) \cdot \left(\theta_s + \int_o^t a(t)\, dt\right) \qquad (15)$$

in which

θ_{HH} is the temperature increase [K]

C_{cal} is the apparent heat capacity of the calorimeter [J/K]

C_s is the heat capacity of the sample [J/K]

θ_s is the temperature increase of the sample [K]

a is the coefficient of temperature loss [K/h]

t is the time [h]

$$a(t) = \frac{T_s(t) - T_a}{\tau} \quad (16)$$

in which

T_s is the temperature of the sample [K]

T_a is the temperature of the surroundings [K]

τ is a time constant [h]

$$\tau = \frac{C_T}{h} \quad (17)$$

in which

C_T is the total heat capacity (C_{cal} + C_s) [J/K]

h is the coefficient of heat loss [J/(h·K)]

The rate of heat generation $Q_H(t)$ [W/m³] was calculated using Equation (18):

$$Q_H(t) = H_\infty \cdot \left(\frac{\tau}{t_e}\right)^\beta \cdot \left(\frac{\beta}{t_e}\right) \cdot \alpha(t_e) \cdot \frac{E}{R}\left(\frac{1}{273 + T_r} - \frac{1}{273 + T_c}\right) \quad (18)$$

in which

H_∞ is the total heat of hydration of the concrete [J/m³]

t_e is the equivalent age

β is a hydration parameter

$\alpha(t_e)$ is the degree of hydration at an equivalent age

E is the apparent energy of activation of cement [J/mol]

R is the universal gas constant = 8.314 [J/(mol·K)]

Tr is the temperature of the environment [°C]

Tc is the temperature of the specimen [°C]

The hydration parameter is calculated according to Schindler and Folliard (2003)

$$\beta = 181{,}4 \cdot p_{C_3A}^{0{,}146} \cdot p_{C_3S}^{0{,}227} \cdot Blaine^{-0{,}535} \cdot p_{SO_3}^{0{,}558} \cdot e^{-0{,}647 \cdot p_{SLAG}} \quad (19)$$

in which

p_i is the mass fraction of each mineral *i* in the cement

p_{SLAG} is the mass fraction of blast furnace slag in the binder

Blaine is the fineness of the cement [m²/kg]

$$\alpha(t_e) = \alpha_u \cdot e^{\left(-\left(\frac{\tau}{t_e}\right)^{\beta}\right)} \quad (20)$$

in which

α_u is the ultimate degree of hydration, which was calculated according to Mills (1966):

$$\alpha_u = \frac{1{,}031 \cdot w/c}{0{,}194 + w/c} \quad (21)$$

in which

w/c is the water/cement ratio

In order to study the hydration process and hydration products in more detail, the cement pastes were prepared for study in thermogravimetric analysis (TGA) and x-ray diffraction (XRD) tests. The hydration heats of the cement pastes were also measured. For the purpose of this study, the heat generation was limited by means of cooling. This was done in order to acquire a more realistic understanding of the hydration products in normal concreting conditions.

The cement pastes were cast in watertight, sealed plastic containers with a volume of 0.450 dm³ with a thermo sensor linked to a data logger to monitor the temperature development. The containers were placed in a large water tank of 0.7 m³. In the water tank a pump equipped with a thermostat kept the water circulating steadily at a

temperature of 20 ± 1.5 °C. Temperature data was collected every 60 seconds for a total of 28 days.

13 different cement pastes were prepared for study. For each paste 4 specimens for the ages of 1, 2, 7 or 28 days were cast, marked and placed in the water tank. Measurement of the heat of hydration was stopped once the sample reached the desired age and with the help of a chisel and hammer a part of the sample was broken into small (approximately 0.5 cm x 2 cm) pieces that were placed in an evacuated desiccator, containing also silica gel, for a minimum of 7 days. These samples were used in the TGA/DTA and XRD analysis.

Thermoanalysis of cement pastes

The samples were ground using a Herzog rotary sample grinder that consists of a heavy steel and tungsten carbide grinding vessel. The sample material was filled manually into the grinding vessel and into the grinder. Samples were ground for 10 seconds, since the high speed of the drive motor enables short grinding times and constant particle size. The thermoanalyses were performed with a Thermogravimetric Analyzer from Du Pont Instruments. The heating profile of the samples was the following:

- Heating from 20 °C to 200 °C at a rate of 20 °C/min
- Maintaining the temperature at 200 °C for 2 minutes
- Heating from 200 °C to 1000 °C at a rate of 20 °C/min

The weight of the test samples was 50 ± 5 mg and they were heated in nitrogen, with flowing rate of 40 ml/min. Each paste was analysed three times

Five types of pastes were analysed; a reference paste without mineral powders, pastes with 10, 20, 30 or 40 per cent of the cement replaced by limestone powder, pastes with 10, 20, 30 or 40 per cent of the cement replaced by Nilsiä quartz powder, pastes with 10 or 40 per cent of the cement replaced by Kemiö quartz powder and pastes with 10 or 40 per cent of the cement replaced by EHK quartz powder. The water to cement ratios ranged from 0.3 to 0.5, depending on the amount of cement replaced. The amount of superplasticiser was kept constant at 0.38% of the fine material (cement + mineral powder).

The amount of chemically bound water in the paste was used to calculate the degree of hydration according to Fagerlund (2009). Since the CO_2 is dissipated from the limestone at ignition, a

correction for this must be made when calculating the amount of chemically bound water:

$$w_{n,sample} = W_s - W_i - \Delta CO_2 \quad (22)$$

in which

$w_{n,sample}$ is the amount of chemically bound water [mg]

W_s is the mass of the sample prior to ignition [mg]

W_i is the mass of the sample after ignition [mg]

ΔCO_2 is the weight loss at ignition of the limestone [mg]

The effective cement amount used to calculate the degree of hydration is defined as:

$$c_{sample,eff} = (1 - g) \cdot c_{sample} \quad (23)$$

in which

$c_{sample,eff}$ is the effective limestone-free amount of cement in the sample [mg]

g is the weight-% of limestone

c_{sample} is the cement content in the sample [mg]

The degree of hydration of the limestone-free part of the cement is calculated by:

$$\alpha = \frac{\frac{w_{n,sample}}{c_{sample,eff}}}{\frac{w_n^0}{c}} \quad (24)$$

in which w^0_n/c is the chemically bound water at complete hydration of the cement content c and the value varies between 0.18 and 0.26, according to Powers and Brownyard (1948). In this study a common value of 0.25 was used.

The procedure described above requires that the loss on ignition of the cement before mixing is known, since this shall not be included in $w_{n,sample}$. The loss on ignition of the cement before mixing is determined by drying and igniting a cement sample.

X-ray diffraction of cement pastes

The tests were performed on 1-, 7- and 28-day-old cement pastes which were dried in a desiccator for at least 28 days prior to testing. The samples were ground using the Herzog rotary sample grinder. Five consecutive tests were performed for each sample.

A Philips PW1710 diffractometer with CuKα radiation was used (40kV and 40mA). The measurements were performed from 2θ angles of 5,015 to 99.965 with a step of 0.03. The samples were prepared by adding 5 % by weight of CaF_2 manually as an internal standard. The hydration products and cement minerals were identified using diffraction data from the National Institute of Standards and Technology (Stutzman (1996)) and Taylor (1990).

The data was processed using a method described in Mannonen (1996). In the process, the values of the counts for each step were first divided by the net intensity of the internal standard CaF_2 at 2θ angles from 28.265 to 28.295 and then multiplied by 100. The net intensity was calculated by calculating the net average intensity of the background at 2θ angles from 25.925 to 26.045 and subtracting it from the measured intensity of the internal standard. The pattern was then smoothed by calculating a moving average for each step from the intensities of four consecutive steps. After smoothing, the average and standard deviation of the replicate tests were calculated. Because of the standardisation, the peaks of the internal standard disappeared.

The data was analysed by calculating the intensities of the crystal phases of alite and Portlandite from the standardised patterns using diffraction data from Stutzman (1996) and Taylor (1990). The net intensity of a peak was calculated by subtracting from the net area of the peak, the corresponding area of the background measured near the peak. Table 10 presents the 2θ angles of the peaks and backgrounds used in the calculations. C_3S also has a distinctive peak at 2θ angles of 29.37 to 29.52 but this was not used since it overlaps with the peak of $CaCO_3$ at 2θ angle of 29.4 (Stutzman (1996)).

Table 10. 2θ angles of the peaks and backgrounds used in the calculations of intensities.

Phase	Abbreviation	Peak		Background		Source
		Lower limit [2θ]	Upper Limit [2θ]	Lower Limit [2θ]	Upper limit [2θ]	
Alite	C_3S	51.725	51.935	52.715	52.925	Taylor (1990), Stutzman (1996)
Portlandite	$Ca(OH)_2$	18.035	18.155	17.015	17.225	Stutzman (1996)

3.3.7 Durability tests

Freeze-thaw resistance

Freeze-thaw durability was determined according to CEN/TS 12390-9:2006 "Testing hardened concrete – Part 9: Freeze-thaw resistance – Scaling" and CEN/TR 15177:2006 "Testing the freeze-thaw resistance of concrete – Internal structural damage". The concrete specimens were cast separately and had dimensions of 150 x 110 x 70 mm^3. The test surface was against a teflon surface and no oil was used. Demoulding was done 24 hours after casting and the specimens were stored for 6 days at ≥ 95% relative humidity, after which they were removed into 60% RH, where they were stored to dry for 21 days until the freeze-thaw test started. Exceptionally, the specimens which contained 50% or 70% blast furnace slag were removed from 95% into 65% RH 35 days after casting and testing for freeze-thaw resistance started at 56 days. In this way all the test specimens had 21 days to dry. On the 22nd day after casting, or on the 50th for the concretes with blast furnace slag, respectively, the specimens were measured and aluminium foil with self-adhesive bitumen was attached to the lateral surfaces of the specimens. Following dry storage, freeze-thaw testing was preceded by 7 days of capillary suction, in which the specimens were placed in the test containers on 5 ± 0.1 mm-high spacers with the test surface downwards and de-ionised water was poured into the container to a height of 10 ± 1 mm. Figure 21 illustrates the arrangement principle of the CIF test. The weight gain of the specimens was measured before the freeze-thaw cycles were started. One freeze thaw-cycle took 12 hours, during which the temperature changed from +20 °C to -20 °C and back to +20 °C, as illustrated in Figure 22. All the tests were continued for 56 freeze-thaw cycles, i.e. 28 days

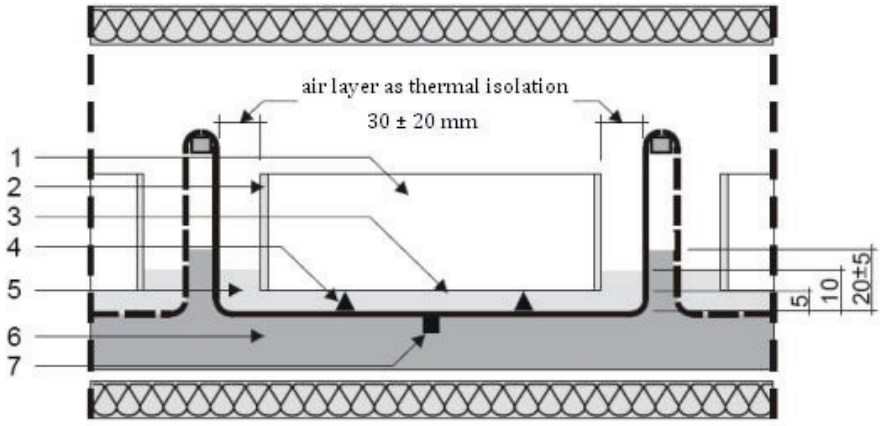

Figure 21. General arrangement of the CIF test. 1. specimen, 2. lateral sealing, 3. test surface, 4. spacer 5 mm high, 5. test liquid, 6. cooling liquid, 7. reference point.

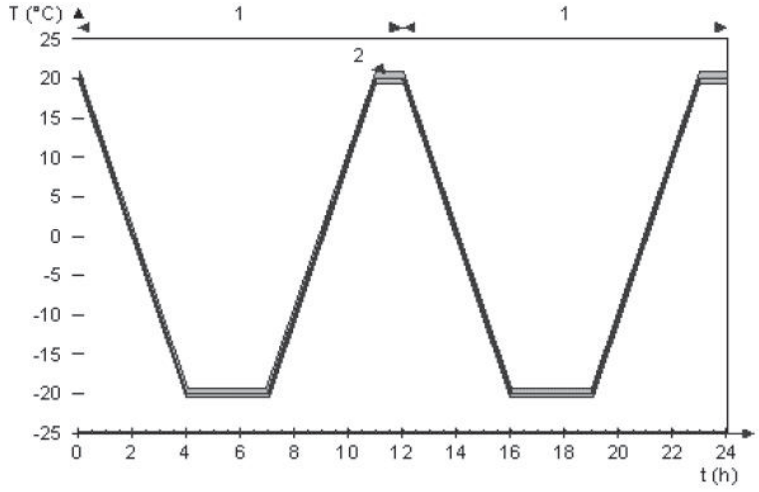

Figure 22. Temperature change within one freeze-thaw cycle in the CIF test.

Surface scaling, internal damage and water uptake were measured during the test. Internal damage was studied by means of the relative dynamic modulus (RDM) of the concrete calculated from the ultrasonic pulse transfer time data. The relative dynamic modulus was calculated according to the following formula:

$$RDM_{UPPT,n} = \left(\frac{l_{t,n}}{l_{t,0}} \times \frac{t_{t,0} \times l_{t,0} - t_{cm,0} \times l_{t,0} + t_{cm,0} \times l_s}{t_{t,n} \times l_{t,n} - t_{cm,n} \times l_{t,n} + t_{cm,n} \times l_s}\right)^2 \times 100[\%] \qquad (25)$$

in which RDM_{UPTT} is the relative dynamic modulus of elasticity in %, t_t is the total transit time (specimen + coupling medium) in μs, t_{cm} is the transit time through the coupling medium without the specimen in the container in μs, l_t is the total length between the transducers in mm and l_s is the length of the specimen in mm before the sealing of the lateral surfaces. The index n characterises the measure after a number of freeze-thaw cycles and the index 0 characterises the initial measure after the capillary suction period. Figure 23 illustrates the basic principle of the test.

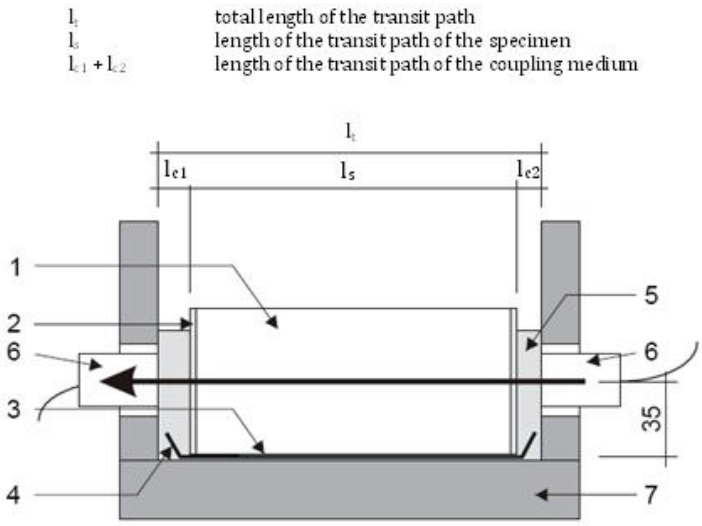

Figure 23. Test equipment for measuring ultrasonic transit time. 1. specimen, 2. lateral sealing, 3. test surface, 4. steel plate (1 mm V2A steel), 5. coupling medium test liquid, 6. transducers, 7. test container.

In order to evaluate the pore structure of the concretes an additional capillary suction test according to SINTEF (1994) was used. In the test, pre-cut concrete slices (h ~ 25 mm), presented in Figure 24, were dried at 105 °C until the weight change was < 0.5‰/day and were left to cool overnight. The concrete compositions made with cement as the only binder were cut at the age of 28 days and the concretes with cement and ground granulated blast furnace slag as a binder were tested at the age of 56 days.

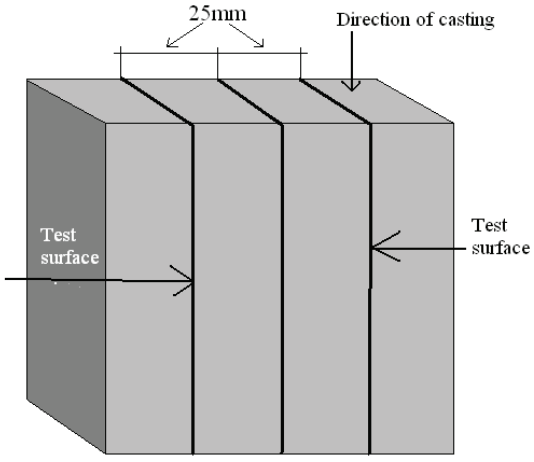

Figure 24. Cutting of test specimens for capillary suction test.

Capillary suction test commenced on the following day by placing the specimens in a test container in water so that the other surface was 1 mm below the water line (Figure 25). The weight increase of the concrete was measured as a function of the square root of time until a point of vertical intersection was achieved (see Figure 26). This is the point where the capillary and gel pores become saturated.

Figure 25. General arrangement of the capillary suction test.

After the capillary suction, the specimens were immersed in water for 3 days. Subsequently, the pore structure was filled with water at a pressure of 150 bars for 24h. Prior to the pressure test, the concrete specimens were weighed in air and under water. After the pressure test, the specimens were weighed in air. The protective pore ratio was calculated by dividing the volume of the pore space, which is not filled with water in the capillary suction test, by the total pore volume of concrete. The porosity of the concrete can be calculated by using these equations:

$$\varepsilon_{total} = \frac{W_3 - W_1}{V} \qquad (26)$$

$$\varepsilon_{suc} = \frac{W_2 - W_1}{V} \qquad (27)$$

$$\varepsilon_{air} = \frac{W_3 - W_1}{V} \qquad (28)$$

in which

W_1 is the dry weight of the specimen

W_2 is the weight of the specimen after capillary suction

W_3 is the weight of the specimen after being filled with water under pressure

ε_{total} is the total porosity

ε_{suc} is the capillary porosity

ε_{air} is the air porosity

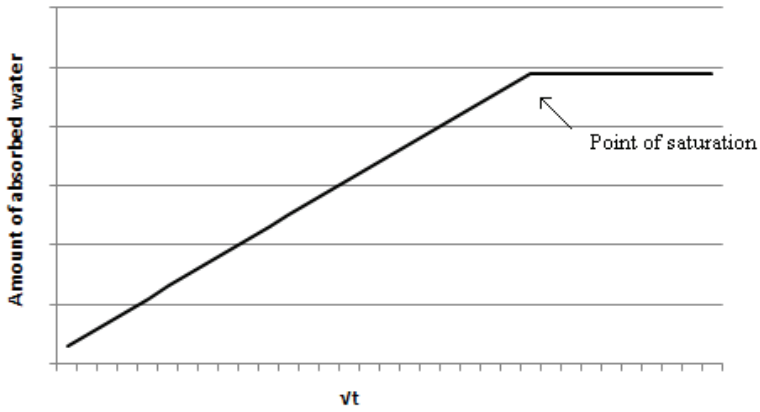

Figure 26. An illustration of an ideal capillary suction test: weight increase of the specimen in which the abscissa (time) is given on a square-root-of-time scale and a point of vertical intersection (saturation point).

4. RESULTS AND DISCUSSION

4.1 Initial laboratory studies of cement paste

According to the literature review, mineral powders have the potential to reduce the water requirement of cement pastes and concretes and they may also have a positive effect on strength development. The optimal packing, and thus water demand reduction, of a mixture consists of differently-sized particles so that the smaller particles fill up the voids between the larger particles. The purpose of the initial laboratory studies of cement paste was to investigate and evaluate the effects of different mineral powders with cements and to find the blends that are the most compatible. The effects on fresh cement paste properties, such as water demand, flowability and air content, and the effects on mechanical strength were tested.

4.1.1 Results of the particle analysis

The particle shape analysis of the fillers was performed using an environmental scanning electron microscope (ESEM). The images provided insights into the particulate properties of the mineral powders. Figure 27, Figure 28 and Figure 29 illustrate the differences between two of the quartz powders and the limestone powder. All the images were taken at a magnification of 1000X. In the images the measure at the bottom of the picture marks 10 µm.

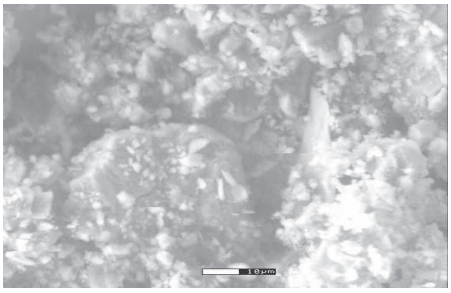

Figure 27. EDS image of limestone powder at a magnification of 1000X. The white measure at the bottom of the picture marks 10 µm.

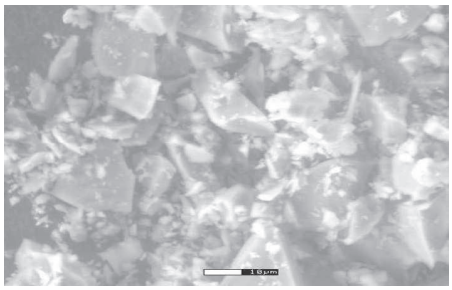

Figure 28. EDS image of Nilsiä quartz powder at a magnification of 1000X. The white measure at the bottom of the picture marks 10 µm.

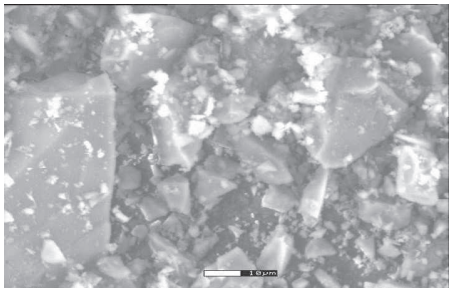

Figure 29. EDS image of Kemiö quartz powder at a magnification of 1000X. The white measure at the bottom of the picture marks 10 µm.

The particle shapes of both quartz powders exhibited characteristically angular and split-like forms, originating from the crushing of relatively hard quartz minerals. The particle surfaces appeared to have a dense glassy structure and were mostly even. The particle shapes of the limestone powder were more roundish but also flakier, as a result of the softer structure of the limestone mineral. There was no apparent porosity on the surfaces of either of the quartz powders or the limestone powder capable of absorbing excess water in cementitious pastes.

In addition to particle shape, particle packing is also influenced by grading. When evaluating the optimal replacement ratio of cement with mineral additions, the size distributions of the powders fractions must be taken into account so that powders are compacted to as dense a structure as possible. The particle-size distribution of the fines fraction should be such that the peaks of the size distributions are at separate locations on the distribution curve, in which case the different fractions of the powders can compensate and complete the combined granulometric distribution. Thus using a mineral filler with a similar size distribution to replace cement will probably not result in notably improved packing density.

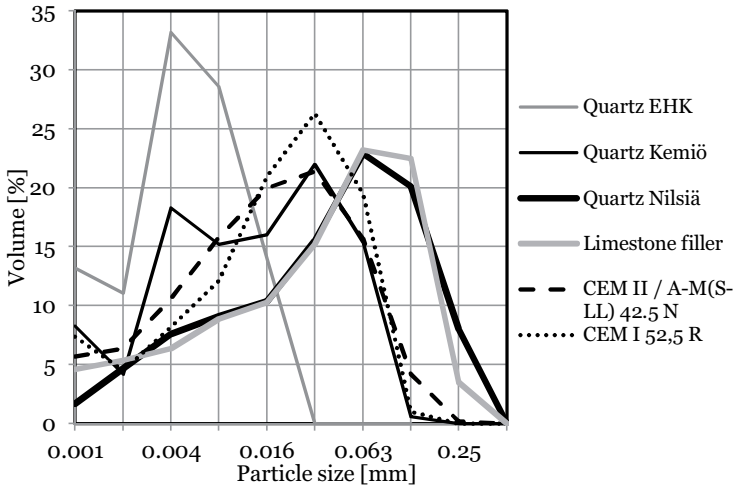

Figure 30. Particle size distributions of the studied mineral powders and cements performed by laser diffraction.

The frequencies of the size distributions of the powders are presented in Figure 30. From the figure one can see for example that about 33% of EHK quartz particles are the size of 0.004mm. According to the particle size analyses, the size distributions and distribution peaks of the limestone powder and Nilsiä quartz were very similar. This is also obvious in the cases of Kemiö quartz, CEM I and CEM II. However, the size distribution peaks of the limestone and Nilsiä quartz seemed to complement those of the cements, as was the case for EHK quartz and the cements.

Furthermore, according to Hunger and Brouwers (2009) and Ma and Lim (2002), a broader particle size distribution with as many overlapping fractions as possible results in an improved mix packing. When the particle size distribution curves were studied, all of the powders except for the EHK quartz had a broad grain size distribution, especially those of CEM II, Nilsiä quartz and limestone.

4.1.2 Testing water demand

No single method is generally accepted to determine the maximum packing density or water demand of wet fine particles and hence various test methods are used. In this research project, the water demand was determined by using a method developed by Puntke, which allows the approximation of the packing density by the determination of the water demand of the dry particle system. The basic principle of the test is that the added water fills in the voids between the dry particles and acts as a lubricant, which causes the materials to pack efficiently. The test yields information on the water content at the point of saturation, in other words, the transition from coherent packing to a suspension.

The determined water demand consists of filling and adsorbed water. The filling water is related to the packing density of the system, whereas the absorbed water creates a water film on the surfaces of the particles and its thickness determines the fluidity.

$$W_D = W_F + W_A \qquad (29)$$

in which W_D is the water demand according to Puntke,

W_F is the filling water determining the packing density and

W_A is the adsorbed water contributing to the flow

Thus the Puntke method does not directly give the packing density of the mixture. In order to obtain the filling water demand alone, an additional estimation of the adsorbed water requirement on the particle size distribution curves would need to be performed. For the purposes of this research a simplification was made so that the water demand determined by the Puntke method is evaluated as corresponding directly to the packing density. This generalisation was made since the results from the water demand tests were used exclusively to evaluate and compare the effects of different cements and powders on the water demands of the cement pastes.

The water demands were determined for different cement and mineral powder combinations in steps of 10%. Figure 31 shows the water demands for different combinations of cement and mineral powder. According to the results of the Puntke tests, the packing density increased, i.e. the water demand decreased with the replacement of cement by mineral powder in nearly every mix. Only the mixes with the very fine EHK quartz attained a minimum packing density when 40% of the cement was replaced by mineral powder for CEM I and 50% for CEM II. No suitable minimum was found at any point of the replacement combinations of Kemiö and Nilsiä quartz or limestone powder, since the use of 100% mineral powder as a replacement for cement is not possible in cement pastes.

The lowest water demands for CEM I were obtained by using EHK quartz as the replacement powder and for CEM II by selecting limestone powder or Nilsiä quartz as the replacement powder. In addition, the water demands of Nilsiä quartz and limestone powder with both cements were almost identical, presumably because of the similar particle sizes of the Nilsiä quartz and limestone (see Figure

31). Substituting cement with Kemiö quartz reduced the water demand of all the replacement amounts but by a lower quantity than with the other powders. The results also revealed that in almost all the combinations of mineral powder and cement, smaller water demand values were obtained with the use of CEM II.

Using limestone powder to replace CEM II resulted in the lowest water demand values. In all cases no feasible water demand minimum was found. However, by using either Nilsiä quartz or limestone powder in an amount of 30 to 40 per cent to replace CEM II, a high gradient in the water demand was obtained in addition to the already lowest water demands. The easily-ground limestone had a wide particle size distribution which presumably allows the limestone particles to fill the gaps between the cement particles and thus the water demand was reduced.

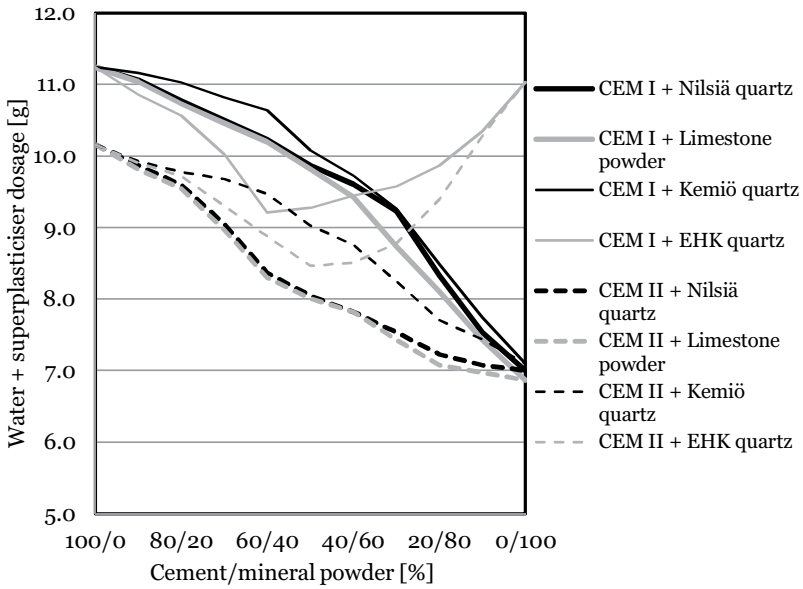

Figure 31. Water demands for different combinations of cement and mineral powder

4.1.3 Discussion about particle analysis and water demand

The particle size distributions of the Kemiö quartz and both cements were very similar. Thus, insufficient divergence between the particle sizes may have caused nearly total interaction between the materials and as a result the particles could not fully fill the free spaces between each other. For this reason the effects of the Kemiö quartz on the water demand of the mix were less pronounced.

An unexpected result was the relatively high water demand values of EHK quartz with cement, since the particle size distribution data would have suggested that the fine powder would improve the packing of the mix because of the sufficient discrepancy in the particle size distributions. Although optimal packing was obtained with a cement replacement of 40% for CEM I and 50% for CEM II, the water demand values were nevertheless notably larger than with, for example, Nilsiä quartz powder. This may have been due to the larger surface area of the EHK quartz, which may have needed more superplasticiser than the other powders. However, since the results of the Puntke tests were meant to be compared with each other and besides, high amounts of superplasticiser can result in slower hydration, no additional superplasticiser was added to the mix containing EHK quartz.

Thus, on the basis of the Puntke tests the lowest water demand values were obtained using either limestone powder or Nilsiä quartz with CEM II. Although the narrow particle size distribution of EHK quartz combined with the cement created a distinct minimum, the broad particle size distributions of the Nilsiä quartz and limestone powders with sufficient discrepancy in their distribution peaks compared to the cements were able to pack the best.

4.1.4 Cement paste results

Cement pastes were prepared in order to determine the flow and compressive strength values of the cement and mineral powder combinations on the basis of the Puntke tests. As indicated by the water demand tests, CEM II was used for the experiments since it had the lowest water demand values and thus less water and superplasticiser would be needed to make the pastes flowable. All the mix compositions are listed in Table 11. The use of mineral powder to replace the cement took place on a weight basis and, therefore, there is a deviation in the volume of the mixes. Only the reference paste P0 is exactly 4.5 dm^3. The amounts of water and superplasticiser were kept constant in all the mixes in order to determine the effect of the mineral powder on flow properties.

Table 11. Mix proportions of the cement pastes used in the preliminary laboratory tests.

Mix	Cement	Limestone powder	Quartz Nilsiä	Quartz Kemiö	Quartz EHK	Water	Superplasticizer
	[kg]	[kg]	[kg]	[kg]	[kg]	[kg]	[kg]
P0	7.181	0	0	0	0	2.154	0.027
PL10	6.463	0.718	0	0	0	2.154	0.027
PL20	5.745	1.436	0	0	0	2.154	0.027
PL30	5.027	2.154	0	0	0	2.154	0.027
PL40	4.308	2.872	0	0	0	2.154	0.027
PN10	6.463	0	0.718	0	0	2.154	0.027
PN20	5.745	0	1.436	0	0	2.154	0.027
PN30	5.027	0	2.154	0	0	2.154	0.027
PN40	4.308	0	2.872	0	0	2.154	0.027
PK10	6.463	0	0	0.718	0	2.154	0.027
PK20	5.745	0	0	1.436	0	2.154	0.027
PK30	5.027	0	0	2.154	0	2.154	0.027
PK40	4.308	0	0	2.872	0	2.154	0.027
PEHK10	6.463	0	0	0	0.718	2.154	0.027
PEHK20	5.745	0	0	0	1.436	2.154	0.027
PEHK30	5.027	0	0	0	2.154	2.154	0.027
PEHK40	4.308	0	0	0	2.872	2.154	0.027

Consistency

From the spread flow of the pastes, the relative flow area ratio Γ_m was calculated using the equation (Okamura et. al 1995):

$$\Gamma_m = \left(\frac{F}{F_0}\right)^2 - 1 \qquad (30)$$

in which Γ_m is the relative flow area

F is the mortar flow value (mm)

F_o is the bottom diameter of the flow cone (100 mm)

The relative flow area ratio represents the extent of the cement paste flow relative to the bottom of the flow cone; the higher the relative flow area, the greater the deformation of the cement paste. The results of the flow are presented in Figure 32.

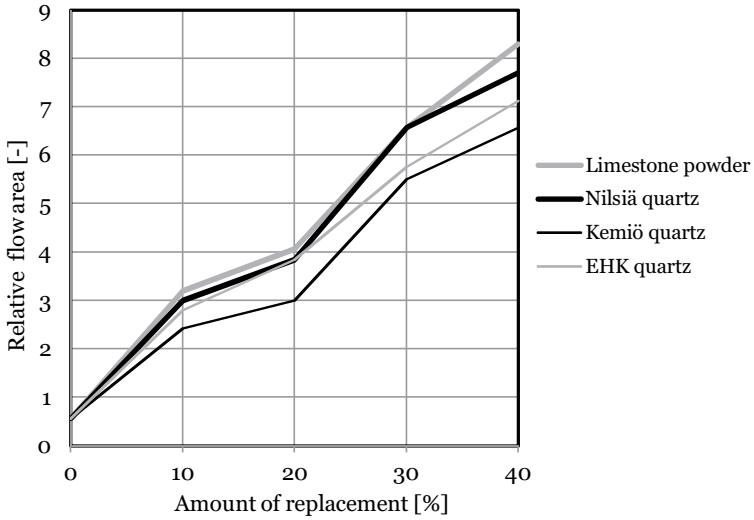

Figure 32. Relative flow area of the cement pastes, plotted against the amount of replacement of cement.

For evaluating the effect of mineral powders on viscosity, the relative funnel speed ratio Rm was calculated using the equation (Okamura et al. 1995):

$$Rm = \frac{10}{t} \qquad (31)$$

in which t is the measured time for paste to flow through the funnel (sec)

The relative funnel speed is obtained from the funnel discharging time during 10 seconds; the higher the funnel speed ratio, the lower the viscosity of the cement paste. The results are presented in Figure 33.

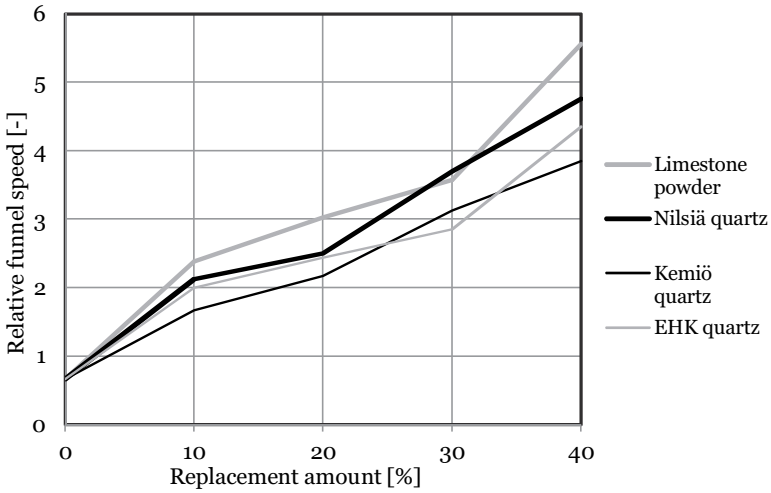

Figure 33. Relative funnel speed of the cement pastes, plotted against the replacement amount of cement.

The flow and funnel speed results were consistent with the results of the Puntke tests: adding mineral powders improved the consistency of all the pastes and the results of the limestone powder were congruent with the results of the Nilsiä quartz, as predicted by the Puntke tests. This is because in mixes with a higher packing density the fine particles replace some of the water from the voids between the coarser particles, making it available to act as an additional lubricant. At replacement levels of 10 and 20% the flow of cement pastes with limestone, EHK and Nilsiä quartz were very similar but as the replacement amount increased the differences in flow also increased. This was also observed from the water demand tests. The highest flow values and smallest funnel speeds were obtained for cement pastes with limestone powder as the substituting material.

The results also revealed that the substitution of cement with Kemiö quartz was less influential in terms of improved consistency in comparison to the other powders. This is in line with the results obtained from the water demand tests and particle size distribution analyses that the cement and Kemiö quartz have too small a discrepancy in their particle sizes and thus the increase in consistency is less effective.

The funnel speed results were mostly in compliance with the flow area results. However, variation in relative funnel speeds was observed, mainly as a result of operational error in measuring the exact start and stop times for the funnel test. Even a 0.2-second error in the start and stop times can cumulate to an error greater than one second in the calculated relative funnel speed of the cement paste. The flow test is also susceptible to operational error, but when it is

performed by the same skilled operator the results are reasonably reproducible.

Compressive strength

Using a mineral powder as a replacement for cement while keeping the water amount constant, increased the water cement ratio and thus had an effect on the strength of the pastes. Figure 34 shows the results of the 28-day compressive strength tests against the water/cement ratio. As expected, the compressive strength at the age of 28 days decreased with an increase in the w/c ratio. It seemed that the strength decreased almost linearly with increasing replacement levels, with the mineralogy of the powder having some effect on the results.

However, replacement level of 10 % had no significant unsatisfactory effect on the strength of the pastes, except for the compressive strength of paste with Kemiö quartz, which was about 4 to 5 MPa lower. In fact, using limestone powder to replace 10% of the cement increased the compressive strength of the cement paste by about 2.5 MPa compared to the reference mix P0. The measured air contents of all the pastes were 0.4 to 0.5 %. The standard deviation of the compressive strength results was, on average, 0.8 MPa.

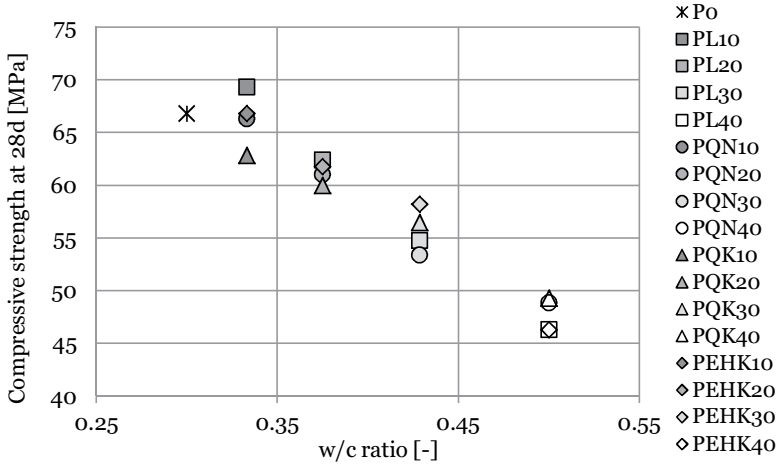

Figure 34. Compressive strengths of the test pastes at the age of 28 days.

No early-age strength gain was observed in the mixes containing limestone powder, although some investigators have reported increases in early-age strength with calcareous fillers (Gutteridge and Dalziel 1990, de Larrard 1989 and Soroka & Setter 1977). Actually, as shown in Figure 35, the replacement of cement did have some

retarding effect on the short-term (1, 2 and 7 days) strengths of the cement pastes. For the most part, using mineral powder to replace 10 to 40% of the cement retarded the strength development notably during the first 24 hours. The retardation was most substantial in the pastes with larger replacement amounts, especially in the pastes with either Nilsiä or Kemiö quartz.

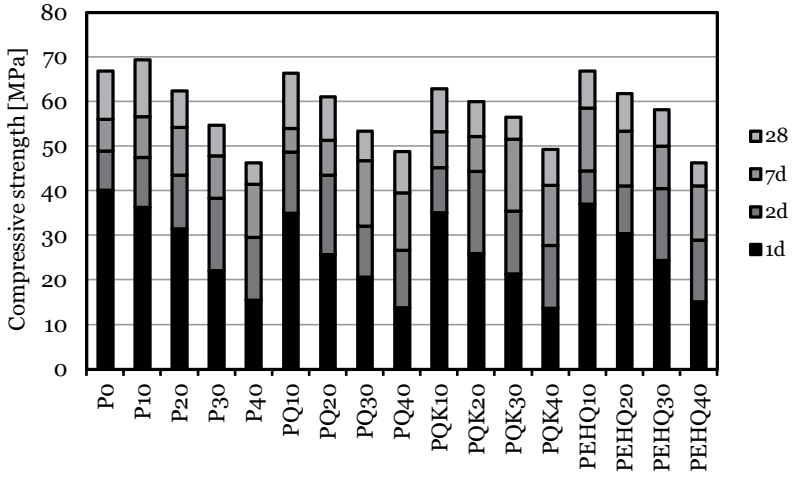

Figure 35. Strength gain at different ages

4.1.5 Discussion concerning cement paste results

The differences in relative flow areas and funnel speeds caused by different fillers, as presented in Figure 32 and Figure 33, can be assumed to be caused by differences in the physical and surface chemical features of the fillers. The physical characteristics include particle size distribution and the shape and roughness of the particles, while the surface chemical properties are subject to the mineralogy of the particle. Statistical analysis of the results showed a negative correlation between the measured water demand and the measured relative flow area of a cement paste, i.e. a reduction in water demand caused an increase in the relative flow area, as presented in Figure 36.

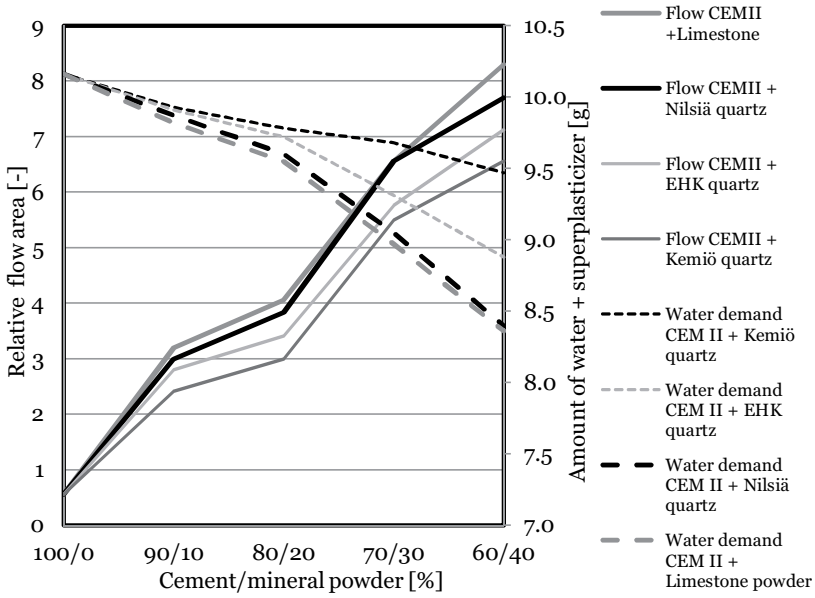

Figure 36. Relative flow areas and water demands of pastes plotted against cement/mineral powder ratio.

The different powders induced different effects on the consistency of the cement paste. As described earlier, the effect of mineral powders on viscosity can be evaluated by means of the relative funnel speed ratio Rm and the relative flow area ratio Γm, which represents deformation of the cement paste. The limestone powder had a larger Rm value for the same Γm value than the other powders, i.e. the limestone powder had the strongest viscosity-reducing effect on the cement pastes. An interesting observation was also obtained by studying the results of the Kemiö and EHK quartz. According to the results, the Kemiö quartz produced a greater viscosity-reducing effect than the EHK quartz.

Reducing the cement content reduced the strength of almost all of the cement pastes. However, replacing cement also reduced the water requirement in all of the mixes, especially in the cement pastes produced with limestone powder. Thus, according to the results, compensation for the loss of strength would be possible through reduction of the water content while maintaining the same workability of the mix.

4.1.6 Conclusions of the initial laboratory studies of cement paste

The effects of different mineral powders on water demand, consistency and strength were investigated. The following conclusions can be drawn:

- the use of mineral powders seemed to reduce the water demand of all the cement and mineral powder combinations, and in general the measured water demands were lower for CEM II than for CEM I. The effect was the most pronounced when CEM II and limestone powder with replacement amounts of 30 to 40 per cent were used;
- as a result of the lower water demand, the cement paste flow and funnel speed values increased when mineral powder was used to replace cement and the amount of water was kept constant;
- the results of the consistency tests exhibited good correlation with the results of the Puntke tests;
- in general, the replacement of 10% of the cement did not significantly impair the strength of the pastes but greater substitutions of cement reduced the strength almost linearly.

According to the preliminary laboratory test results on the cement pastes, the reduction of the cement content in concrete may be possible by substitution with inert powder. However, at the same time the water content also needs to be lowered since the non-hydraulic powder cannot compensate for the total strength loss.

The results from the Puntke tests and experiments with cement paste were used in the second part of the experimental tests – the full-scale concrete tests, which focused on the mix design optimisation of mineral powder concretes. Using the results from the initial laboratory studies, the optimisation procedure included a combination of strength and rheology in normal-strength mineral powder concretes, as well as quantitative recommendations for suitable mineral powder contents.

CEM II was chosen for the second part of the experiments in accordance with the results described in the previous sections. In addition, on account of ecological and economic factors there is a clear trend towards the use of blended cements all over Finland and the rest of Europe, which was also taken into account. Also according to the preliminary laboratory test results, limestone was chosen as the major powder to replace cement. However, no powder was discarded at this point of the research.

4.2 Mix design optimisation of mineral powder concretes

On the basis of the results of the preliminary laboratory studies, over 70 mix compositions with different mineral powders and superplasticisers were produced in the laboratory. Mix compositions with binder contents ranging from 250 kg/m^3 to 340 kg/m^3, mineral powder contents from 0 to 265 kg/m^3 and amounts of superplasticiser of about 0.4% of the total amount of fines (cement + mineral powder) were used. Limestone powder was used as the main powder substituting for cement but compositions with quartz powders were also produced. All the mix compositions are presented in Appendix 1. A detailed description of the materials and test methods used can be found in the chapter titled "Materials and methods".

The purpose of the second part of the research was to quantify the effects of mineral powders on fresh concrete properties and strength. Eventually, the main goal was to develop general mix design rules for normal-strength concretes containing mineral powders. A particle packing model, grading curves and statistical analysis were used. In conclusion, the effects of different factors on the consistency and the strength of the concrete were estimated.

4.2.1 Results of fresh concrete properties

Consistency

As a result of increasing amounts of inert mineral powder being used to replace part of the cement, the workability of the concretes improved. Table 12 presents the flow values of "lean" concrete mixes with 250 kg to 265 kg of cement in one cubic metre of concrete. The influence of the amounts of powder on the consistency was the most substantial feature of these test mixes. The concretes R1-R5 are reference concretes, i.e. they did not contain any mineral powders. Slump values, represented by a dash (-), denote that no slump was obtained or the test resulted in a collapsed slump cone, since the concrete was highly flowable.

Table 12. Workability of concretes containing 250-265 kg/m3 of cement.

Name	Cement [kg]	MP [kg]	Type of powder	Water [kg]	SP [%]	Air [%]	Flow [mm	Slump [mm]
R1	265	0	-	185	0.38	2.4	200	30
R2	265	0	-	185	0.43	2.9	200	30
R3	265	0	-	195	0.43	1.9	200	110
R4	265	0	-	185	0.53	2.7	200	40
R5	265	0	-	180	0.53	2.8	200	10
C25L7	250	175	Limest.	175	0.47	2.6	325	90
C25L6	250	145	Limest.	171	0.41	3.2	275	60
C26L60	262	152	Limest.	158	0.48	2.4	370	130
C26L3	265	80	Limest.	170	0.58	1.9	300	60
C26L45	265	119	Limest.	169	0.47	3.2	300	120
C26L61	265	153	Limest.	169	0.47	2.8	300	120
C26L62	265	159	Limest.	185	0.33	2.0	435	-
C26N60	265	159	Q. Nilsiä	185	0.38	2.4	415	-
C26K6	265	159	Q. Kemiö	185	0.44	2.3	435	-
C26L63	265	159	Limest.	185	0.38	2.6	470	-
C26N61	265	159	Q. Nilsiä	185	0.47	1.5	525	-
C26EHK6	265	159	Q. EHK	185	0.43	1.8	575	-
C26L65	265	159	Limest.	185	0.47	0.9	510	-
C26L35	265	95	Limest.	185	0.33	1.7	430	-
C26K4	265	95	Q. Kemiö	185	0.33	2.4	470	-
C26EHK3	265	80	Q. EHK	185	0.46	1.1	505	-
C26L8F0	265	205	Limest.	185	0.40	2.3	400	-
C26L66	265	165	Limest.	185	0.47	2.5	455	-
C26L80	265	215	Limest.	185	0.47	1.6	540	-
C26L95	265	250	Limest.	185	0.46	2.6	455	-
C26L31	265	80	Limest.	185	0.58	1.3	430	140
C26L32	265	80	Limest.	185	0.20	3.6	300	50
C26L33	265	80	Limest.	190	0.26	2.1	445	-
C26L50	265	135	Limest.	185	0.45	0.9	550	-
C26L70	265	186	Limest.	185	0.40	1.7	555	-
C26L81	265	212	Limest.	185	0.38	1.7	565	-
C26L100	265	265	Limest.	185	0.55	2.0	510	-
C26L67	265	159	Limest.	185	0.47	1.7	490	-
C26L68	265	159	Limest.	185	0.47	1.7	490	-
C26L69	265	159	Limest.	185	0.47	1.2	520	-
C26L71	265	159	Limest.	185	0.47	1.0	500	-

Increasing the superplasticiser content up to 0.53% of the total amount of powder (cement + mineral powder) did not significantly improve the consistency of the reference concretes containing only 265 kg/m3 cement and no mineral powder, but with higher SP dosages some bleeding was observed visually. Increasing the amount of water by 10 kg/m3 (composition R3) improved the slump but still

no flow value was obtained. However, when mineral powder was added to the mix, so that its proportion of the total amount of powder was about 30 to 40%, the water requirement of the mix decreased notably, i.e. the workability of the concretes improved. For example, adding 119 kg of limestone powder and reducing the amount of water to 169 kg/m^3 in a mix with 265 kg/m^3 cement (mix C26L45) generated a composition with similar workability features as in the reference mix R3 with no mineral powder and 195 kg/m^3 water; see Table 12. This complies with the results of the Puntke tests, which predicted an average water reduction of 12% with a replacement amount of 30%. By keeping the water-cement ratio constant, the addition of mineral powder increased the flow values of the test concretes by up to as much as 615 mm. All the test results are presented in Appendix 1.

The addition of mineral powder to richer concrete compositions had a similar influence on water demands as in leaner mixes. However, the effect became less significant as the cement content rose. Table 13 present results for concretes containing 322-340 kg/m^3 of cement. At these cement contents, the mineral powder concretes started to resemble self-compacting concretes when the fine material content was increased. However, the concretes were not self-compacting as such and with the increase in fine material, the amount of plasticising admixture also had to be increased.

Table 13. Workability of concretes containing 322 – 340 kg/m^3 of cement.

Name	Cement [kg]	MP [kg]	Type of powder	Water [kg]	SP [%]	Air [%]	Total ≤0,125mm [kg]	Flow [mm]	Slump [mm]
R8	340	0	-	200	0.41	3.8	420.84	425	-
R9	322	0	-	202	0.26	1.0	409.52	440	100
R10	322	0	-	202	0.31	0.9	399.13	465	-
R11	322	0	-	202	0.31	0.9	407.50	505	-
R12	338	0	-	208	0.30	1.8	421.21	440	90
R13	340	0	-	200	0.55	1.3	420.84	535	-
R14	340	0	-	215	0.41	1.6	407.23	490	-
C34L2	340	68	Limest.	200	0.54	0.8	486.41	615	-
C34EHK	340	34	Q. EHK	200	0.55	0.9	455.16	580	-
C32L21	340	100	Limest.	200	0.54	1.0	491.43	610	-
C32L30	322	100	Limest.	195	0.47	0.7	491.38	595	-
C32L31	322	100	Limest.	190	0.46	1.3	491.43	525	-

When the results are examined, it can be seen that small differences between the effects of the powders were observed. As predicted, Nilsiä quartz and limestone powders had a similar effect on the consistency of the concrete. But contrary to the results from the Puntke tests and experiments with cement paste, the concretes containing Kemiö quartz reached very similar relative flow area values. In addition, unlike in the water demand tests, the concretes

containing EHK quartz powder attained slightly higher flow values, even with a smaller amount of powder.

Attaining a sufficient amount of superplasticiser was essential because too low an amount generated excessive air (> 3.0%) and too large a dosage of superplasticiser caused bleeding, especially in the leaner mixes without mineral powder, which hindered the flow.

Admixture compatibility

Superplasticisers were an important component of this research and their use was essential to assure the compliance of the cement and mineral powder. But the need for a plasticising admixture was chosen to be kept low since the objective was to produce "ordinary" concrete. Self-compacting or otherwise high-performance concretes were excluded from the research goals. The compatibility of mineral powders and air-entraining admixtures is covered in the section titled "Frost resistance".

Admixture compatibility tests included the production of concretes using the same mix composition but with different superplasticisers. Two types of superplasticisers, both modified polycarboxylate ether types, were tested in the study. Table 14 compares the results of four different concretes with either Kollomen GE or Glenium 51 as the plasticising agent, with and without mineral powder. When the results in Table 14 are examined, it can be seen that the highest flow values were obtained in mixes containing the Kollomen GE superplasticiser. However, even with smaller amounts of plasticiser, Kollomen GE generated large (> 6%) amounts of air into the concrete mix.

Table 14. Comparison of superplasticizers Glenium (GL) and Kollomen GE (KO)

Name	SP type	Cement [kg]	MP [kg]	Water [kg]	SP [%]	Air [%]	Total ≤0,125mm [kg]	Flow [mm]
R14	GL	340	0	215	0.41	1.6	407.23	450
R15	KO	340	0	215	0.41	8.1	407.12	630
C34L30	KO	340	100	200	0.35	7.3	495.3	650
C28L35	KO	283	100	180	0.31	7.0	451.6	440
C29L31	KO	293	88	185	0.39	6.3	448.6	615
C29L30	GL	293	88	185	0.42	1.9	448.6	480

4.2.2 Concrete strength

Mineral powders mainly had a positive effect on the strength of the concrete. As expected, the compressive strength decreased with an increase in the w/c ratio, as can be seen from Figure 37. But in general the mineral powder concretes reached higher compressive

strength results than the reference concretes at the same (water + air)/cement ratio.

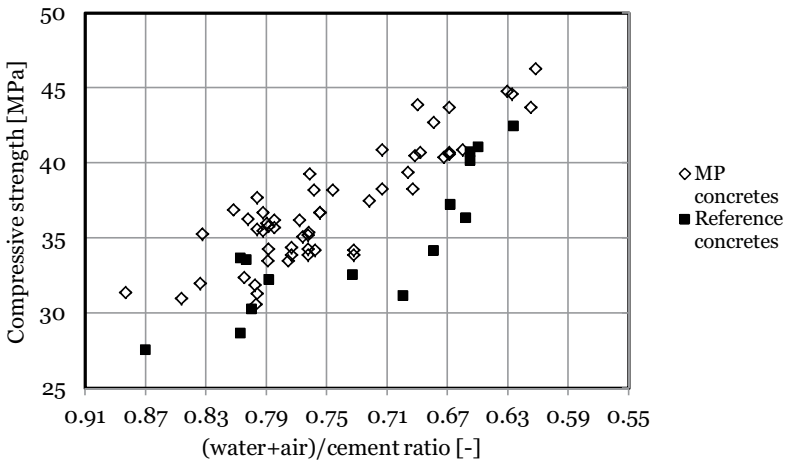

Figure 37. Compressive strengths of concretes with and without mineral powders at the age of 28 days.

When Figure 37 is examined carefully, it can be seen that the effect of the addition of mineral powder itself on the strength of the concrete is apparent, but nevertheless only minor, at about 0 to 5 MPa on average. This increase in strength could be due to heterogeneous nucleation. Lawrence et al. (2003 and 2005) and Cyr et al. (2005 and 2006) studied the influence of mineral admixtures in mortars and accounted for the strength increase caused by inert powders by the physical effect of the mineral admixture, i.e. heterogeneous nucleation in which the surfaces of the mineral powder act as nucleation sites for the early reaction products of CH and C-S-H (see the section titled “Studies of inert mineral powders in concrete”).

However in the present study, the addition of mineral powder also led in most cases to a decrease in the water demand, which resulted in increased workability. In other words, the effect of mineral powders on the strength of the concrete can be considered to consist of cement reduction, heterogeneous nucleation and water reduction. Figure 38 presents the compressive strength results of lean concrete mixtures with 265 kg/m^3 of cement and 185 kg/m^3 of water and with and without mineral powders, plotted against the relative flow area ratio Γ_m. In the case of mineral powder concretes the increase in workability was clear and flow values over three times higher than in the reference mixes were observed. Thus, by the addition of mineral powder to a mix, the amounts of cement and/or water could be lowered in order to obtain the same consistency and strength results as in the reference concrete mixtures.

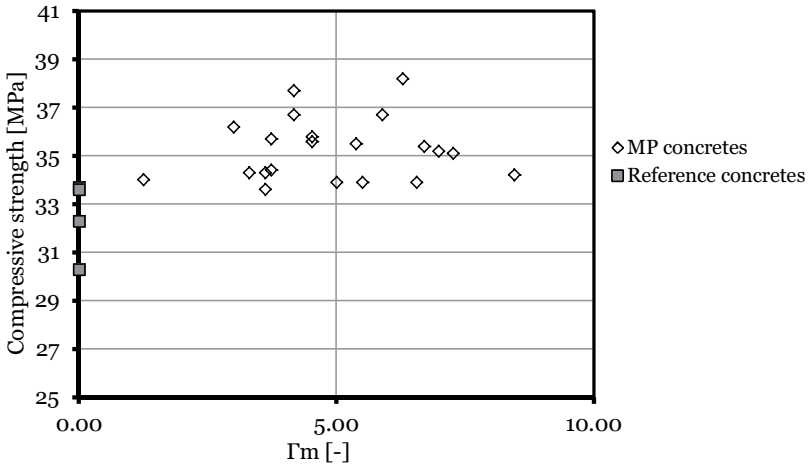

Figure 38. Compressive strengths of reference and mineral powder concretes with 265 kg/m³ of cement and 185 kg/m³ of water, plotted against relative flow area ratio Γ_m.

This effect is demonstrated in Table 15, in which the reference concrete R3 has been modified so that the amount of water is reduced by 12% and limestone powder is added to the concrete mix. This resulted in an increase in strength of about 10 MPa (C26L45). As a result of adding limestone powder and reducing both the water and cement contents, the difference in strength decreased (reference concrete R4 and mineral powder concrete C25L6).

Table 15. The plasticising effect of the addition of limestone powder.

Name	Cement [kg]	MP [kg]	Water [kg]	SP [%]	Air [%]	Total ≤0,125mm [kg]	Flow [mm]	Slump [mm]	Compressive strength [MPa]
R3	265	0	195	0.34	1.9	364.0	200	110	28.7
C26L45	265	119	169	0.47	3.2	453.3	300	120	39.3
R4	265	0	185	0.43	2.7	364.0	200	40	30.3
C25L6	250	145	171	0.41	3.2	469.1	275	60	36.9

Unlike in the results with the cement pastes, the use of mineral powders seemed to increase the early-age strength of the concretes. However, no specific distinction between the effect on early-age strength between the limestone powder and the quartz powder concretes was observed. Conversely, larger amounts of superplasticiser retarded the early-age strengths but this effect was, for the most part, compensated for by the addition of mineral powder since the micrometer-sized mineral particles act as nucleation sites for hydrates such as calcium silicate hydrates (C-S-H) (Soroka and Stern (1977), Bonavetti et al. (2000), Ezziane (2010)).

In addition to slightly higher flow results, the concretes made with EHK quartz powder also attained somewhat greater compressive strengths than the concretes with the other mineral powders. No statistical differences in strengths between the limestone, Nilsiä quartz and Kemiö quartz powders were observed.

The C26L65, C26L67, C26L68, C26L69 and C26L71 concretes were all cast with an identical mix design but on different dates. This was done in order to establish natural variation in the results. The flow and strength test results are presented in Table 16. The flow results and 28-day strength results of the concretes varied by ± 15mm and ± 1.4 MPa, respectively.

Table 16.Flow results and compressive strength data of concretes used to formulate the natural variation in the results.

Name	Air [%]	Flow [mm]	Γm	Compressive strength 1d [MPa]	Compressive strength 7d [MPa]	Compressive strength 28d [MPa]	Compressive strength 91d [MPa]
C26L67	1.7	490	5.00	9.0	26.6	33.6	38.9
C26L68	1.7	490	5.00	11.7	29.2	35.9	40.6
C26L69	1.2	520	5.76	10.9	28.8	36.1	42.0
C26L71	1.0	500	5.25	11.0	30.3	36.4	41.9
C26L65	0.9	510	5.50	10.0	28.3	34.2	41.9

4.2.3 Discussion

The results showed that cement could be partially replaced by mineral powders by utilising the water reduction effect of the addition of mineral powder. Figure 39 plots the relative flow area ratios Γ_m with the required amounts of water for the mineral powder and reference concretes. Since there were large deviations in the consistencies of the concrete, mainly because of the different amounts of cement and mineral powder, the observation of the quantity of the water reduction becomes more difficult. On average, the addition of mineral powder reduced the amount of water needed by 20 litres/m^3 concrete.

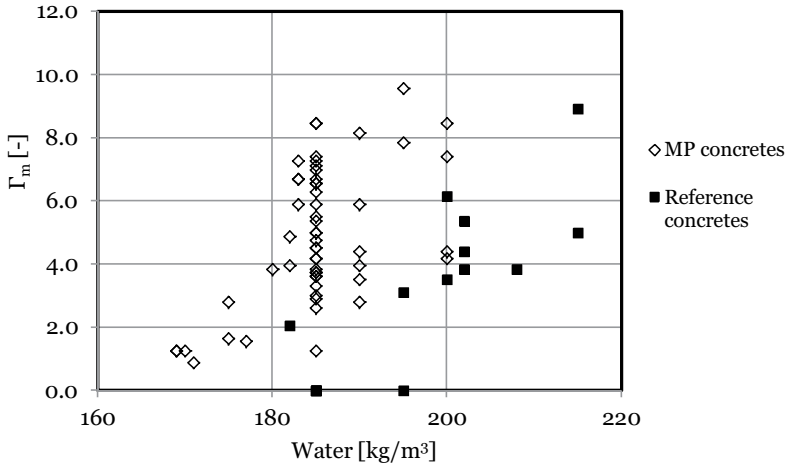

Figure 39. Relative flow area ratios (Γ_m) of reference and mineral powder concretes plotted against amounts of water utilised.

The higher the initial amount of cement was, the greater the cement reduction. Table 17 displays groups of concretes with similar workability and strength with and without mineral powders. Cement reductions of up to 75 kg/m^3 were observed. However, cement reduction amounts of 15 to 47 kg/m^3 were more common.

Table 17. Comparison of concretes with and without mineral powders with similar workability and strength.

Name	Cement [kg]	MP [kg]	Water [kg]	SP [%]	Air [%]	Total ≤0,125mm [kg]	Flow [mm]	Slump [mm]	Compressive strength 28d [MPa]
R13	340	0	200	0.55	1.3	420.84	535	-	42.5
C29L32	293	98	183	0.41	1.4	459.76	555	-	42.4
C29N31	293	98	183	0.41	1.6	459.76	555	-	42.7
R5	265	0	185	0.43	2.8	364.01	200	40	33.6
R3	265	0	195	0.34	1.9	363.97	200	110	28.7
C25L7	250	175	175	0.47	2.6	494.56	325	90	36.3
C25L6	250	145	171	0.41	3.2	469.10	275	60	36.9
R6	300	0	195	0.50	2.5	388.54	405	-	30.6
C26L33	265	80	190	0.20	2.1	412.61	445	-	31.3
C26L35	265	95	185	0.33	1.7	428.75	430	-	34.3

Increasing the mineral powder content had a greater effect on the water demand of the concrete than directly on the strength. The direct strength gain resulting from the chemical activation of the hydration of the cement, presumably via heterogeneous nucleation, was, on average, 0 to 5 MPa. Increasing the amount of mineral powders enhanced the nucleation effect since the probability of nucleation sites being near cement particles grew with the amount of

foreign particles in the concrete. But after the addition of about 20 to 30% no increases in the strengths as a result of nucleation were observed. Table 18 presents the results for concretes with 340 kg/m3 cement and 200 kg/m3 water.

Table 18. Test results on concretes with 340 kg/m3 cement and 200 kg/m3 water.

Name	Cement [kg]	MP [kg]	Water [kg]	SP [%]	Air [%]	Total ≤0,125mm [kg]	Flow [mm]	Compressive strength 28d [MPa]
R13	340	0	200	0.55	1.3	420.84	535	42.5
C34EHK	340	34	200	0.55	0.9	455.16	580	44.7
C34L2	340	68	200	0.54	0.8	486.41	615	46.3
C32L21	340	100	200	0.54	1.0	491.43	610	46.5

Furthermore, an increase in the fineness and specific surface area of a mineral admixture enhances the effect of heterogeneous nucleation, since the decrease in particle size favours nucleation. The effect was especially seen in the higher compressive strength values obtained with the EHK quartz powder. Figure 40 compares the compressive strength and flow results of different mineral powder concretes all containing the same amount of cement, water, mineral powder and superplasticiser.

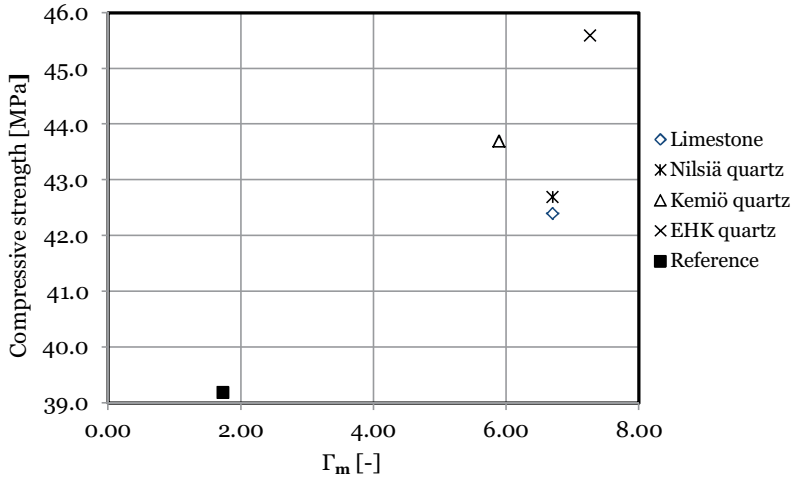

Figure 40. Compressive strength results plotted against Γ_m of concretes containing 293 kg/m3 cement, 183 kg/m3 water and 98 kg/m3 mineral powder. The reference concrete does not contain any mineral powder.

Contrary to the preliminary test results with the cement paste, the concretes made with the finer EHK quartz obtained slightly higher strength and flow table test results. The main reason for this discrepancy in the results could be the greater amounts of fine material in the concrete, such as the fine natural sand and the rock

dust originating from the coarse aggregate, which altered the grading and packing of the fine material under the sieve passing value of # 0.125 mm.

4.2.4 Modelling the effects of mineral powder concretes on concrete properties

One aim of this research project was to gain a better understanding of the basic features affecting the consistency and strength of mineral powder concrete and to quantify the combined effects of these factors. Particle packing models were used to predict the water demands of mixtures of cement paste and concrete with varying results.

Jones and his co-workers (Jones et al. 2002) compared four particle packing models on their suitability to predict a minimum voids ratio. They concluded that each model could be used to calculate the minimum voids ratio and that they all gave broadly the same output and suggested similar combinations when the mean size of the two particle groups was similar. In other cases the models appeared to be less suitable. In addition, the packing degree tended to be overestimated by LPDM (Stovall et al. 1986), whereas it was underestimated by the CPM (de Larrard 1999). According to Jones et al. (2002), the Modified Toufar model (Toufar et al. 1976 and Goltermann et al. 1997) showed the best agreement with the experimental data. However, the calculation procedures of the Toufar model are not suitable for being expanded to a large number of size classes, which would be needed for the design of mineral powder concretes. Fennis (2011) found that by modifying the Compressible Packing Model (CPM), the model could be adequately used to calculate the optimal packing densities of mixtures to be used in concretes with reduced amounts of cement. On the other hand, Kronlöf (1997) came to the conclusion that the Linear Packing Density Model (LPDM) was not suitable for estimating the water requirement of concrete.

In general, the problem with packing models is that they estimate the water requirement of compact mixes, which are, in fact, non-workable compositions. The amount of water needed to transform a mix so that it is workable varies from mix to mix, depending on factors such as the composition of the concrete and the preferred workability. In addition, almost all packing models require the measurement of the packing density of each individual material, for which there are no standardised methods. In particular, the experimental determination of the packing densities of fine powders depends heavily on the amount and method of compaction, as well as on the admixtures used to prevent agglomeration and flocculation of the fine particles.

For these reasons, the decision was made to study the elements affecting the properties of mineral powder concretes and the quantification of these factors by generating a statistical model to quantify the effects of the addition of powder on the flow and compressive strength of the concrete. The use of a particle packing model to account for the effect of water reduction and to find an optimal amount of powder was not studied.

Formulation of a statistical model

The effects of the mineral powders on the water demand and strength of concrete were analysed statistically using the Statgraphics Plus software. The most influential variables were first determined using linear regression by means of 11 predictor variables:

- amount of water, cement, mineral powder, superplasticiser and aggregate (crushed and total amount) in kg/m^3
- air content measured by the pressure method (%)
- water/cement ratio
- total amount of material passing through the # 0.125-mm sieve (kg/m^3)

In addition, new parameters termed H_p and H_v were introduced, in which H_p and H_v are fineness moduli calculated from grain sizes from 1 μm to 0.125 mm in weight fraction or by volume, respectively. The specific calculation of the parameters H_p and H_v is described in detail in Appendix 2.

In addition, the significance of each parameter and their interactions in the models were defined using the analysis of variance (ANOVA). The F-tests in the ANOVA chart identified the significant factors and the p values determined the statistical significance of each factor and their interactions in the models. This was done to determine whether the models could be simplified. The t-test was performed for all possible predictor variables. The results showed that in some cases $p > 0.05$, which indicated that there was not enough evidence to reject the null hypothesis for those particular cases at the confidence level of 95%.

According to the results obtained from the fitting of various multiple regression models to describe the relationship between the flow and the predictor variables, the most influential variables to model the flow were the amounts of water, cement, mineral powder and air, as well as the parameter H_p.

After the most relevant variables had been defined, several models were constructed with an alternating amount of variables by nonlinear regression. The most suitable equation to model the relative flow area ratio was chosen:

$$\Gamma_m = a + b \cdot \left[\left(\frac{C}{H_p} \right)^c \cdot \left(\frac{W}{A} \right)^d \cdot H_p^e \right] \qquad (32)$$

in which

C is the cement content [kg/m³]

H_p is the fineness modulus in weight fraction

W is the water content [kg/m³]

A is the air content [%]

and a, b, c, d and e are constants.

The R^2 statistic indicates that the model as fitted explains 77.9% of the variability in the flow table test values. Table 19 presents the values for the constants a, b, c, d and e. Figure 41 displays the observed flow values versus the predicted values.

Table 19. The model constants of Equation (32).

a	b	c	d	e
-463.39	396.87	0.007	0.006	0.03

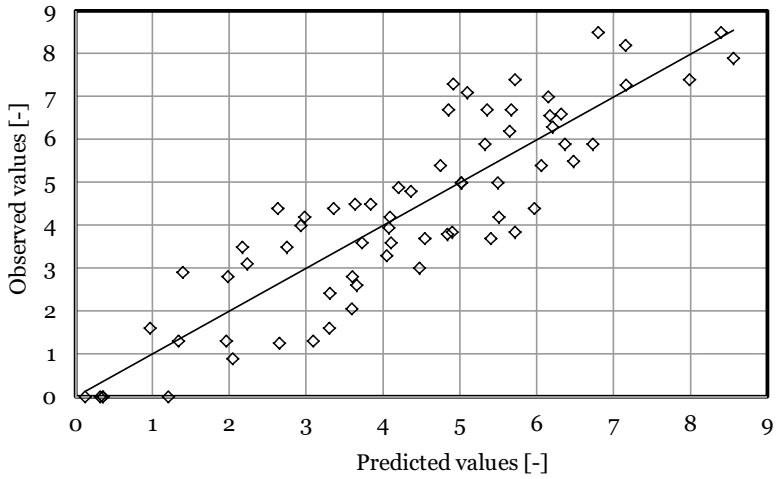

Figure 41. The predicted versus the observed values of relative flow area ratio of Equation (32).

The Durbin-Watson (DW) statistic, which tests the residuals to determine if there is any significant correlation based on the order in which they occur in the data file, was greater than 1.4. This means that according to the DW statistic, there was probably not any serious autocorrelation in the residuals. Figure 42 shows the residual plot of the flow model, which expresses the difference between the actual observation of the model and the estimated function values.

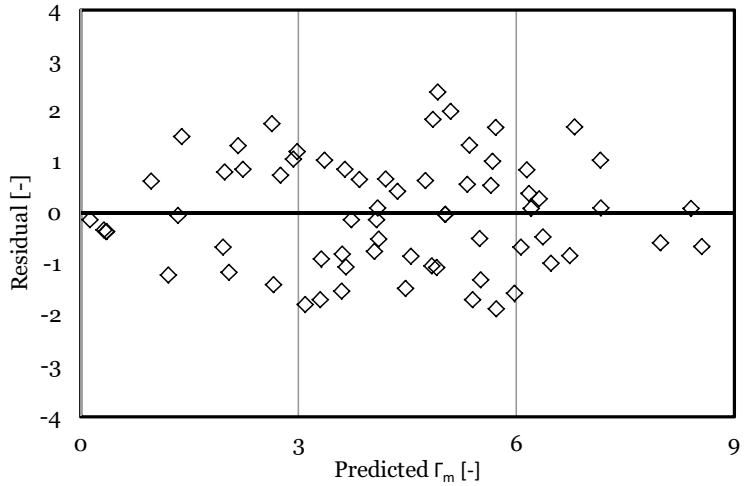

Figure 42. Residual plot of the flow model.

In addition to containing the information on the amount of fine material, the parameter H_p also takes into account the fineness of the

fine material. In other words, the H_p value also reflects the grading of the fine material. According to the model, increasing the amount of fine material (cement or mineral powder), i.e. H_p, increased the flow table test results of the test concretes. Figure 43, Figure 44 and Figure 45 present the contours of the estimated response surface of Γ_m by using Equation (32).

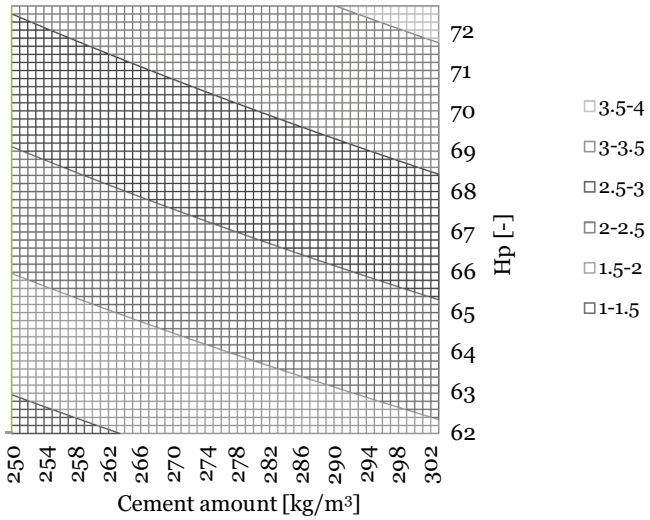

Figure 43. Contours of estimated response surface of relative flow area ratio with water content of 190 kg/m3. The defined areas represent the predicted relative flow area ratios.

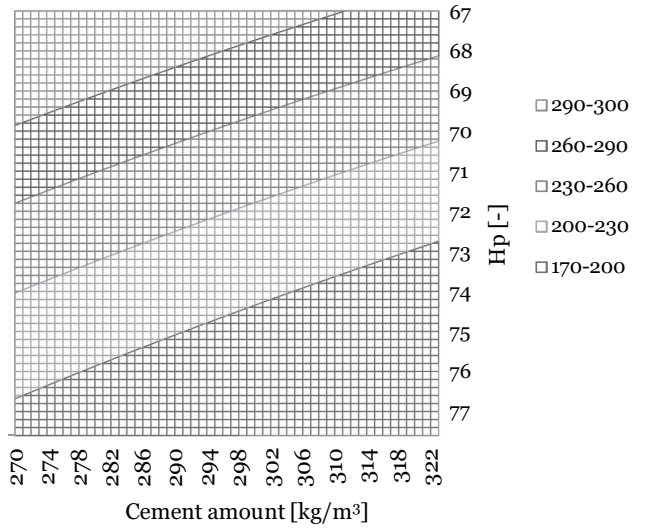

Figure 44. Contours of estimated response surface of relative flow area ratio. The defined areas represent the required water amount in kg/m3 in order to achieve relative flow area ratio of 4,0.

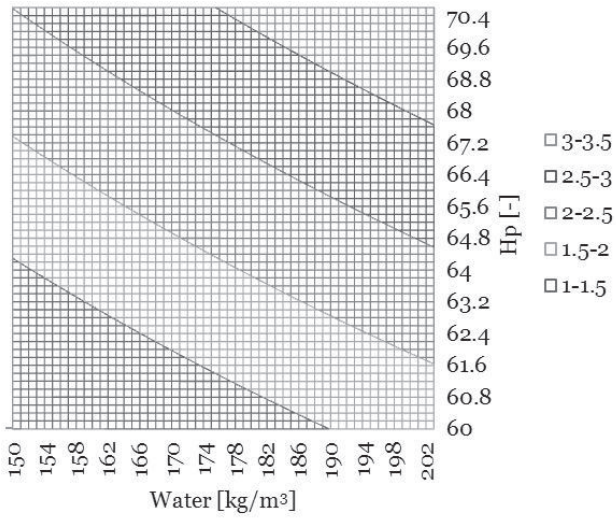

Figure 45. Contours of estimated response surface of relative flow area ratio for cement content of 265 kg/m3. The defined areas represent the predicted relative flow area ratios.

From Figures 43 to 45 the effect of increasing the amount of fine material on the predicted flow areas can be observed. Fox example, From Figure 43, it can be seen that increasing the amount of fine material (increasing H_p) while keeping the amount of water constant increased the flow table test results of the concretes. In other words, with cement amount of 290 kg/m3, increasing H_p from a value of 62 to 67, increases the predicted relative flow area ratio from 1.5-2 to 2.5-3. In all the figures the amount of air is kept constant at 2,5 %.

The R^2 statistic of the model of 77.9% can be considered to be satisfactory, taking into consideration the diversity in the amounts and types of powders and the different amounts of superplasticiser in the concrete compositions.

The strength of the concrete at 28 days was modelled in the same manner as the flow. The most influential variables to model the strength were found to be the amounts of cement, water, mineral powder and air. Several models were also constructed for compressive strength with an alternating amount of variables by nonlinear regression. The best nonlinear regression model of the compressive strength results was formulated as:

$$f_c = a + b \cdot \left[\left(\frac{P + C}{C} \right)^c \cdot \left(\frac{W}{C} \right)^d \cdot \left(\frac{W}{A} \right)^e \right] \qquad (33)$$

in which

P is the mineral powder content [kg/m^3]

C is the cement content [kg/m^3]

W is the water content [kg/m^3]

A is the air content [dm^3/m^3]

and a, b, c, d and e are constants

Table 20 displays the values for the constants a, b, c, d and e. The R^2 statistic indicates that the model explains 84.6% of the variability in the 28-day strength results. The DW statistic was greater than 1.4. This means that according to the DW statistic, there was probably not any serious autocorrelation in the residuals. Figure 46 presents the estimated response surface of strength by using Equation (33).

Table 20. The model constants of Equation (33).

a	b	c	d	e
21.45	1.38	0.6	3.61	0.16

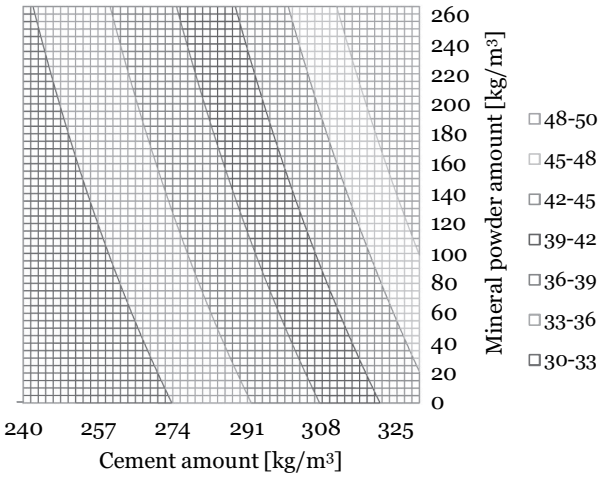

Figure 46. Contours of estimated response surface of strength. The coloured areas represent the strengths obtained with a water content of 185 kg/m^3 and air content of 2%.

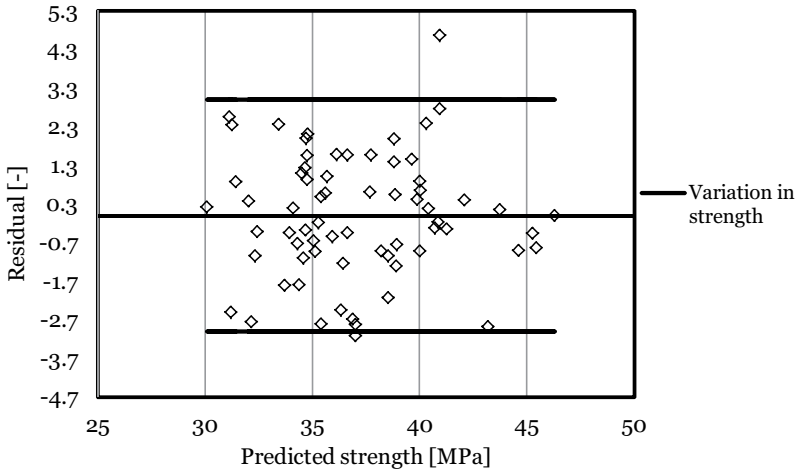

Figure 47. Residuals of the modelled strengths.

Figure 47 shows the residual plot of the strength model, which expresses the difference between the actual observation of the model and the estimated function value. From the tests with the concretes C26L65, C26L67, C26L68, C26L69 and C26L71, which were all cast with exactly the same mix design but on different dates, it was known that the strength results can vary by approximately 3 MPa. When examining the residual plot of the predicted and observed values of the strength model in Figure 47, it can be observed that nearly all of the model residuals fit inside this range of deviation and thus higher values of R^2 would be very hard to achieve. Figure 48 displays the observed values of the 28-day strengths versus the predicted values.

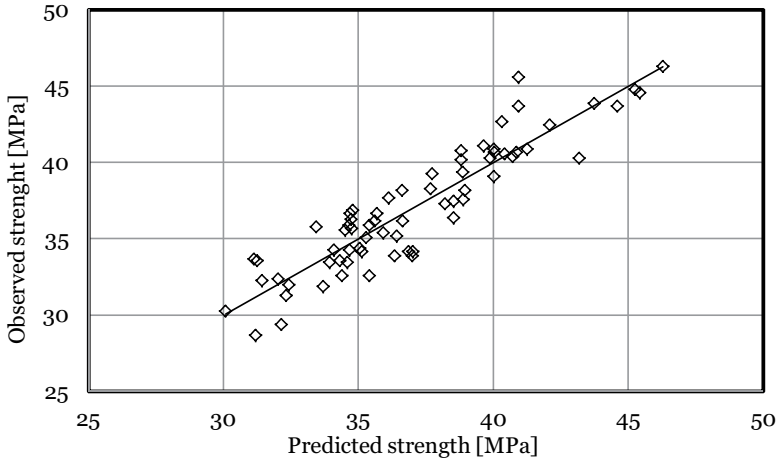

Figure 48. The predicted versus the observed values of the 28 day strengths of Equation (33)

4.2.5 Conclusions of the mix optimisation

The reduction of the cement content in concrete was possible by substitution with an inert powder by lowering the water content at the same time, since the non-hydraulic powder cannot compensate for the strength loss. It was observed that the amount of cement and mineral powder alone does not account for the changes in the flow table test results, since the fineness, and thus the combined gradation curve, also has an effect.

The following general conclusions can be drawn from the second part of the research:

- the water requirement of the concretes appeared to decrease as a result of the addition of mineral powders and therefore, the strength of the concretes was increased by reducing the amount of water compared to normal concretes possessing similar workability and in which no mineral powders were used;
- increasing the mineral powder content had a greater effect on the water demand of the concrete than directly on its strength. The direct strength gain, presumably the result of the chemical activation of the hydration of the cement via heterogeneous nucleation, was, on average, from 0 to 5 MPa. The optimum amount of mineral powder for heterogeneous nucleation was found to be about 20 to 30% of the cement content;
- the results revealed that the fineness of the mineral powders was more relevant to the strength and flow than the origin or mineral composition of the powder. Concretes made with the finer ground EHK quartz obtained slightly higher strength and flow table test results;
- the most important variables influencing the flow table test results were found to be the contents of mineral powder, cement, water and air. In general, increasing the amount of fine material in concretes also increased the flow table test values. The R^2 value of the model that was created was 78%;
- the most important variables affecting the compressive strength of mineral powder concretes were found to be the contents of mineral powder, cement, water and air. The R^2 value of the model that was created was 85%.

4.3 Frost resistance

The third part of the study focused on basic concrete properties, including freeze-thaw durability and characteristics affecting the air entrainment of inert mineral powder concretes. Frost damage was measured by means of surface scaling and internal damage. Water uptake was measured during the CIF test. The cooperation of ground granulated blast furnace slag (GGBS) with mineral powders at levels of 50% and 70% was also studied in this part of the research. All the values presented in this section are calculated as a mean value of 3 specimens measured after 14, 28, 42 and 56 cycles of freezing and thawing.

The compositions of the test concretes are given in Table 21. The amounts of mineral powder used were 0, 10 and 20%, which either replaced cement or was added to the mix without any reduction of the cement. No reductions of water were made to the concretes containing mineral powders, although the additions of the minerals increased the flow of the test concretes. This was done in order to test only the effect of the mineral powder on frost resistance. Figure 49 shows the increase in the flow of the concretes with either a cement replacement (presented as a negative value) or the addition of mineral powder (presented as a positive value). All the concretes with the same binder combination had the same amount of superplasticiser (kg/m3).

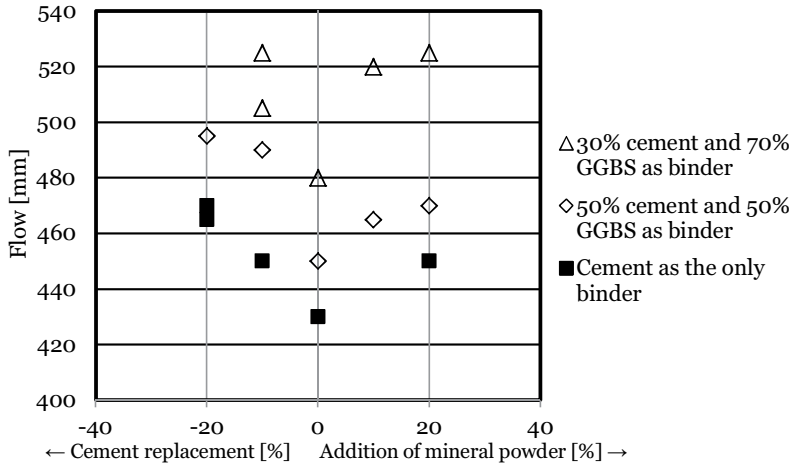

Figure 49. The effect of the replacement of cement or the addition of mineral powder on the flow of air entrained concretes.

4.3.1 Effect of mineral powders on air entrainment

All the concretes used in the freeze thaw tests were air-entrained. In order to obtain the desired 6.0% (± 0.5%) of air, an alternating amount of air-entraining admixture was used. The proportions of the

mixture for the concretes are given in Table 21. The recommended dosage for the air-entraining admixture from the supplier was 0.01 to 0.08% of cement weight but for the test concretes amounts of 0.0049 to 0.0145% of the total amount of fines (cement + blast furnace slag + mineral filler) were enough.

Fine material is known to increase the amount of admixture needed (Neville 1995) but only a marginally larger amount of air-entraining agent was needed for the concretes with a mineral addition of limestone powder or Nilsiä quartz. However, the concretes with EHK quartz, which is produced by the additional grinding of Nilsiä quartz, required a greater quantity of admixture in order to attain the desired amount of entrained air. The use of ground-granulated blast furnace slag (GGBS) reduced the air-entraining admixture requirement notably. Nearly three times less admixture was needed for the concretes containing 50% or 70% GGBS than for the concretes containing only cement as a binder. GGBS also increased the concrete flow.

In addition, the stability of the air entrainment was studied. Figure 50 presents the measured air contents of the concretes 15 and 45 minutes after the addition of water to the mix. The loss of air was greater in the concrete compositions with GGBS. In the mixes with cement as the only binder, the addition of mineral powder did not affect the stability of the entrained air. However, the concrete composition with 50% or 70% GGBS and the addition of 10% and 20% mineral powder experienced an entrained air loss of over 1%.

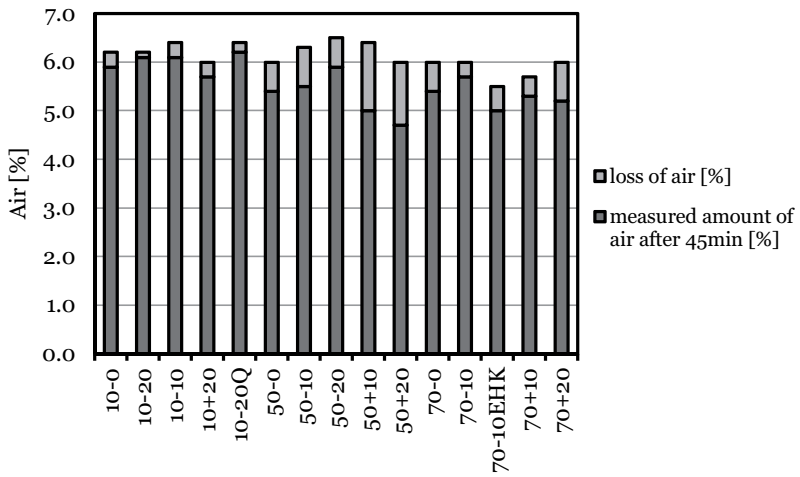

Figure 50. Loss of entrained air in the test concretes.

Table 21. Mix proportions of the test concretes.

	10-0	10-20	10-10	10+20	10-20Q	50-0	50-10	50-20	50+10	50+20	70-0	70-10	70-10EHK	70+10	70+20
Cement [kg/m^3]	330	264	297	330	264	170	153	136	170	170	102	92	92	102	102
Blast furnace slag [kg/m^3]	0	0	0	0	0	170	153	136	170	170	238	214	214	238	238
Limestone powder [kg/m^3]	0	66	33	66	0	0	34	68	34	68	0	34	0	34	68
Quartz powder [kg/m^3]	0	0	0	0	66	0	0	0	0	0	0	0	34 EHK	0	0
Aggregate [kg/m^3]	1701	1692	1696	1634	1692	1632	1628	1623	1598	1564	1632	1632	1627	1598	1564
Water [kg/m^3]	190	190	190	190	190	182	182	182	182	182	182	182	182	182	182
Superplasticizer [kg/m^3]	1.4	1.4	1.4	1.4	1.4	1.05	1.05	1.05	1.05	1.05	1.05	1.05	1.05	1.05	1.05
Air entraining-agent [kg/m^3]	0.048	0.048	0.048	0.048	0.048	0.02	0.03	0.02	0.022	0.02	0.022	0.025	0.03	0.033	0.033

Table 22. Air content, strength and scaling of the test concretes.

	10-0	10-20	10-10	10+20	10-20Q	50-0	50-10	50-20	50+10	50+20	70-0	70-10	70-10EHK	70+10	70+20
Air content [%]	6.2	6.2	6.4	6.0	6.4	6.0	6.3	6.5	6.4	6.0	6.0	6.0	5.5	5.7	6.0
Strength at 28 or 56 days [MPa]	33.4	24.5	28.0	35.0	23.8	41.2	33.7	29.3	44.2	44.9	32.9	28.2	31.6	35.9	36.1
Scaling after:															
7 d = 14 cycles [g]	1.7	1.8	1.8	0.7	1.5	0.6	1.2	1.4	0.3	0.3	1.3	1.7	1.9	0.7	0.7
14 d = 28 cycles [g]	0.9	1.8	2.2	0.9	2.4	0.9	1.4	1.7	0.6	0.6	0.9	1.3	1.7	0.7	0.9
21 d = 42 cycles [g]	0.8	2.4	3.1	1.2	2.4	1.0	1.5	2.0	1.0	0.9	1.4	2.0	2.4	1.3	1.1
28 d = 56 cycles [g]	1.0	3.1	2.0	1.5	3.4	1.1	1.7	2.0	1.2	1.0	1.6	1.7	2.4	1.4	1.2
Sum [g]	4.4	9.1	9.1	4.3	9.7	3.6	5.8	7.0	3.1	2.8	5.1	6.6	8.5	4.2	3.9
Scaling total [g/m^2]	267.8	551.4	549.6	261.1	588.7	216.2	351.5	424.2	187.1	167.5	309.7	402.6	513.1	255.2	238.2

* Concretes with 50% or 70% GGBS were tested at the age of 56 days.

4.3.2 CIF

CIF means "capillary suction, internal damage and freeze-thaw test". In the test, CIF specimens were subjected to freeze-thaw attack by using de-ionised water. A detailed description of the test procedure is given in the section titled “Materials and methods – Testing durability”.

Scaling

The freeze-thaw resistance was evaluated by the measurement of mass scaled from specimens after 14, 28, 24 and 56 freeze-thaw cycles. Table 22 and Figure 51 present the scaling results of the test concretes after being subjected to the freeze-thaw cycles. The test results showed that using mineral powder to replace cement, and thus reducing the amount of cement in the mix, increased the scaling of the test concretes during the freeze-thaw cycles. The amount of scaled material increased with cement reduction by as much as over 100%. The deterioration of freeze-thaw durability was the highest in the test concretes with cement as the only binder. The test concretes produced with 50% or 70% GGBS seemed to endure the cyclic freezing and thawing better.

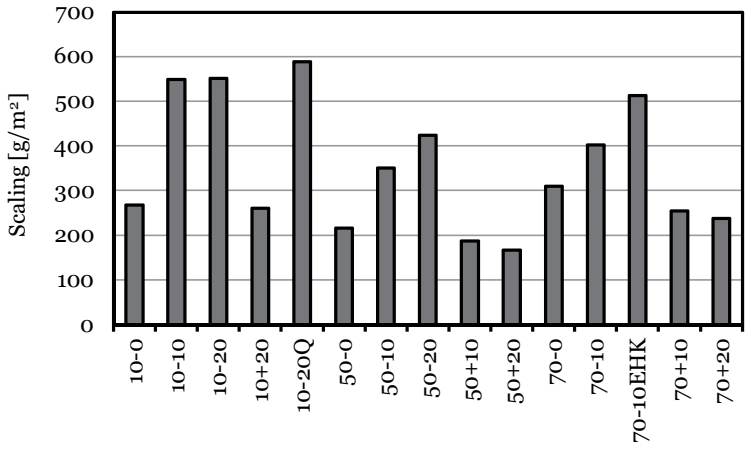

Figure 51. Scaling results measured after 56 freeze-thaw cycles.

However, adding mineral powder without cement reduction seemed to reduce the amount of scaled material slightly, especially in the compositions made with 70% GGBS as a binder. The concrete compositions with Nilsiä quartz behaved in a similar manner to the concretes with limestone powder, but using 10% EHK quartz to replace the binder produced a higher scaling, although a higher

strength was attained than in the compositions with limestone powder. In other respects resistance to freezing and thawing seemed to comply with the compressive strengths of the test concretes, as can be seen in Figure 52.

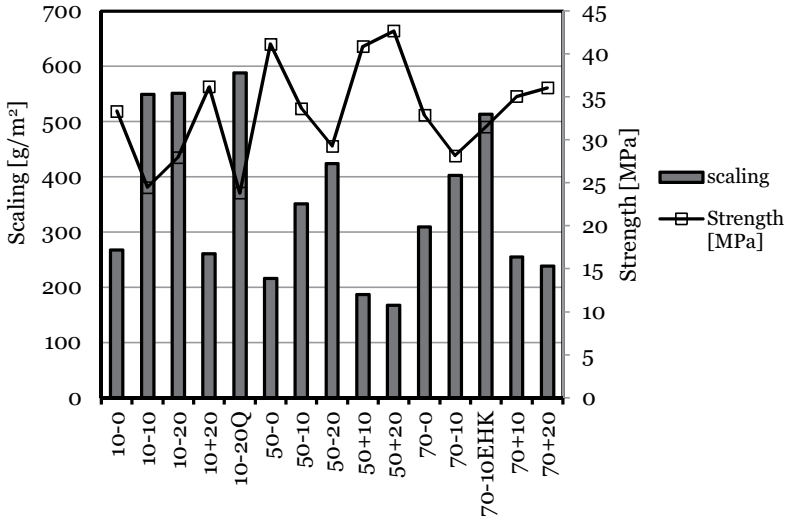

Figure 52. Freeze-thaw resistance and concrete strength.

Water uptake

Figure 53, Figure 54 and Figure 55 show the water uptake results measured during the freeze-thaw cycles of 28-day-old (with cement as the only binder) and 56-day-old (with a blend of GGBS and cement as the binder) test concretes.

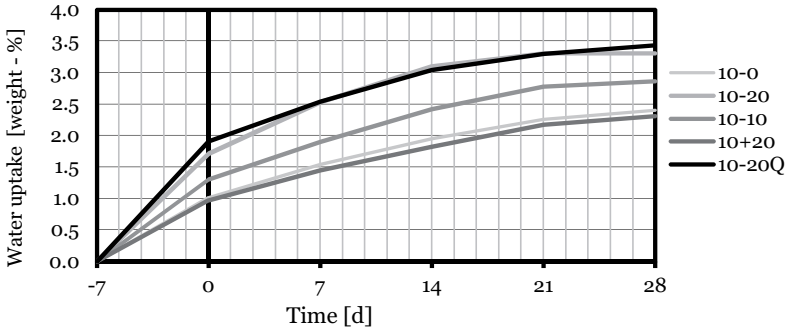

Figure 53. Water uptake of concretes with cement as the only binder. Time -7→0 = capillary suction before the freeze-thaw testing. Time 0→28 capillary suction during the freeze-thaw testing.

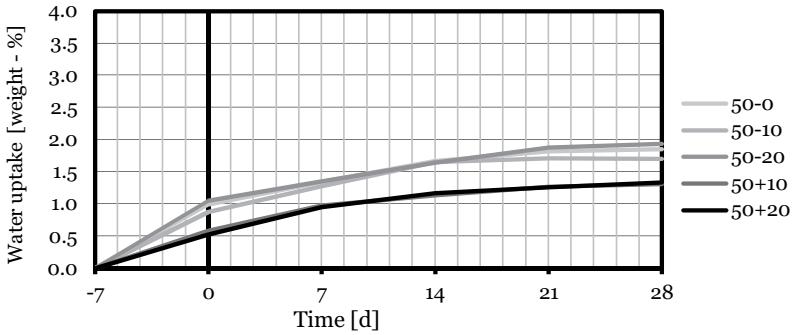

Figure 54. Water uptake of concretes with 50% cement and 50% GGBS as binder. Time -7→0 = capillary suction before the freeze-thaw testing. Time 0→28 capillary suction during the freeze-thaw testing.

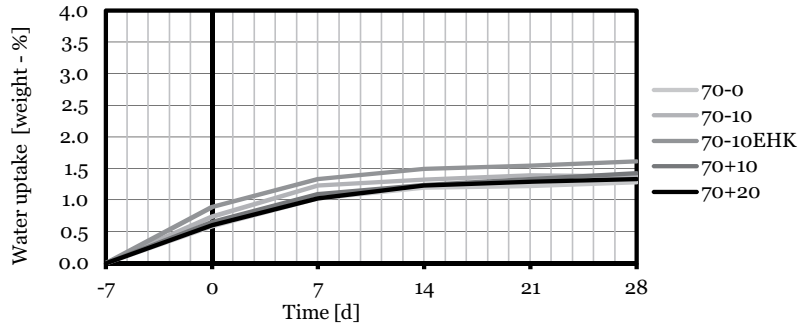

Figure 55. Water uptake of concretes with 30% cement and 70% GGBS as binder. Time -7→0 = capillary suction before the freeze-thaw testing. Time 0→28 capillary suction during the freeze-thaw testing.

The concretes with 50% or 70% GGBS became saturated during the test, i.e. the water absorption levelled out at around 21 and 14 days respectively. The smallest water uptake values were also measured for these concretes. Nearly all the test concretes with 70% GGBS reached saturation at 1.3 to 1.4 weight-%, except for the test concrete with EHK quartz powder being used to replace 10% of the binder, which reached a water uptake value of 1.6 weight-% at 28 days.

The differences between the amounts of cement replacement and mineral powder additions on the water uptake seemed more apparent for the concretes with 50% GGBS as a binder. The concretes with mineral powder added (without cement reduction) attained lower water uptake values of about 1.3 weight-%, whereas the concretes with no additions or binder replacements of 10 or 20% reached saturation levels at about 1.7 to 1.9 weight-%.

Notably higher water uptake levels were measured for concretes containing only cement as a binder. Using a mineral powder to replace cement increased the water uptake value by 19 to 43%. However, adding mineral powder without reducing the amount of cement slightly lowered the water uptake. In all, the concretes with cement as the only binder reached higher water uptake values than the concretes with GGBS and did not become fully saturated even towards the end of the freeze-thaw cycles.

Internal damage

Internal damage was studied by the relative dynamic modulus (RDM) of concrete, calculated from the ultrasonic pulse transfer time data during the freeze-thaw testing. The internal damage results are presented in Figure 56, Figure 57 and Figure 58. Contrary to scaling, the results showed insignificant internal damage values for all the test concretes, especially for concretes with cement as the only binder. In the figures the 67% line, the dashed line at the bottom of the figures, denotes the limit value for internal damage according to the Finnish concrete code (BY 50, 2004).

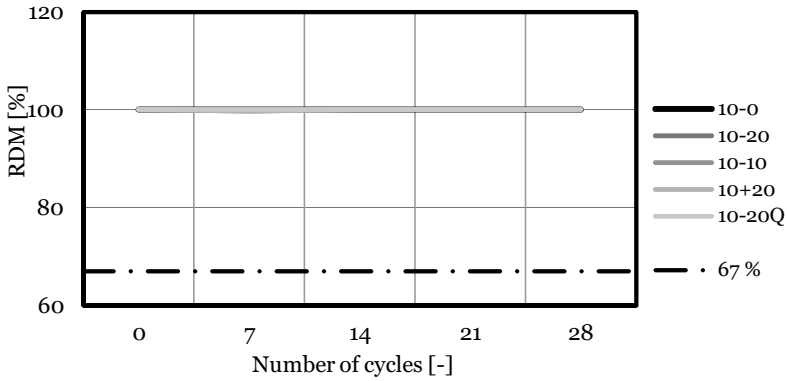

Figure 56. Internal damage (CIF) results of concretes with cement as the only binder. Note that the RDM lines run directly at the 100 % line.

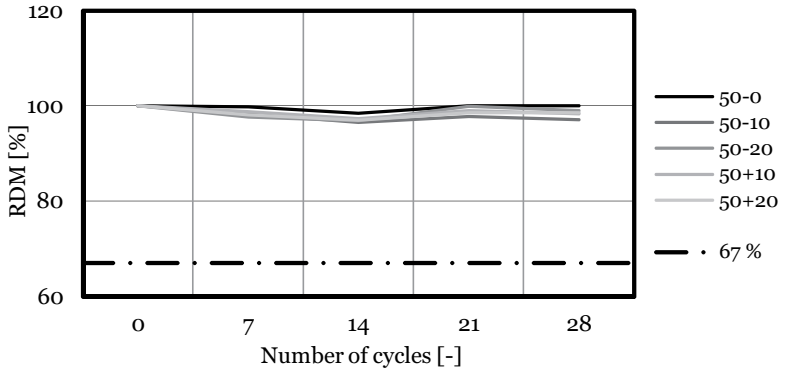

Figure 57. Internal damage (CIF) results of concretes containing 50% ground granulated blast furnace slag (GGBS) and 50% cement as binder.

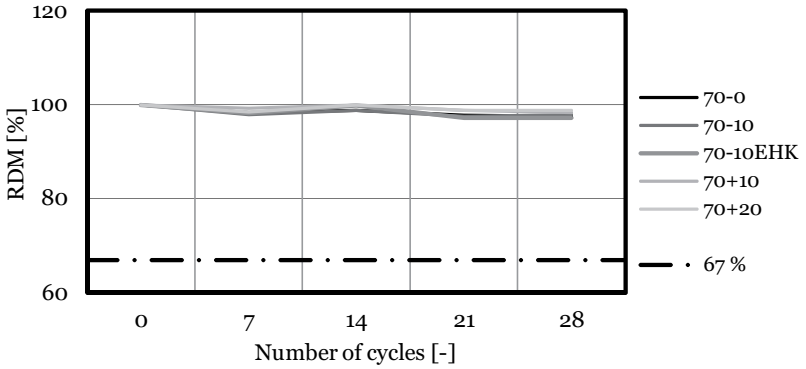

Figure 58. Internal damage (CIF) results of concretes containing 70% ground granulated blast furnace slag (GGBS) and 30% cement as binder.

4.3.3 Capillary water absorption

Figure 59, Figure 60 and Figure 61 present the results of the capillary water absorption tests versus $\sqrt{t}$.

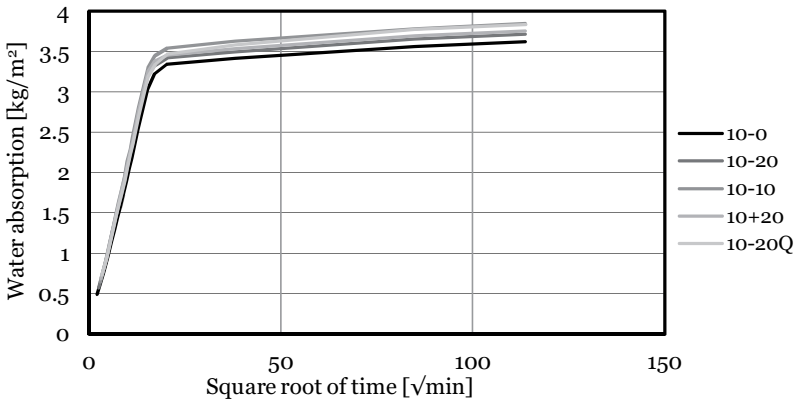

Figure 59. Capillary water absorption of concretes containing only cement as binder.

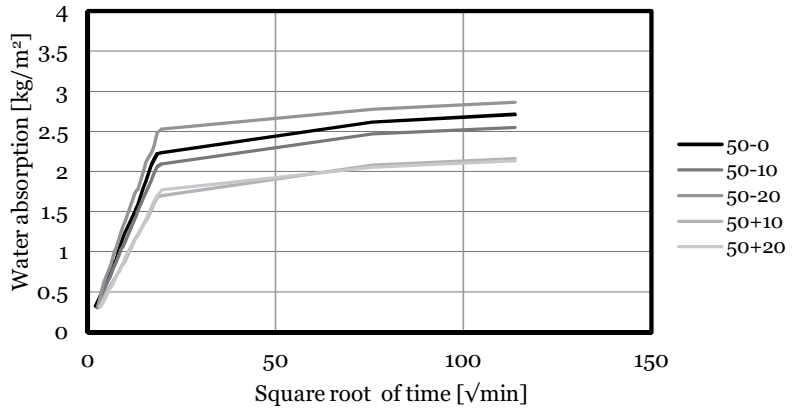

Figure 60. Capillary water absorption of concretes containing 50% cement and 50% GGBS as binder.

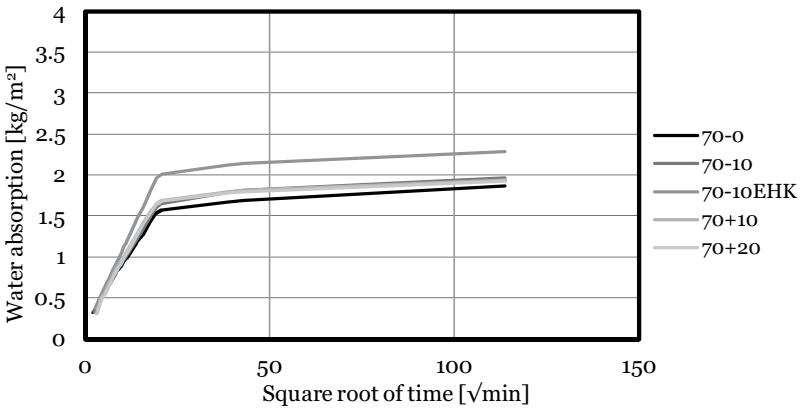

Figure 61. Capillary water absorption of concretes containing 30% cement and 70% GGBS as binder.

The capillary absorption tests gave similar results to the water uptake results during the freeze-thaw testing. The highest water absorptions were measured for the concretes containing only cement as a binder, whereas the concretes containing 50% or 70% GGBS absorbed less water. From the absorption tests the water absorption coefficient and capillary water penetration factor and the total porosity, capillary porosity and air porosity were calculated using Equations (26), (27) and (28) and are presented in Table 23.

Table 23. Total porosity (ε_{total}), capillary porosity (ε_{suc}), air porosity (ε_{air}) and the protective pore ratio ($\varepsilon_{air}/\varepsilon_{total}$), as well as the water absorption coefficients (k) and capillary water penetration factors (m) of the test concretes.

	ε_{total} [%]	ε_{suc} [%]	ε_{air} [%]	$\varepsilon_{air}/\varepsilon_{total}$	k [kg/m^{2}s$^{1/2}$]	m [s/m^2]
10-0	20.49	14.91	5.59	0.272	0.278	2.84E+07
10-10	21.03	15.38	5.65	0.269	0.280	2.49E+07
10-20	21.24	15.66	5.59	0.262	0.282	2.52E+07
10+20	20.19	15.32	4.87	0.241	0.270	2.67E+07
10-20Q	21.62	15.77	5.84	0.270	0.260	2.83E+07
50-0	16.22	10.93	5.29	0.343	0.134	3.15E+07
50-10	15.89	10.62	5.28	0.332	0.119	3.30E+07
50-20	16.89	11.68	5.21	0.308	0.145	3.47E+07
50+10	13.53	8.77	4.76	0.352	0.092	3.94E+07
50+20	13.63	8.85	4.78	0.350	0.096	3.68E+07
70-0	12.96	8.08	4.88	0.377	0.079	4.14E+07
70-10	13.26	8.45	4.81	0.363	0.083	4.42E+07
70-10EHK	14.80	9.78	5.02	0.339	0.103	4.20E+07
70+10	13.23	8.52	4.71	0.356	0.086	4.11E+07
70+20	12.59	8.13	4.46	0.354	0.086	4.04E+07

It can be seen that the total porosity and capillary porosity appeared to be related more to the choice of binder than the amount of mineral powder. According to the results, even using mineral powder to replace as much as 20% of the binder had a smaller effect on total and capillary porosity than changing the binder composition to 50% GGBS and 50% cement or 70% GGBS and 30% cement. However, adding 10% or 20% limestone powder to 50/50 GGBS/cement concrete seemed to somewhat lower the amount of capillary porosity. Figure 62 plots the water penetration factors and capillary porosities of the test concretes. The choice of binder composition also had a greater effect on the protective pore ratio than the use of mineral powders. The calculated protective pore ratios of the GGBS concretes were higher than in the concretes made with cement as the only binder.

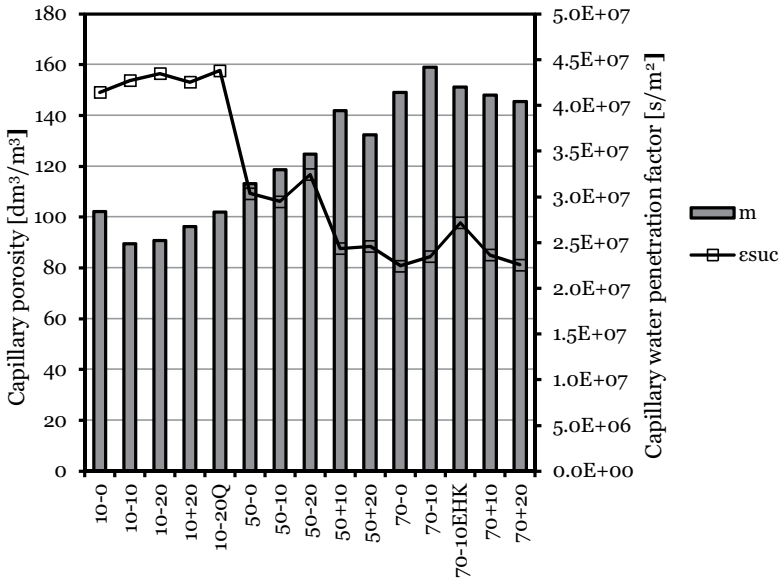

Figure 62. Water penetration factors (m) and capillary porosities (ε_{suc}) of the test concretes.

4.3.4 Discussion on frost resistance of mineral powder concretes

The air contents and protective pore ratios, as well as the water absorptions, of the test concretes that contained only cement as a binder were congruent with each other. Using mineral powder as a replacement for cement appeared to reduce the compressive strength and freeze-thaw resistance of the concretes. Adding mineral powder without any reduction of the cement did not have a notable influence on the freeze-thaw resistance of these concretes but it did appear to improve their compressive strength slightly.

Reductions of the amount of binder also increased the scaling of the test concretes with 50% or 70% GGBS as a binder but not as much as in the concretes made with only cement as a binder. However, the results suggest that adding mineral powder without reducing the amount of binder might somewhat improve the freeze-thaw resistance of the concretes. The slight improvement could also be noticed in compositions where the addition of 10% and 20% mineral powder increased the amount of lost air. As can be seen from Figure 63, the freeze-thaw resistance appeared to be influenced by the water absorption of the concretes during testing to some extent.

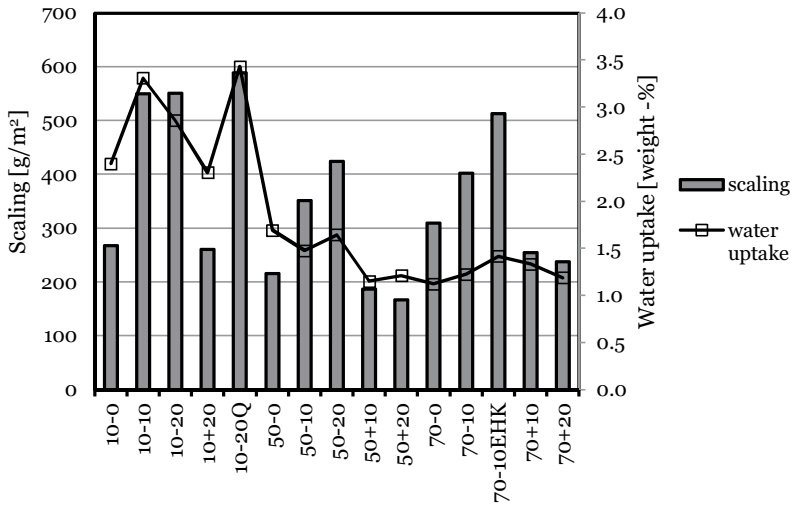

Figure 63. Scaling in relation to the measured water uptake.

One reason for the better freeze-thaw resistance of the GGBS concretes might be the greater age at which the freeze-thaw testing commenced. The compressive strengths of the concretes containing GGBS were higher than those of the concretes containing only cement as a binder. The measured water absorptions of the GGBS concretes were also lower and the water penetration factors (m) higher than in the concretes containing only cement as a binder. This could also be a result of the delayed testing time (56 vs. 28 days) and thus explain the better freeze-thaw resistance. However, the scaling results of the reference concrete containing 70% GGBS and 30% cement without mineral powders were higher than those of the reference concrete containing only cement as a binder. Although the compressive strength was similar and the water penetration factor was higher in the GGBS concrete, it could be that the slower reaction rate of GGBS hindered the frost durability.

In general, the reduction of the amount of cement, coupled with the addition of mineral powder did not impair the freeze-thaw resistances of the GGBS concretes as much as was the case for the concretes made with only cement as a binder. However, the loss of entrained air was greater in the concretes made with GGBS. The freeze-thaw resistances of the mineral powder concretes made with crushed quartz and limestone powder were similar, although slightly larger scaling amounts were measured for the concretes containing quartz. Using finely ground EHK quartz to replace 10% of the binder increased the scaling and water absorption of the concrete, even though higher compressive strength was attained than in the reference. Unlike the scaling, the internal damage results did not indicate internal damage to the test concretes.

Of the calculated parameters, the capillary water penetration factor (m) describes the pore structure of the concrete, as does the water absorption coefficient (k), but the penetration factor is independent of the amount of paste in the concrete. For this reason it is more suitable for the comparison of different concretes. Mineral powder additions did not seem to have a notable effect on the water penetration factors. According to statistical analysis, the factors influencing the scaling of all the concretes were strength, capillary porosity, water uptake during freeze-thaw testing and the F-factor, which describes the freeze-thaw resistance of concrete in a non-saline environment according to the concrete code By50. The F-factor is calculated using Equation (34):

$$F = \frac{1}{max\left\{0{,}25\,;\,7{,}2\,\frac{(w/c)^{0{,}45}}{(a-1)^{0{,}14}} - 4{,}0\right\}} \qquad (\ 34\ )$$

Figure 64 plots the calculated F-factors and scaling of the tested concretes.

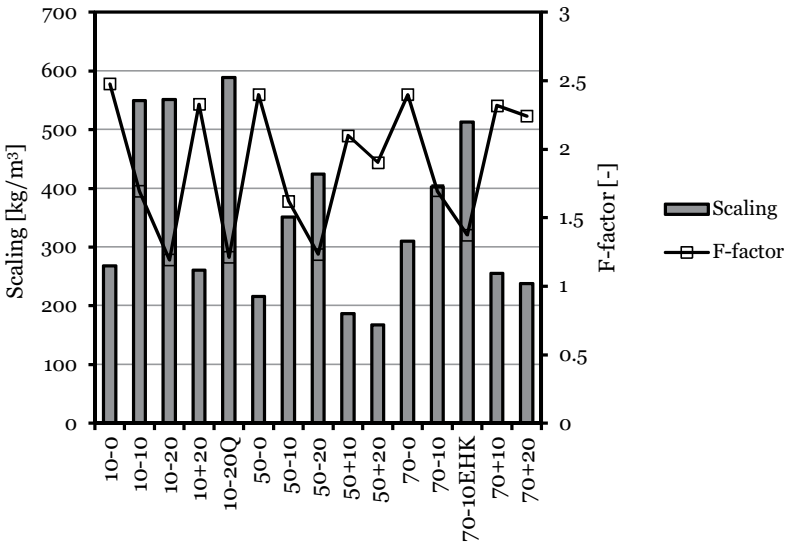

Figure 64. The F-factors and scaling results of the test concretes.

All the mineral powder additions, with or without cement reduction, increased the flow table test results. Therefore, the freeze-thaw resistance of mineral powder concretes may possibly be improved by

reducing the amount of water and thus improving the strength of the concretes.

4.3.5 Conclusions on the frost resistance of mineral powder concretes

From the freeze-thaw tests the following conclusions can be drawn:

- the use of mineral powders increased the amount of air-entraining admixture required to attain the desired amount of entrained air;
- the factors influencing the scaling of all the concretes were found to be strength, capillary porosity, water uptake during freeze-thaw testing and the F-factor;
- the use of mineral powders itself did not have an effect on the freeze-thaw resistance, but the consequent binder reduction and loss of strength impaired the durability;
- using GGBS and, presumably, the consequent later testing time had a positive effect on the freeze-thaw durability;
- the freeze-thaw resistance of mineral powder concretes made with at least 50% GGBS as a binder did not seem to be as strongly affected by the binder reduction as concretes made with only cement as a binder;
- the loss of strength resulting from the replacement of the cement and the consequent fall in the freeze-thaw durability, might be compensated for by reducing the w/c ratio of the mineral powder concretes. This may be possible since the use of mineral powders increased the flow, i.e. reduced the water demand of the test concretes.

4.4 Effects of mineral powders on hydration process and hydration products

In order to investigate the effects of mineral powders on the hydration process and hydration products of cement pastes and concretes, the following experiments were performed. The theoretical background and the equations that were utilised are presented in the previous section, "Materials and methods". All the mix designs for the concretes and cement pastes are presented in Appendix 3

4.4.1 The effects of mineral powders on the hydration of concretes

B0 was the reference concrete, with no mineral powder. The concretes B10, B20, B30 and B40 contained 10, 20, 30 and 40% of added limestone powder of cement weight respectively and the concretes BQ10, BQ20, BQ30 and BQ40 contained 10, 20, 30 and 40% of added Nilsiä quartz powder of cement weight respectively. The mix designs of the concretes and the test results are presented in Appendix 3.

Heat evolution in concretes during hydration – semi-adiabatic tests

Figure 65 and Figure 66 present the temperatures [°C] of the concretes as a function of time [h] as obtained experimentally from the hydration tests. Only the first 72 hours are shown. The temperatures of the concretes have been recalculated to correspond to the adiabatic temperature increase.

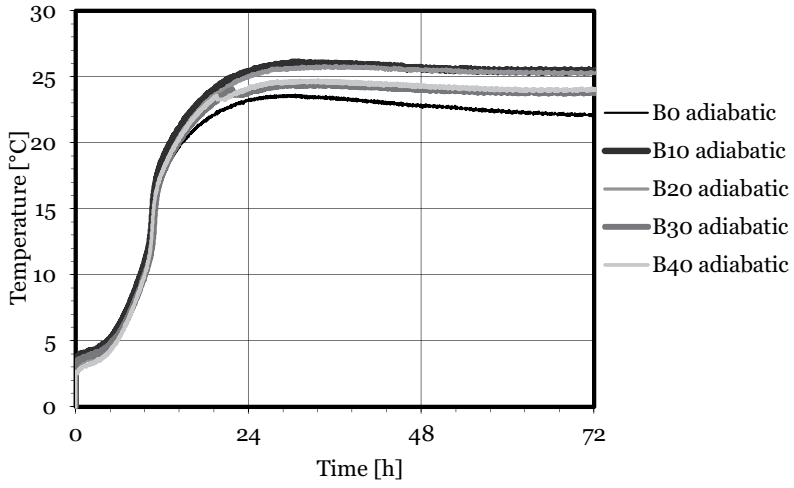

Figure 65. Adiabatic temperature increase of concretes B0, B10, B20, B30 and B40.

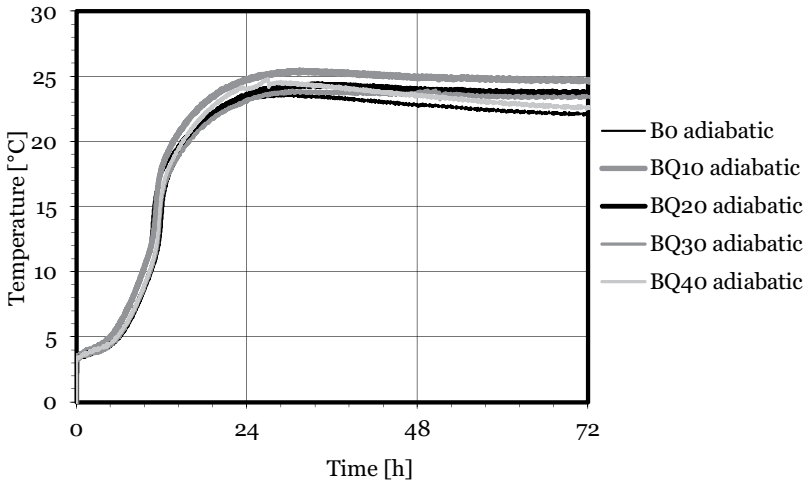

Figure 66. Adiabatic temperature increase of concretes B0, BQ10, BQ20, BQ30 and BQ40.

The heats of hydration were measured with two replicate samples. The variation in the measured heats between the samples was at maximum of 0.5 °C. It is clear from the results that the addition of limestone powder and Nilsiä quartz powder had some effect on the heat of hydration. Limestone powders increased the heat of hydration at all addition levels and maintained a higher heat of hydration during the first 72 hours. Nilsiä quartz powder had a similar effect, except that after the first 24 hours all of the mineral powder concretes had a similar temperature. However, the temperatures were still somewhat higher than those of the reference concrete. A slight retardation of the hydration temperature – about 1 hour – was measured for the concretes containing 20, 30 and 40% of Nilsiä quartz powder.

In all, the addition of 10% mineral powder appeared to have the greatest effect on the heat of hydration during the first 72 hours, followed by the addition of 20%. After the first 72 hours the temperatures of all the concretes levelled out steadily, corresponding finally to the temperature of the environment.

Maturity of mineral powder concretes

Because the measurements were performed in semi-adiabatic conditions and then recalculated to correspond to the adiabatic temperature rise, the data reduction leads to an estimate which is lower than the actual adiabatic temperature increase. The approximation was improved by studying the maturity increase of the concrete through a maturity function based on the Arrhenius equation. Afterward, Freiesleben Hansen and Pedersen developed a

new method of maturity concept using Arrhenius equation in 1977 (Freiesleben Hansen and Pedersen, 1977).

$$k_t = e^{\frac{E_A}{R}\left(\frac{1}{293}-\frac{1}{273+T}\right)} \quad (35)$$

in which

k_t is the temperature factor

E_a is the activation energy [J/mol]

R is the universal gas constant = 8.314 [J/(mol·K)]

T is the temperature [°C]

The maturity function is:

$$M = \int_0^t k_t \, dt \quad (36)$$

The correction was done in compliance with RILEM TC 119-TCE (1997), according to the equations:

$$\theta_{ad}(t) = \theta_{HH}(M) \quad (37)$$

with time

$$t = \int_0^M \frac{1}{k_t} \, dm \quad (38)$$

and

$$T_s - T_o + \theta_{HH}(M) = T_o + \theta_{ad}(t) \quad (39)$$

in which

θ_{ad} is the adiabatic temperature increase [K]

θ_{HH} is the temperature increase [K]

T_s is the temperature of the sample [K]

T_o is the initial temperature of the sample [K]

Figure 67 and Figure 68 present the maturity of the concretes as a function of time [h] during the first 72 hours.

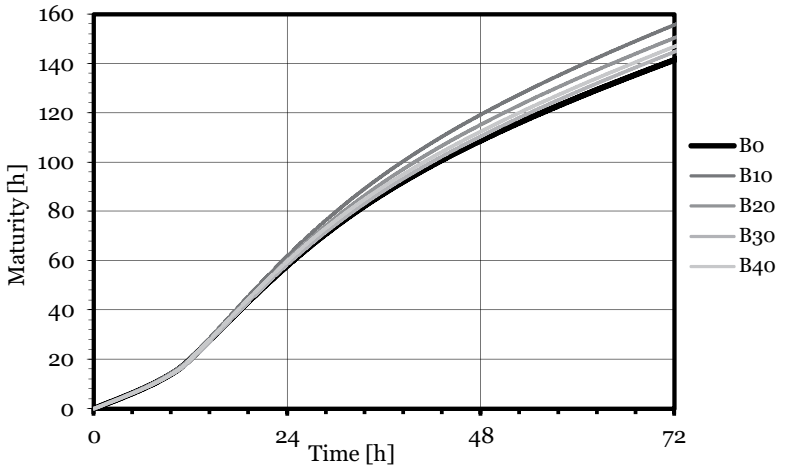

Figure 67. Maturity of concretes B0, B10, B20, B30 and B40.

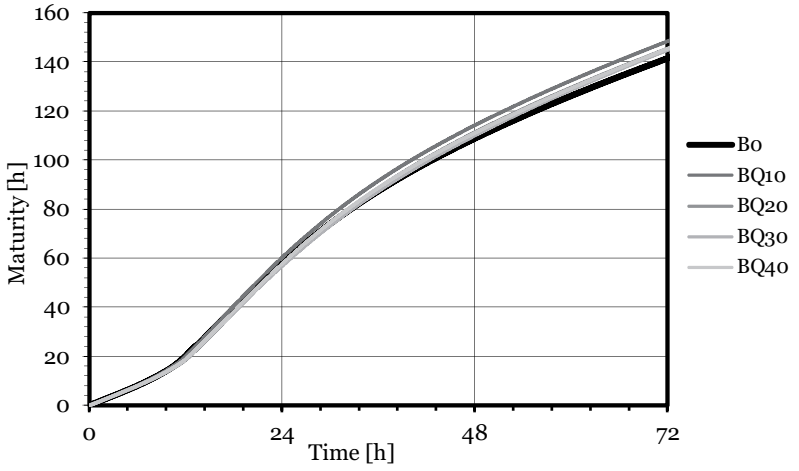

Figure 68. Maturity of concretes B0, BQ10, BQ20, BQ30 and BQ40.

The results were consistent with the results from the measured temperatures; the highest maturity was calculated for the concrete

B10 containing 10% limestone powder, followed by those with the addition of larger amounts of mineral powders. The differences in maturity between the quantities of powder were greater with the limestone powder concretes, as can be seen when comparing Figure 67 with Figure 68. However, all the mineral powder concretes obtained a higher maturity than the reference, even at the end of 28 days.

Influence of mineral powders on the degree of hydration of concretes

The degree of hydration of the concretes was calculated using Equation (20). It has been shown that the heat released divided by the total heat available provides a good measure of the degree of hydration (van Breugel, 1997). Figure 69 and Figure 70 present the degrees of hydration of the concretes at the ages of 1, 2, 7 and 28 days. The results show that the degree of hydration was slightly increased with the addition of mineral powder compared to the reference concrete without mineral additives.

Especially after the first 24 hours, a 10% mineral addition seemed to have the greatest influence on the degree of hydration with both powders. With limestone powder, additions of 10% and 20% were at their most effective during the first 7 days, after which the differences between the amounts of powder were almost non-existent. The addition of 10% Nilsiä quartz powder was slightly more effective during the first 48 hours, after which the differences between the amounts of powder levelled off.

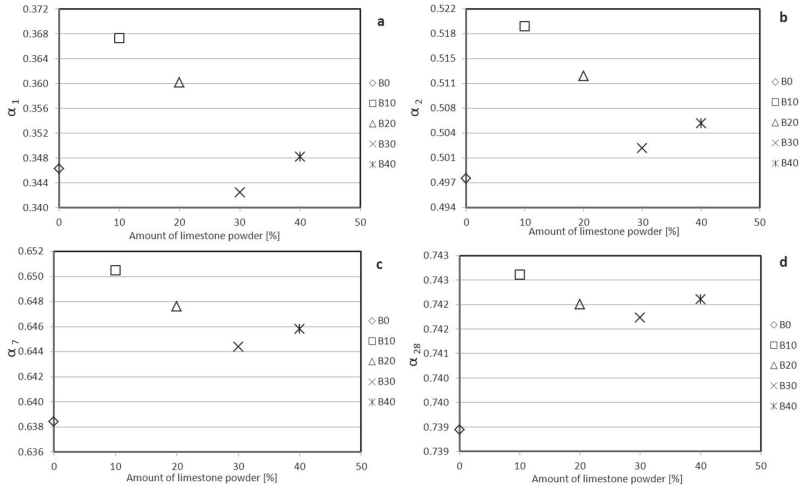

Figure 69. Degrees of hydration (α) for concretes B0, B10, B20, B30 and B40, at the ages of a) 1 day, b) 2 days, c) 7 days and d) 28 days.

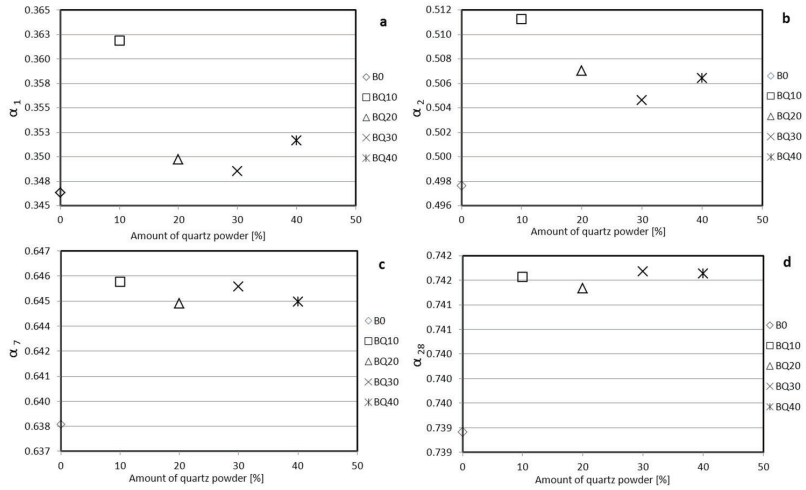

Figure 70. Degrees of hydration (α) for concretes B0, BQ10, BQ20, BQ30 and BQ40, at the ages of a) 1 day, b) 2 days, c) 7 days and d) 28 days.

As illustrated in Figure 69 and Figure 70, the addition of mineral powders seemed to have a positive effect on the hydration of the concrete. This was also observed when the compressive strengths of the concretes were examined, as shown in Table 24. The compressive strength of the mineral powder concretes was 3.9 MPa greater on average than that of the reference at the age of 28 days.

Table 24. Compressive strength [MPa] results of the concretes at the age of 1, 2 7 and 28 days.

	Age [d]			
Name	1	2	7	28
B0	7.0	14.1	23.1	30.9
B10	9.5	16.7	26.9	35.2
B20	9.4	16.8	27.1	34.8
B30	9.0	17.1	26.3	35.1
B40	9.2	16.9	26.8	34.5
BQ10	9.0	16.9	26.5	34.8
BQ20	9.3	17.0	26.7	34.4
BQ30	9.0	16.9	26.6	34.9
BQ40	9.4	16.8	26.5	34.8

4.4.2 Results of the thermoanalysis of cement pastes

The thermal disintegration of the cement pastes with and without mineral fillers was investigated by analysing the weight loss of the

sample during heating. Figure 71 shows the characteristic shapes of TGA/TGA derivative curves of hydrated cement paste. The rapid peak in the TGA derivative at around 210-215 °C is a result of an unfortunate error in the program. All the TGA and TGA derivative data is presented in Appendix 4.

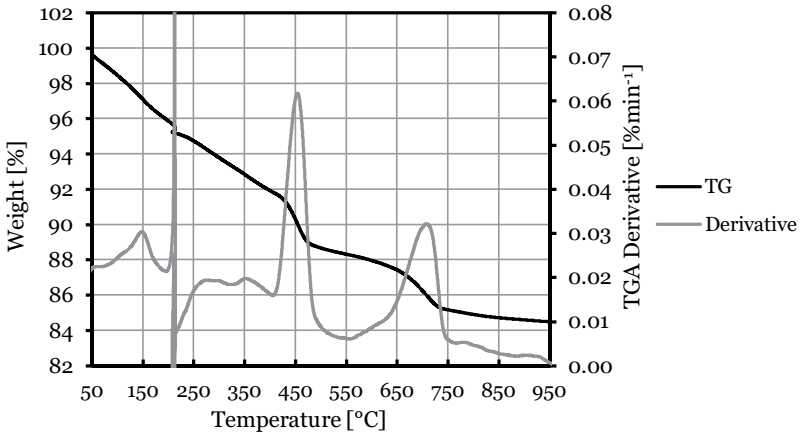

Figure 71. TGA/TGA derivative diagram of P0 cement paste at the age of 28 days in a nitrogen atmosphere.

Calculation of the content of hydration products

The TGA and the TGA derivative curves in Figure 71 show three major weight loss steps at below 400 °C, around 450 °C and around 700 °C which can be attributed to the decomposition of hydration products such as C-S-H gel and ettringite, the decomposition of Portlandite ($Ca(OH)_2$) and the decomposition of $CaCO_3$, respectively (Hewlett 1998). The disintegration equations of Portlandite and $CaCO_3$ can be expressed as:

$$Ca(OH)_2\,(s) \rightarrow CaO\,(s) + H_2O\,(g) \qquad (40)$$

and

$$CaCO_3\,(s) \rightarrow CaO\,(s) + CO_2\,(g) \qquad (41)$$

The amounts of calcium hydroxide and calcium carbonate at the age of 28 days, estimated from the measured weight losses portrayed in Equations (40) and (41), are presented in Table 25. The quantity of Portlandite was slightly lower in all the cement pastes with mineral powders replacing cement. Both the $Ca(OH)_2$ and the $CaCO_3$ amounts are expressed as a percentage of mass.

Table 25. The amounts of $Ca(OH)_2$ and $CaCO_3$ as measured by weight loss [%] in the cement pastes at the age of 28 days and the degrees of hydration (α) at the ages of 1, 2, 7 and 28 days.

	P0	P10	P20	P30	P40	PQ10	PQ20	PQ30	PQ40	PQK10	PQK30	PEHK10	PEHK30
$Ca(OH)_2$	3.10	2.80	2.80	2.60	2.40	2.75	2.70	2.60	2.50	2.80	2.55	2.90	2.15
$CaCO_3$	3.00	6.00	9.70	12.20	16.00	2.70	2.30	2.10	1.85	2.60	2.30	2.90	3.05
α_1	0.349	0.349	0.353	0.380	0.352	0.317	0.316	0.296	0.296	0.331	0.300	0.307	0.342
α_2	0.425	0.455	0.458	0.504	0.450	0.391	0.438	0.444	0.445	0.421	0.420	0.427	0.443
α_7	0.463	0.499	0.546	0.601	0.640	0.433	0.533	0.578	0.600	0.532	0.540	0.500	0.559
α_{28}	0.527	0.535	0.631	0.669	0.654	0.466	0.601	0.617	0.685	0.528	0.653	0.582	0.557

The content of chemically bound water in the cement pastes increased with the hydration of the cement. The amount of chemically bound water in the paste was used to calculate the degree of hydration according to Equation (24). Table 25 presents the degrees of hydration α_1, α_2, α_7 and α_{28} at the ages of 1, 2, 7 and 28 days, respectively.

The degrees of hydration were higher in the pastes containing mineral powders, although the hydration products, in this case $Ca(OH)_2$, were slightly lower. This apparent discrepancy can be accounted for by examining the calculation of the degrees of hydration, and thus it can be seen that the degree of hydration is calculated only for the limestone-free part of the cement. Since the amount of cement was lower in the pastes with mineral powders replacing cement, the amount of Portlandite was also lower.

The intensity of the disintegration peaks changed with the hydration time. The temperature at the peak maxima also seemed to be influenced by the quality and quantity of the mineral filler. The amount of $CaCO_3$ appeared to decrease as the hydration proceeded, even after 7 days in some of the pastes. However, the shape of the peak does not change. Figure 72 presents the evolution of the $CaCO_3$ content and the difference in the peak decomposition temperature of $CaCO_3$ by almost 40 °C in two different cement pastes both containing 20% mineral powder.

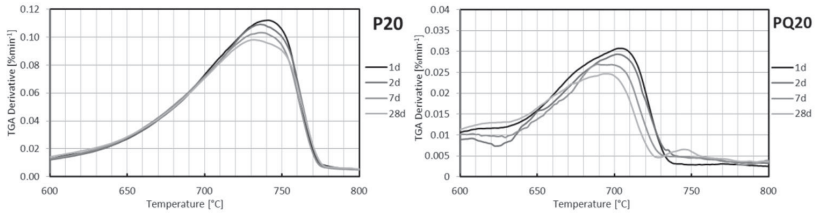

Figure 72. Evolution of $CaCO_3$ content and the change in the peak decomposition temperature of $CaCO_3$ in the pastes P20 and PQ20, with 20% of the cement replaced by limestone powder and quartz powder respectively.

Figure 73 presents the TGA derivative decomposition curves of $CaCO_3$ of the pastes PQ40, P0, P10, P20, P30 and P40, comprising the use of Nilsiä quartz powder to replace 40% of the cement and 0%, 10%, 20%, 30% and 40% limestone powder, respectively, at the age of 28 days. In the figure a change in the peak temperature of the $CaCO_3$ decomposition by as much as 50 °C can be observed with the limestone powder content.

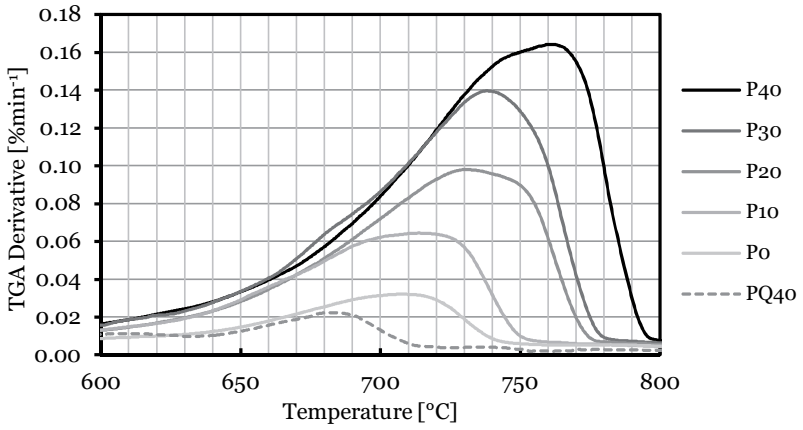

Figure 73. Variation in the peak decomposition temperature of $CaCO_3$ in relation to limestone powder content.

In all, increasing the amount of limestone powder in the cement pastes shifted the $CaCO_3$ decomposition peak temperature towards higher values. However, increasing the amount of quartz fillers appeared to shift the decomposition peak temperature to lower temperatures, as can be seen in Figure 73.

4.4.3 Results of the X-ray diffraction

The processing of the XRD data was presented in the section titled "Materials and methods – X-ray diffraction of cement pastes". The effects of mineral powders on the development of crystal phases were investigated by examining the XRD patterns of cement pastes with and without mineral powders. The pastes that were studied were the same as in the TGA tests and they were examined at the ages of 1, 7 and 28 days. All of the XRD patterns are presented in Appendix 5.

Development of different crystal phases

From the results of the cement pastes the intensities of $Ca(OH)_2$ and C_3S, were examined. No other distinctive peaks, such as those for

C_3A, monosulphate (AFm) or ettringite (AFt), were studied, mainly because of the overlapping of the peaks. For example, the peak of monosulphate (AFm) at a 2θ angle at 31.10° is overlapped by the peak of calcium magnesium carbonate at a 2θ angle at 30.94° (Taylor (1990), Stutzman (1996)).

The measured intensity of the $Ca(OH)_2$ peak as a function of time is presented in Figure 74 and Figure 75 in pastes which have 0%, 10% or 30% of the cement replaced by mineral powder. The amount of $Ca(OH)_2$ was measured from its peak at a 2θ angle at 18.09°. According to the results, the amount of Portlandite was clearly lower in the cement pastes containing 30% less cement than in the reference paste. Reducing the amount of cement by 10% seemed to have less influence on the amount of $Ca(OH)_2$.

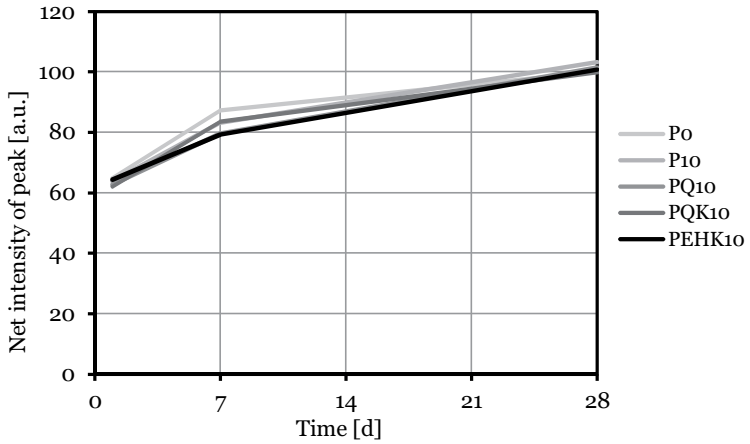

Figure 74. The measured intensity of the $Ca(OH)_2$ peak as a function of time in pastes P10 PQ10, PQK10 and PEHK10 with 10% of the cement replaced by limestone powder, Nilsiä quartz powder, Kemiö quartz powder and EHK quartz powder, respectively. P0 is the reference paste.

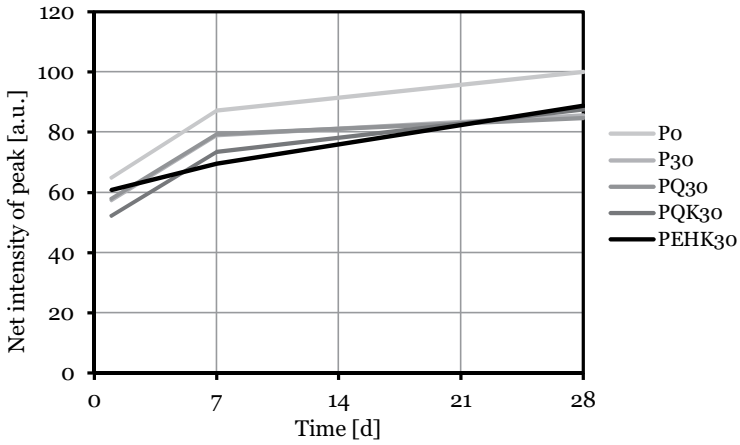

Figure 75. The measured intensity of the $Ca(OH)_2$ peak as a function of time in pastes P30 PQ30, PQK30 and PEHK30 with 30% of the cement replaced by limestone powder, Nilsiä quartz powder, Kemiö quartz powder and EHK quartz powder, respectively. P0 is the reference paste.

During the first 7 days, the increase in the intensity of the $Ca(OH)_2$ peak seemed to be the lowest in the pastes containing the finest EHK quartz. After 28 days all the cement pastes in which mineral powder had been used to replace 10% of the cement had attained almost the same intensity of $Ca(OH)_2$ as in the reference paste. In pastes with 30% replacement the differences in the amounts of $Ca(OH)_2$ were more distinct after 1 and 7 days but at the age of 28 days the intensities were quite similar.

The amount of C_3S was measured from its peak at a 2θ angle at 51.72°. Since the pastes with mineral powders originally contained less cement, the measured intensity peaks for C_3S were, as expected, also lower. Figure 76 and Figure 77 present the measured intensity of the C_3S peak as a function of time. On the basis of the intensity results, the amount of C_3S was measured to be somewhat lower in nearly all of the mineral powder pastes than would be caused by mere replacement.

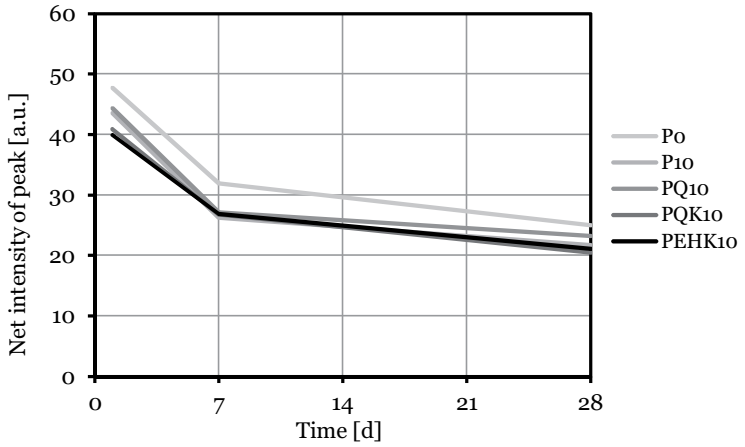

Figure 76. The measured intensity of the C_3S peak as a function of time in pastes P10 PQ10, PQK10 and PEHK10 with 10% of the cement replaced by limestone powder, Nilsiä quartz powder, Kemiö quartz powder and EHK quartz powder, respectively. P0 is the reference paste.

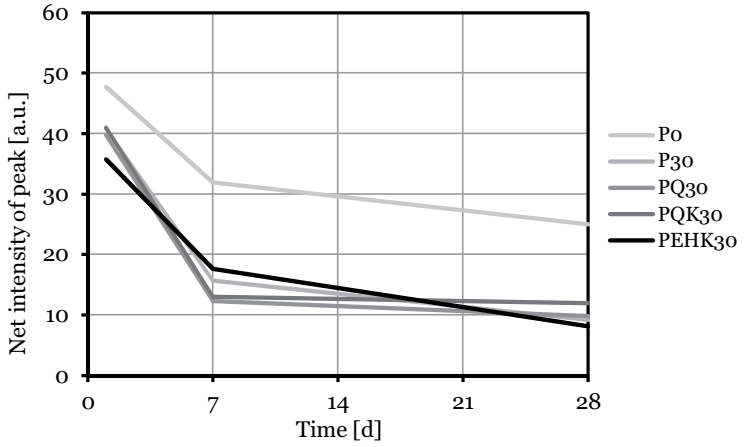

Figure 77. The measured intensity of the C_3S peak as a function of time in pastes P30 PQ30, PQK30 and PEHK30 with 10% of the cement replaced by limestone powder, Nilsiä quartz powder, Kemiö quartz powder and EHK quartz powder, respectively. P0 is the reference paste.

4.4.4 Discussion of the effects of mineral powders on hydration process and hydration products

The results showed that more hydration heat was developed in mineral powder concretes containing up to 40% of either quartz or limestone powder. The hydration temperatures of the concretes containing quartz powder levelled off to match the temperature of the reference concrete more quickly than those of the concretes containing limestone powder. This may indicate that there is a chemical effect that accelerates the hydration of cement in the

presence of limestone powder For example Pera et al. (1999) have reported an acceleration of the C_3S reaction in the presence of limestone. The maturities of all the mineral powder concretes were constantly higher than the reference. This could explain in part why all of the concretes containing mineral powder obtained a higher strength throughout the testing period. The calculated degrees of hydration were higher with the concretes containing limestone powder, although the differences were quite small. In addition, the measured flows of the mineral powder concretes were higher than the reference. Test results of the concretes are presented in Appendix 3.

Overall, additions of 10% and 20% mineral powder seemed to have the biggest influence on the heats of hydration. The effect of the addition of mineral powder on the heats and maturities of the concretes was most apparent in the concretes with limestone powder. However, these small differences in the heats of hydration were not manifested in the concrete strengths, which were similar among the concretes containing mineral powder. As in the previous experiments, the additions of mineral powder increased the flowability of the concretes.

Table 26 presents the compressive strength results of the cement pastes. Although the amount of cement was lower in the pastes containing mineral powders, the compressive strengths were similar or even higher when filler was used to replace 10% of the cement. Higher substitutions caused reductions in the strength of the cement paste.

Table 26. Compressive strength results of the cement pastes.

	Age [d]			
	1	2	7	28
P0	39.4	48.5	56.0	66.7
P10	38.9	48.5	58.9	70.1
P20	33.4	45.5	55.5	64.9
P30	23.6	38.4	48.0	58.4
P40	15.5	29.5	42.3	50.0
PQ10	35.7	48.9	55.9	66.9
PQ20	33.1	45.0	52.1	61.3
PQ30	24.1	33.1	46.6	55.4
PQ40	15.5	26.7	40.1	48.8
PQK10	36.6	49.1	55.4	66.7
PQK30	21.6	36.6	51.7	57.1
PEHQ10	38.8	47.9	59.2	68.7
PEHQ30	28.9	40.3	51.2	59.6

In some studies, for example Greene (1960), the decomposition peak of $CaCO_3$ has been found to increase as hydration progresses because of the longer exposure time to CO_2 in the air. However, in this study the samples were held under water in airtight containers before the samples were transported to the desiccator. In addition, the samples were efficiently ground for only 10 seconds and tested immediately after grinding. The change in the intensity of the disintegration peaks of $CaCO_3$ was presented in Figure 72. The decomposition peak appeared to decrease during the hydration, which might indicate that some of the $CaCO_3$ is being consumed and incorporated in the hydrate phases.

As discussed earlier, in Section 2.1.1 Limestone powder in concrete, limestone reacts with the alumina phases of cement and it can also be incorporated into C-S-H gel. Thus the decrease in the amount of $CaCO_3$ as hydration progresses may be due to its incorporation into the aluminate and C-S-H phases.

Using limestone powder to replace more of the cement caused the peak temperature of the $CaCO_3$ decomposition to shift towards higher temperatures. Figure 78 presents the TGA derivative curve of pure limestone powder in the temperature range from 600 to 900 °C. The peak decomposition temperature was established at 812 °C. Thus it appears that increasing the amount of limestone powder (and reducing the amount of cement) in the cement paste shifted the peak decomposition temperature towards 812 °C.

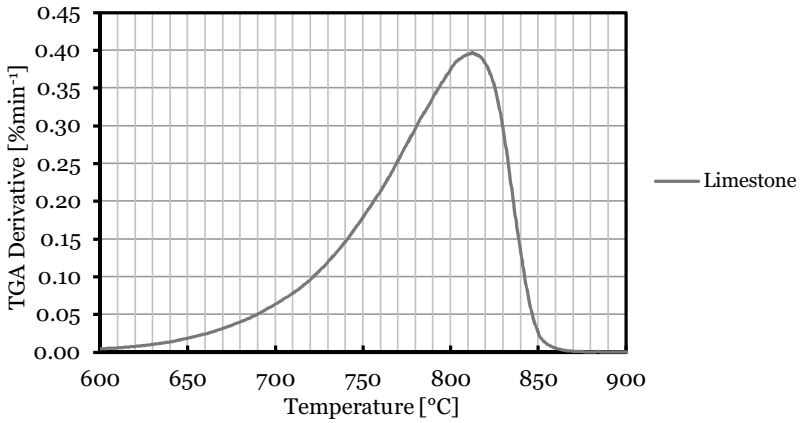

Figure 78. TGA derivative curve of pure limestone powder.

All the TGA data obtained at 1, 2, 7 and 28 days showed a gradual increase in the weight loss at the temperatures between 100 °C and 400 °C and around 450 °C, which denotes the decomposition of the main hydration reaction products of the cement – the C-S-H gel and $Ca(OH)_2$ respectively. Thus the progress of the hydration can be evaluated from the measured weight losses. The weight losses resulting from the decomposition of C-S-H and $Ca(OH)_2$ were lower, especially in those pastes where mineral powder was used to replace more than 10% of the cement. However, the measured compressive strengths were quite similar up to 20% replacement with limestone powder.

According to the XRD results, using mineral powder to replace 10% of the cement did not seem to have much effect on the amount of $Ca(OH)_2$. The measured peak of C_3S seemed to correlate well with the measured net intensity of $Ca(OH)_2$ in all the cement pastes. The XRD patterns for $Ca(OH)_2$ were also consistent with the compressive strength results in Table 26. Figure 79 and Figure 80 present the correlation between C_3S and $Ca(OH)_2$ in pastes in which mineral powder was used to replace 10% or 30% of the cement, respectively. The regression line is also presented.

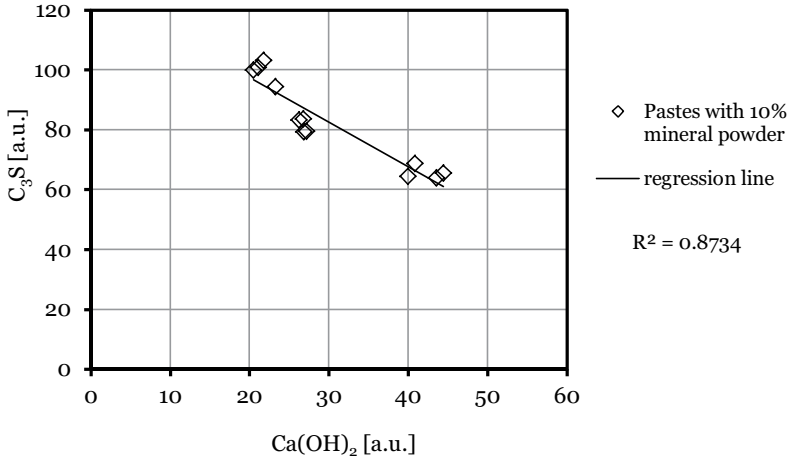

Figure 79. Correlation between C_3S and $Ca(OH)_2$ in pastes with 10% of the cement replaced by mineral powder.

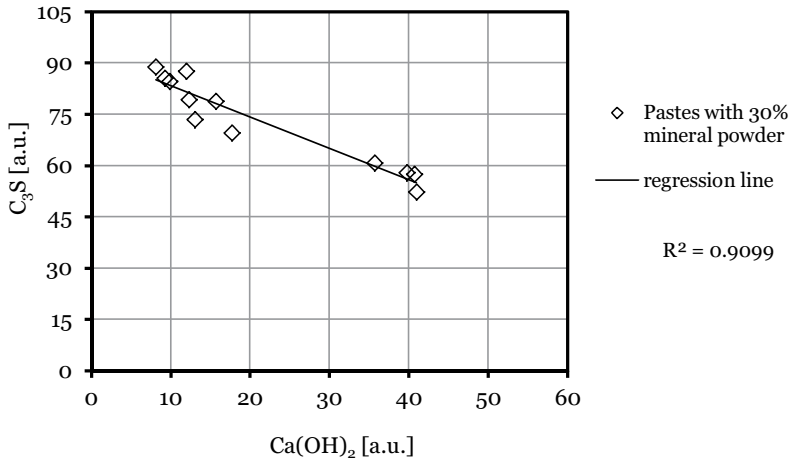

Figure 80. Correlation between C_3S and $Ca(OH)_2$ in pastes with 30 % of cement replaced with mineral powder.

The net intensity of the C_3S peak was lower in most pastes than could be expected as a result of mere cement replacement. This could indicate that more cement is being hydrated in the pastes with mineral powder. The corresponding $Ca(OH)_2$ net intensity peaks of the pastes without mineral powders and with mineral powders used to replace 10% of the cement and the similar compressive strength results support this.

As a result of the overlapping of peaks, the amount of $CaCO_3$ could not be measured using XRD. However, the XRD results in relation to $Ca(OH)_2$ backed up the TG results. Figure 81 presents the correlation between the TG and XRD results. The regression line is also presented

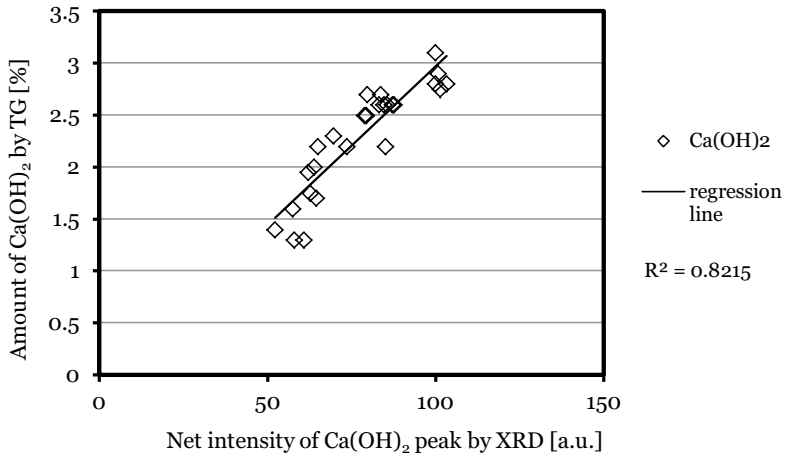

Figure 81. Correlation between the amount of $Ca(OH)_2$ as measured by TG and XRD.

4.4.5 Conclusions

On the basis of the tests the following general conclusions can be drawn:

- the results showed that the heat evolution is influenced by the mineral powders. The maturities of the concretes containing mineral additions were continuously higher than the reference. According to the hydration data, mineral additions of 10 % and 20 % appeared to be the most effective. The effect was most apparent in limestone powder containing concretes;
- adding mineral powders also increased the compressive strengths and the flowability of the test concretes. These results support the previous conclusions that the amounts of cement might be lowered using mineral powders;
- the measured amount of $CaCO_3$ decreased as hydration proceeded, which might indicate that some of the limestone is being incorporated into the aluminate and C-S-H phases;
- replacing 10% of the cement with mineral powder did not seem to have much effect on the amount of $Ca(OH)_2$ or the compressive strength results. The results of the XRD in relation to $Ca(OH)_2$ backed up the results of the TG. It could be that in pastes with mineral powders more cement is being hydrated. Findings on the amount of Portlandite and the compressive strength results support this.

4.5 Effects of mineral powders on concrete microstructure

The concretes were investigated with ESEM/BSE with the purpose of determining the effects of the mineral powders on the microstructure of the concretes. Factors such as the paste structure, porosity and the structure of the interfacial transition zone (ITZ) were studied. In this section the microstructure of the air-entrained concretes is also considered.

The microstructure was studied according to the procedure by Scrivener and Pratt (1987), described earlier in the section titled "Materials and methods – Microstructure". The threshold values were defined manually. Figure 82 presents an example of the separation of the phases according to the method. However, it should be kept in mind that the captured ESEM/BSE images represent only a small section of the whole concrete specimen, which should be taken into consideration when drawing conclusions from the images.

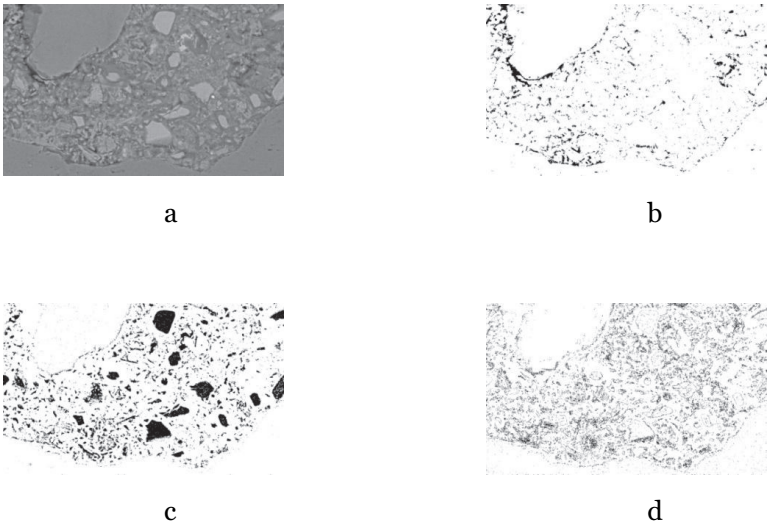

Figure 82. An example of the phase separation according to the method by Scrivener (1987): a) original image, b) porosity c) unhydrated cement d) $Ca(OH)_2$

4.5.1 Microscopy analyses

Figure 83, Figure 84 and Figure 85 present the ESEM/BSE images of the concretes R14, C29L32 and C29N31 and the image of the porosity of the particular concrete, separated according to the method. All of the concretes that are depicted had a w/c ratio of 0.62 or 0.63. All the samples had been hydrating for 28 days. In the pictures the measure at the bottom of the image marks 50 μm.

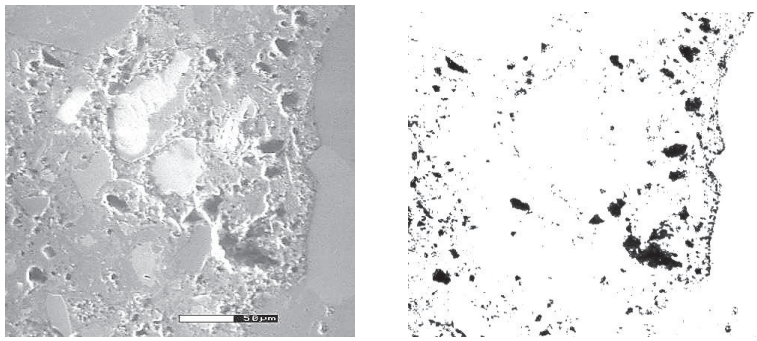

Figure 83. BSE image and the separated porosity phase of concrete R14 with a w/c ratio of 0.63 and cement content of 340 kg/m³. The white measure at the bottom of the picture marks 50 µm.

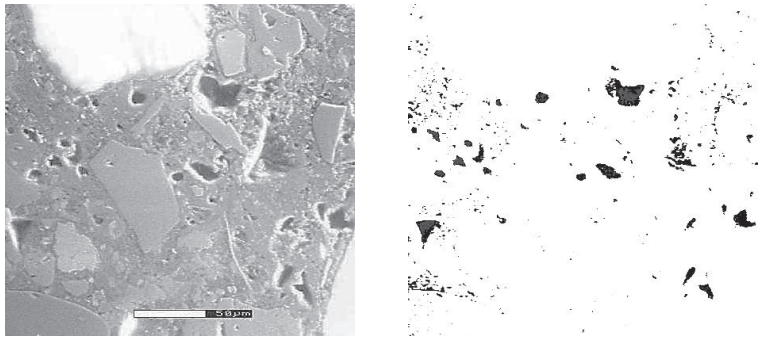

Figure 84. BSE image and the separated porosity phase of concrete C29L32 with a w/c ratio of 0.62 and cement content of 293 kg/m³. The white measure at the bottom of the picture marks 50 µm.

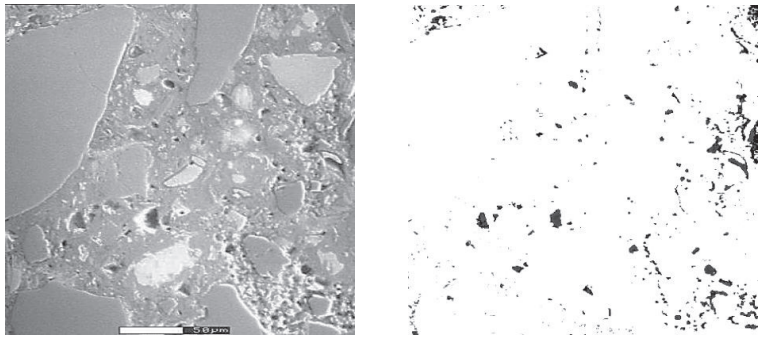

Figure 85. BSE image and the separated porosity phase of concrete C29N31 with a w/c ratio of 0.62 and cement content of 293 kg/m³. The white measure at the bottom of the picture marks 50 µm.

The separated porosity phase of the concrete R14 in Figure 83 revealed increased porosity compared to the concretes containing mineral powder in Figure 84 and Figure 85, despite the higher amount of cement. The amount of anhydrous cement, which appears

as bright/whitish on the BSE images, appeared to be somewhat higher in the reference concrete without mineral powders, as can be seen from Figure 86. Cracking was not found in any of the samples.

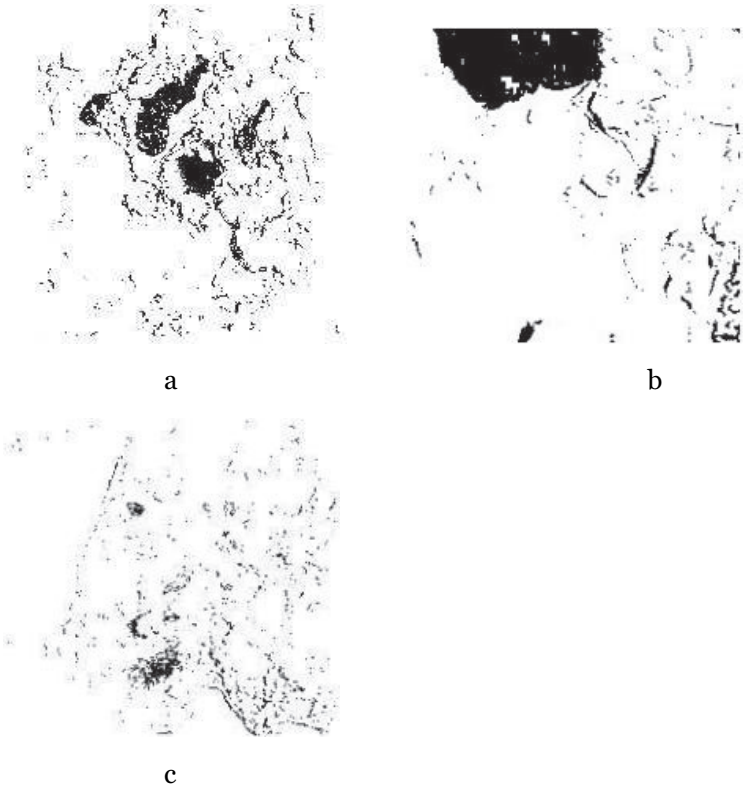

Figure 86. Phase segmentation of unhydrated cement in a) concrete R14, b) concrete C29L32 and c) concrete C29N31

The microstructures of the mineral powder concretes appeared similar in the ESEM images. No distinct differences were observed between the quartz and limestone powder concretes. In addition, no significant agglomerates of quartz particles were found in any of the images. The distribution of limestone particles could not be detected with the ESEM/BSE since the calcium appears as the same greyish colour as the C-S-H-gel.

Microstructure in the interfacial transition zone

The influence of mineral powders on the microstructure in the ITZ was also studied using the ESEM. The BSE images revealed porosity all around the cement paste, but especially around the aggregate particles. In Figure 83 a fairly large piece of aggregate can be seen on the right of the image. In the separated porosity phase image a black border defining the porosity in the transition zone between the

cement paste and aggregate is visible. In Figure 84 and Figure 85 the outlines of the aggregate are also noticeable in the porosity phase images but they are not as distinct.

Figure 87 and Figure 88 present a more detailed picture of the ITZ of the concretes C29N31 and C29K30 containing mineral powder equivalent to 1/3 of the weight of the cement. In the pictures the measure at the bottom of the image shows 20 µm. In both of the pictures the larger aggregate particle is located in the lower right-hand corner.

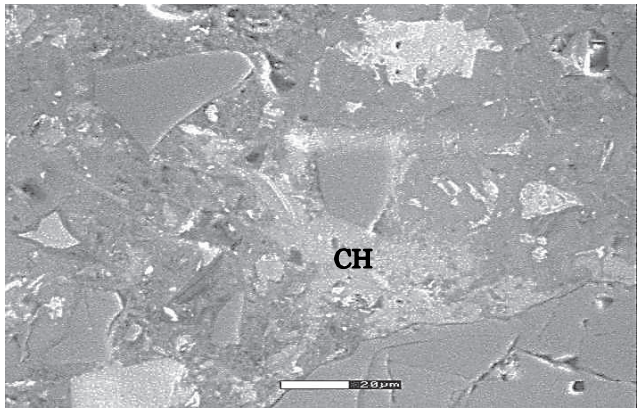

Figure 87. ITZ of concrete C29N31 with a cement content of 293 kg/m^3 and mineral powder addition equivalent to 1/3 of the weight of cement. Portlandite in the picture is marked as CH. The white measure at the bottom of the picture marks 20 µm.

The small quartz particles in the vicinity of the aggregate can especially be observed in Figure 88. The quartz particles are visible as brighter spots, owing to their higher atomic number caused by the predominance of silica in the quartz mineral. In the ITZ pictures one can also see unhydrated cement particles, for example in Figure 88 in the middle on the left. In addition, Portlandite – amorphous lighter grey areas going across the cement paste all the way to the aggregate – was observed. In general, both images presented a moderately uniform structure of the cement even at the aggregate/paste boundary.

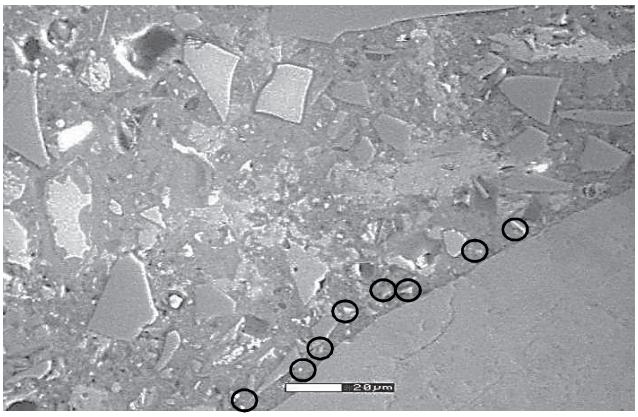

Figure 88. ITZ of concrete C29K30 with a cement content of 293 kg/m³ and mineral powder addition equivalent to 1/3 of the weight of cement. Small quartz particles near the aggregate are circled. The white measure at the bottom of the picture marks 20 µm.

Although mineral powders seemed to improve the structure of the ITZ, adding mineral fillers did not completely eliminate the existence of transition zones between the aggregates and paste especially at these relatively high water/cement ratios. A magnification of 1000X in Figure 89 reveals a clear transition zone between the aggregate on the right and the cement paste in the concrete C29L32.

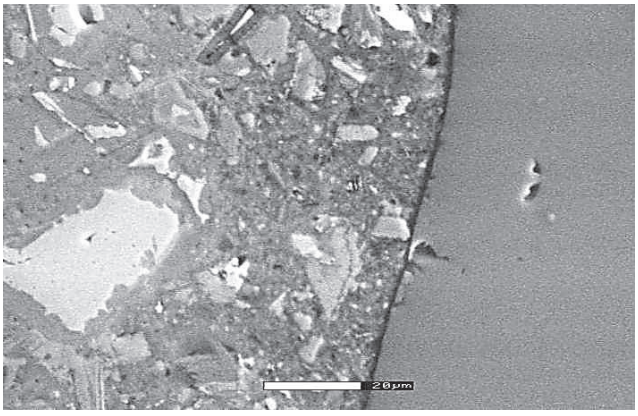

Figure 89. A magnification of ITZ of concrete C29L32. The white measure at the bottom of the picture marks 20 µm.

Influence of mineral powders on the air entrained concretes

The microstructure of air-entrained concretes was also studied with ESEM/BSE. The focus was on the effect of the use of mineral powders to replace the cement on the microstructure and the spacing and quality of the entrained air. Figure 90 and Figure 91 present BSE and separated porosity images of the concretes 10-0 and 10-10, which contained 330 kg/m³ and 297 kg/m³ cement and 0 kg/m³ and 33

kg/m^3 of added limestone powder, respectively. Figure 92 and Figure 93 present BSE and separated porosity images of the concretes 10-20 and 10+20, which contained 264 kg/m^3 and 330 kg/m^3 cement and 66 kg/m^3 and 66 kg/m^3 of added limestone powder respectively. All the samples had been hydrating for 28 days. All the images have a magnification of 250X and the measure at the bottom of the image shows 50 µm.

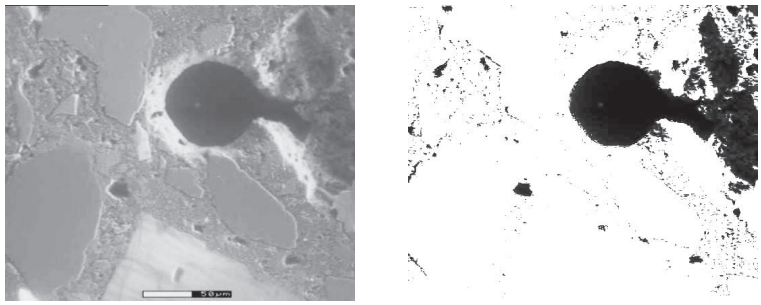

Figure 90. BSE image and the separated porosity phase of concrete 10-0 with a w/c ratio of 0.58 and cement content of 330 kg/m^3. The white measure at the bottom of the picture marks 50 µm.

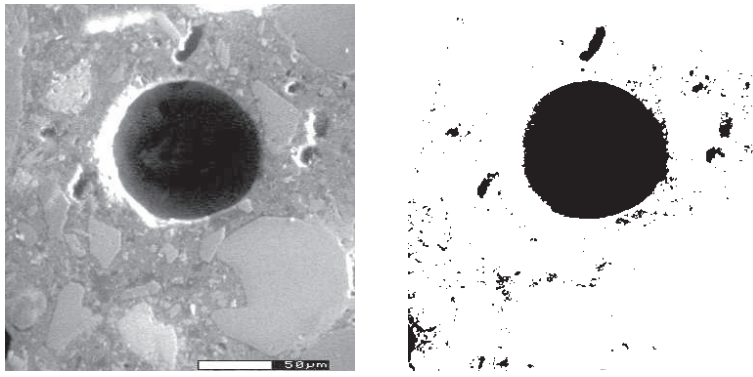

Figure 91. BSE image and the separated porosity phase of concrete 10-10 with a w/c ratio of 0.64 and cement content of 297 kg/m^3 with 33 kg/m^3 of limestone powder. The white measure at the bottom of the picture marks 50 µm.

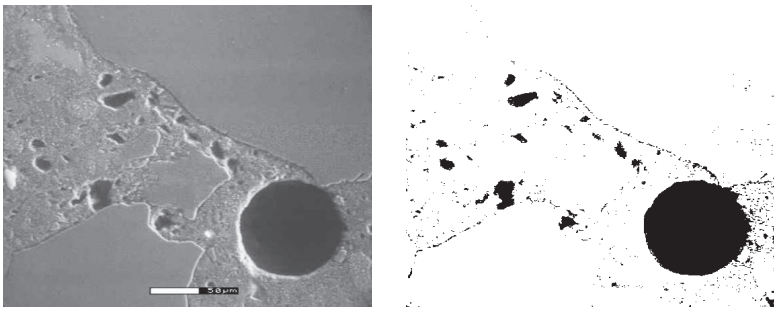

Figure 92. BSE image and the separated porosity phase of concrete 10-20 with a w/c ratio of 0.72 and cement content of 264 kg/m^3 with 66 kg/m^3 of limestone powder. The white measure at the bottom of the picture marks 50 µm.

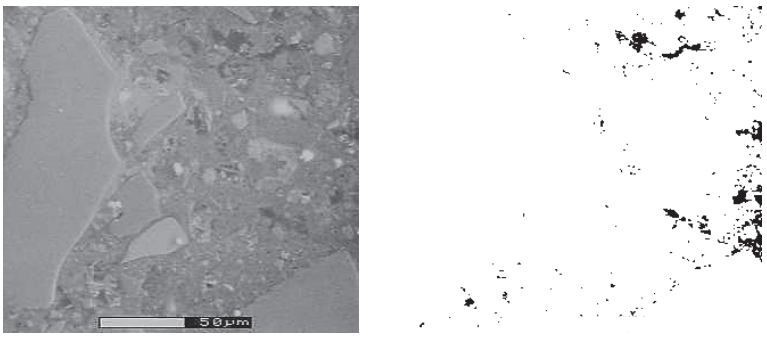

Figure 93. BSE image and the separated porosity phase of concrete 10+20 with a w/c ratio of 0.58 and cement content of 330 kg/m^3 with 66 kg/m^3 of limestone powder. The white measure at the bottom of the picture marks 50 µm.

The images revealed a rather similar microstructure which was consistent with the results obtained from the capillary water absorption tests. The differences were the most distinct between the concretes 10-20 and 10+20, which contained 264 kg/m^3 and 330 kg/m^3 of cement respectively. For comparison, Figure 94 presents the BSE and the separated porosity phase images of the concrete R3 with 265 kg/m^3 cement without mineral powders.

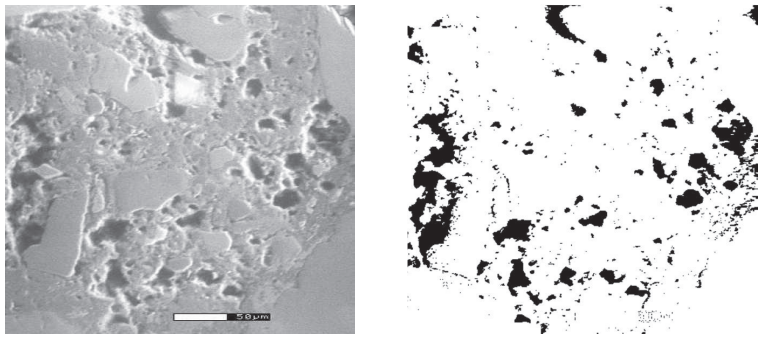

Figure 94. BSE image and the separated porosity phase of concrete R3 with a w/c ratio of 0,74 and cement content of 264 kg/m3. The white measure at the bottom of the picture marks 50 µm.

The concretes containing 50% or 70% GGBS presented similar results, although the porosities were lower than in the concretes with cement as the only binder, as expected from the absorption tests. BSE images with the separated porosity phase images of concretes with 50% or 70% of the binder consisting of GGBS are presented below in Figure 95, Figure 96, Figure 97, Figure 98, Figure 99 and Figure 100. All the samples had been hydrating for 56 days. The measure at the bottom of the images shows 20 µm.

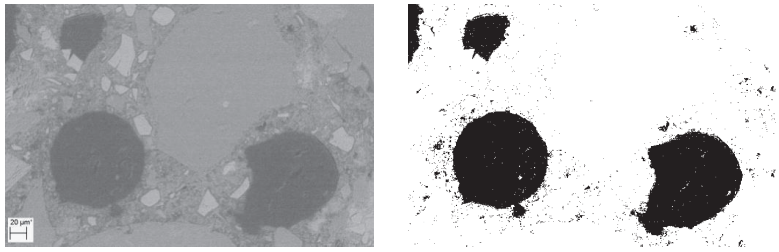

Figure 95. BSE image and the separated porosity phase of concrete 50-0 with a w/b ratio of 0,54 and binder content of 340 kg/m3.

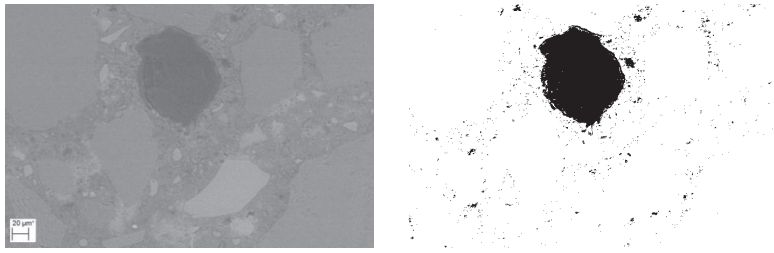

Figure 96. BSE image and the separated porosity phase of concrete 50+10 with a w/c ratio of 0,54 and binder content of 340 kg/m3 and 34 kg/m3 limestone powder.

As with the air-entrained concretes containing only cement as a binder, the microstructures of the samples with either 50% or 70% of the binder being GGBS were quite similar; however, some differences were observed. The addition of mineral powder seemed to have a positive effect on the porosity. Even when the amount of binder was reduced, the porosity of the concrete did not appear to have been significantly increased. However, the porosity of the concrete 70-10EHK seemed to be slightly higher than that of the other mineral powder concretes.

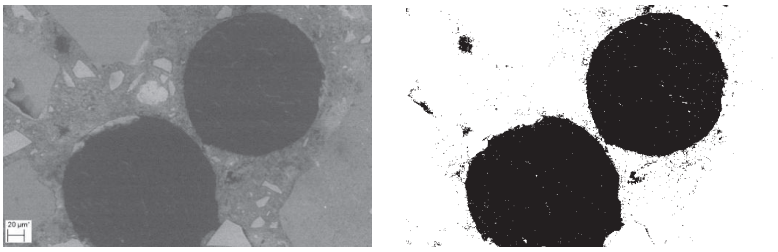

Figure 97. BSE image and the separated porosity phase of concrete 70-0 with a w/b ratio of 0.54 and binder content of 340 kg/m³.

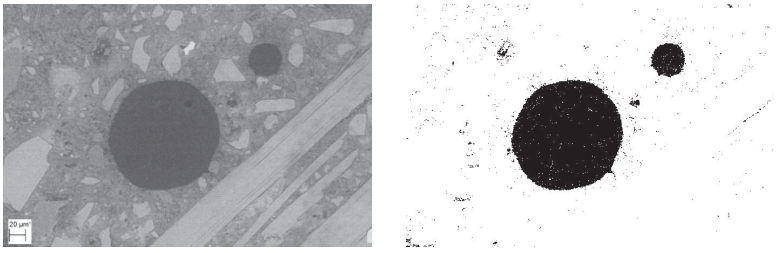

Figure 98 BSE image and the separated porosity phase of concrete 70+10 with a w/b ratio of 0.54 and binder content of 340 kg/m³ and 34 kg/m³ limestone powder.

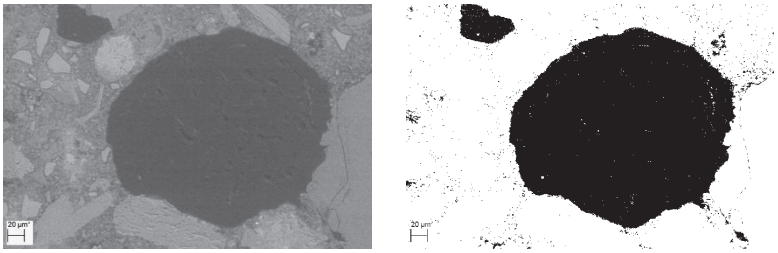

Figure 99 BSE image and the separated porosity phase of concrete 70-10 with a w/b ratio of 0.59 and binder content of 306 kg/m³ and 34 kg/m³ limestone powder.

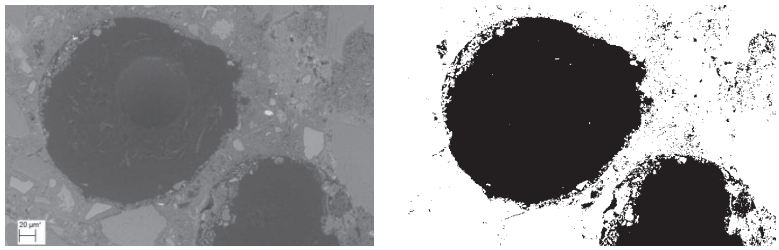

Figure 100 BSE image and the separated porosity phase of concrete 70-10EHK with a w/b ratio of 0.59 and binder content of 306 kg/m^3 and 34 kg/m^3 EHK quartz powder.

The distribution and quality of the entrained air was studied using optical microscopy and ESEM/BSE. No differences were found between the reference concrete and those containing mineral powder with respect to the spacing and shape of the entrained air. Figure 101 presents an optical microscope image of the specimens 10-10 and 10-0, where the larger entrained air bubbles are clearly visible.

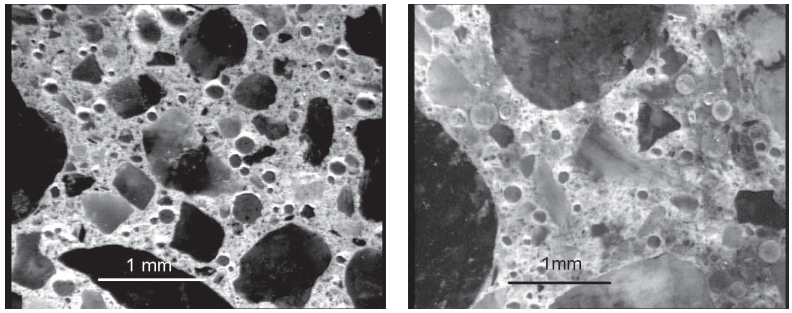

Figure 101. Optical microscope images of specimens 10-10 on the left and 10-0 on the right.

The smaller air bubbles are visible in the ESEM/BSE images in Figure 102 and Figure 103. In general, no differences between the different concretes were found in terms of the spacing or the shape of the entrained air. In Figure 102 and Figure 103, in a few of the air bubbles some residue from the sample cutting process has got stuck in the resin.

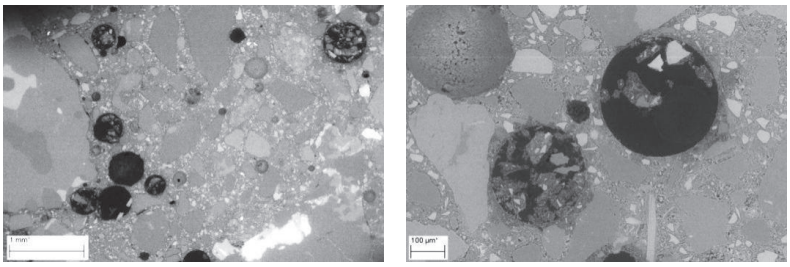

Figure 102. BSE images of concrete 70-10, showing the spacing and quality of the entrained air.

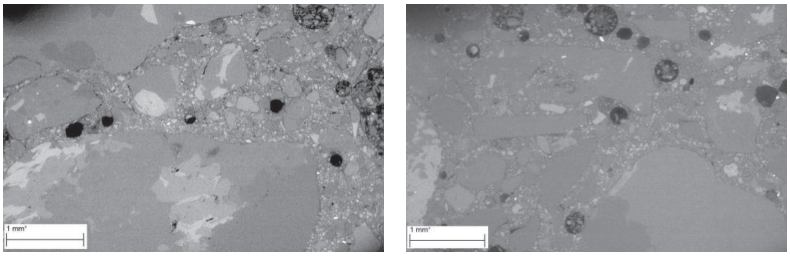

Figure 103. BSE images of concrete 50-0 on the left and 50-10 on the right, showing the spacing and quality of the entrained air.

Although no differences were found between the specimens with and without mineral powder, a peculiar phenomenon was found among the concretes containing GGBS. Large cracks stretching across the specimen were observed in all samples. Figure 104 presents BSE images of the specimens 70-10EHK and 70-0 where cracks filled with resin are visible as black lines. The cracking was not connected with the use of mineral powders but only with the utilisation of GGBS. No specific origin or terminal points were observed. The cracking was found to propagate though the cement paste without cutting the aggregate. Since the cracking was observed only in the concretes containing either 50% or 70% GGBS as a binder, it was concluded that most probably use of GGBS induced the cracking.

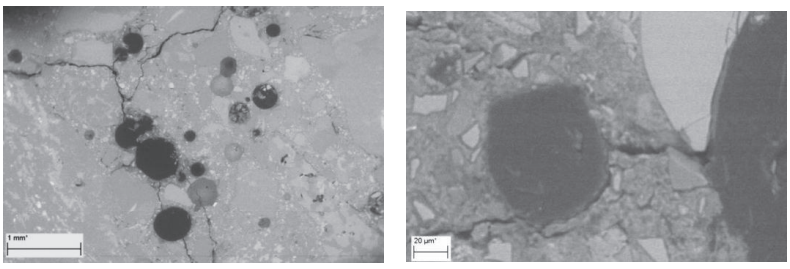

Figure 104. BSE images of specimen 70-10EHK on the left and a 500X magnification of the cracking in specimen 70-0 on the right. The cracks filled with resin are visible as black lines.

Concretes containing GGBS can be more prone to drying shrinkage cracking because of the increased setting time and a reduced rate of strength gain. However, the purpose of this research was not to study the susceptibility of GGBS concretes to cracking and thus this subject has not been covered further in this research. Nevertheless, this could be an important area for future research.

4.5.2 Conclusions

According to the results, a moderate cement reduction did not seem to have detrimental effects on the microstructure of the concrete. Actually, the amounts of unhydrated cement and the amount of porosity appeared to be somewhat lower in the concretes containing mineral powders than in the reference sample. This supports the higher compressive strength results obtained for the mineral powder concretes.

The formation of an ITZ, marked by increased capillary porosity, could not be avoided with these rather high water/cement ratios, but the BSE images revealed a denser cement paste structure in the ITZ of the mineral powder concretes. The less porous structure of the mineral powder concretes in the ITZ could be attributable to the heterogeneous nucleation theory. This theory was supported by the existence of small quartz particles in the vicinity of larger aggregate, which is visible in the ITZ, for example in Figure 88.

Although the use of mineral powders did seem to have some influence on the microstructure of the concrete, no evidence was found that the origin of the powder would have significant effects. The microstructures of the concretes containing either limestone or quartz powders were almost identical. Agglomerates of quartz particles were not found in any of the samples. The distribution of the limestone filler could not be investigated since they appear as the same greyish colour as the C-S-H gel. However, since the quartz particles did not form clusters, it would be safe to assume that the limestone particles would behave in a similar manner.

In the air-entrained concretes the studies showed that the pore distribution and the pore quality of the entrained air were similar in all of the test specimens. No evidence was found that the use of mineral powders would affect the spacing or the quality of the entrained air bubbles. The separated porosity phase images were congruent with the porosity data obtained during the freeze-thaw testing. Using GGBS to replace 50% or 70% of the cement reduced the porosity of the concretes. No evidence was found that replacing binder by 10 % or 20 % with limestone powder would notably

increase the porosity of the concrete. However, according to the separated porosity phase images, concrete containing EHK quartz powder had a slightly higher porosity than the other concretes consisting of 70/30% GGBS/cement.

The use of GGBS appeared to induce (drying shrinkage) cracking in the air-entrained concretes containing 50% or 70% of GGBS as the binder. The cracking was observed in concretes with and without mineral powders. Most probably, the cracking originated from the drying process of the polished samples (see the alcohol exchange method in the section titled “Materials and methods; Microstructure”), since no indication of cracking was discovered or indicated from the freeze-thaw test results. It is concluded that this phenomenon could be an important area for future research, but it is not discussed further in this study.

5. SUMMARY AND GENERAL CONCLUSIONS

The effects of different mineral powders on the properties of cement pastes and concrete were investigated. In the past, studies of the influence of fillers in concrete have mainly been focused on high-performance, high-strength and self-compacting concretes. However in the current research, the focus was on normal-strength concretes, which have been studied relatively little. Particular focus was on the effect of the mineral powders on concrete consistency, strength, microstructure and frost resistance. Of these, especially frost resistance and microstructure have previously received little attention.

In the study, one type of limestone powder and three types of quartz powders were investigated. All of the powders that were used were considered inert, although the $CaCO_3$ in limestone reacts with the alumina phases of the cement, but since it does not actively form cement gel it was considered as inert in this study, see section 2.1.1. Limestone powder in concrete. According to the results, the mineral powders had a considerable effect on the properties of the cement paste and concrete.

The research was divided into three parts:

- initial laboratory studies,
- mix design optimisation and
- definition of the effects of mineral powders on basic concrete properties, such as microstructure, the hydration process & products and frost durability

The initial laboratory studies suggested that nearly all mineral powder and cement combinations lowered the water requirement of cement pastes. However, for most of the cement and mineral powder combinations no distinct minimum, i.e. the lowest packing, was found for any cement-mineral powder combination. Because of the non-hydraulicity of the powders, the loss of strength was noticeable in all the combinations in which more than 10% of the cement was

replaced. On the other hand, replacing cement also reduced the water requirement in all of the mixes and thus it was concluded that some of the loss of strength might be compensated for by water reduction. The choices of material made in the subsequent parts of the research were mainly based on the results of the initial laboratory studies.

The second part of the research focused on quantifying the effects of mineral powders on the properties and strength of fresh concrete with the help of a statistical model. The following conclusions were drawn from the second part of the study:

- as predicted by the initial laboratory studies, the water requirement of the concretes that were studied appeared to decrease with the addition of mineral powders. The direct effect of the mineral powders on the strength of the concrete was estimated to be 0 to 5 MPa. Most of the strength gain occurred with additions of mineral powder up to 30%, and it did not change much at higher quantities. Although the direct strength effect of the powders was minor, because of the decrease in the water requirement of concretes with the addition of powders, the loss of strength resulting from replacing the cement could be compensated for with water reductions, while the workability could be maintained at the same level as that of the reference;
- increasing the fineness of the powder appeared to enhance the effect of heterogeneous nucleation and reduce the water requirement in concretes, since somewhat higher compressive strengths and flow table values were obtained for concretes made with the finest quartz powder;
- the statistical models formulated for the flow and strength of mineral powder concretes explained 78% and 85% of the variability in the test values, respectively.

The frost durability of mineral powder concretes, which was studied in the third part of the research, was found to be conditional on factors such as strength, capillary porosity, water uptake during the freeze-thaw testing and the calculated F-factor. No evidence was found that the use of mineral powders in itself would reduce the freeze-thaw resistance; however, the use of an inert powder to replace cement and the resulting higher water/cement ratio did have a negative effect on the durability. In addition, indications that the use of mineral powders would increase the required amount of air-entraining agent were found. The freeze-thaw durability of concretes made with at least 50% GGBS were not as heavily influenced by the reduction of the binder as was the case for concretes made with cement as the only binder. This was presumably the result of the delayed testing age and increased compressive strength of the GGBS concretes.

According to the results from the tests on the hydration process and hydration products, heat evolution appeared to be somewhat affected by the use of mineral powders. Greater hydration heat and thus higher maturities and compressive strengths were obtained for concretes containing up to 40% added mineral powder. However, increasing the amount of mineral powder did not proportionally increase the amount of hydrated heat. Altogether, the additions of 10% and 20% mineral powder were measured as having the greatest effect on the heat of hydration values.

TGA test results revealed that the amount of $Ca(OH)_2$ was, in general, lower in the mineral powder pastes but the degree of hydration was greater. The use of mineral powder to replace 10% of the cement had no effect or only a small one on the amount of Portlandite and compressive strength of the pastes. However, replacing a higher amount of cement reduced the amount of Portlandite and compressive strengths notably. In addition, the results from the TGA also suggested that some of the $CaCO_3$ from the limestone was being incorporated into the hydration phases.

The results with XRD backed up the results from the TGA. A 10% cement replacement appeared to have almost no effect on the amount of Portlandite at the age of 28 days. However, using mineral powders to replace 30% of the cement affected the amount of Portlandite notably. In many of the cement pastes in which mineral powders replaced cement, the net intensity of C_3S measured by XRD was lower than could be expected to happen as a result of mere cement replacement. It could be that in pastes with mineral powders more cement is hydrated. The findings on the amount of Portlandite and the compressive strength results support this.

Studies with the ESEM/BSE of mineral powder concretes revealed that a moderate cement reduction did not seem to have harmful effects on the microstructure of the concrete. The results suggested that incorporating mineral powders into the concrete mix might actually somewhat reduce the porosity and improve the structure of the ITZ.

In view of the results of this study, it seems that incorporating mineral powders into a concrete mix could have positive effects on the properties of fresh and hardened concrete. The most notable effect was the improved packing of the concrete mixtures, which resulted in a lower water requirement of the mineral powder that contained concretes. This property could be utilised by reducing the amount of cement in the mix by lowering the amount of water without compromising the strength or by increasing the strength by lowering the amount of water. Thus, in order to use mineral powders

to replace cement the amount of water needs to be lowered in order to compensate for the cement reduction, since the direct strength effect of the powders that were studied was, on average, from 0 to 5 MPa.

However, mineral powders reduced the compressive strengths of concretes when they were used to replace cement without compensation of the amount of water. Some indications that the use of mineral powders would require a larger amount of air-entraining agent were also found. In addition, although no remarkable differences in the properties under study were found between the different powders, it should be recognised that the use of limestone filler exposes concrete to the thaumasite form of sulphate attack; see the section titled “Literature review – Durability issues”. Thus, the origin of the mineral powder should be taken into account in design.

The use of mineral powders as a partial replacement of cement also requires the use of superplasticisers. Increasing the amount of fine powders requires an increase in the superplasticiser dosage, which can conversely affect the short-term development of strength. In the current study, however, the amounts of superplasticiser and mineral powder were kept at a moderate level.

Of the powders that were studied, the origin of the powder played only a minor role: powders with similar grading curves behaved in a similar manner and gave almost identical results. The most considerable effect was on the fineness of the powder – a finer powder appeared to improve the packing of the concretes and thus lower the water requirements the most. There was also some evidence that the pure strength effect, defined as heterogeneous nucleation, was larger with the finer powder. Since a finer grading of the powder can be regarded as favourable, co-grinding harder cement clinker with the desired amount of much softer limestone could produce the preferred concrete composition.

In the future, reducing the amount of cement of ordinary Portland cement concrete would help lower the CO_2 emissions and the energy consumption of concrete production. Lowering the amount of cement could also improve the cost-effectiveness of concrete production; in addition, a more economical and ecological concrete would conform well to the requirements of modern building material technology. However, this requires more research and it was not covered in this thesis. In conclusion, on the basis of the results of this study, it may be technically and economically beneficial to replace notable amounts of cement by fine mineral powders without pozzolanic or latent hydraulic properties, without impairing the properties of the fresh or hardened concrete.

6. REFERENCES

Abrams, D. A. 1918. Design of Concrete Mixtures. Bulletin, Vol. 1. Structural Materials Research Laboratory, Lewis Institute, Chicago.

Adams, L. D. and Race, R., M. 1990. Effect of limestone additions upon drying shrinkage of Portland cement mortar, Carbonate Additions to Cement, STP 1064, ASTM, Philadelphia. P. Klieger, R.D. Hooton, Editors , pp. 41-50.

Aïm, R. B., Goff, P.L. 1968. Effet de paroi dans les empilements désordonnés de sphères et application à la porosité de mélanges binaires. Powder Technology, Vol. 1, No. 5. pp. 281-290 (in French).

Aïtcin, P. C. 1998. High-performance concrete, E&FN Spon, London.

Amziane, S. 2006. Setting time determination of cementitious materials based on measurements of the hydraulic pressure variations. Cement and Concrete Research Vol. 36, No. 2, pp. 295-304.

Andreasen A. H. M., Andersen, J. 1930. Ueber die Beziehung zwischen Kornabstufung und Zwischenraum in Produkten aus Losen Körnern (mit einigen Experimenten), Kolloid-Zeitschrift Vol. 50, No.3, pp. 217-228 (in German).

Barnes, B.D., Diamond, S. and Dolch, W.L. 1978. The contact zone between portland cement paste and glass “aggregate” surfaces. Vol. 8, No. 2, pp. 233-243.

Bentur, A. 1991. Microstructure, interfacial effects and micromechanics of cementitious composites. In Advances in Cementitious Materials, ed. S. Mindess, Ceramic Transactions 16. American. Ceramic Society, Westerville, Ohio, pp. 523-550.

Bellmann, F. and Stark, J. 2007. Prevention of thaumasite formation in concrete exposed to sulphate attack. Cement and Concrete Research, Vol. 37, No. 8, pp.1215-1222.

Bensted, J. 1980. Some hydration investigations involving Portland cement - effect of calcium carbonate substitution of gypsum. World Cement Technology, Vol. 11, No. 8, pp. 395-406.

Bensted, J, 1999. Thaumasite - background and nature in deterioration of cements, mortars and concretes. Cement and Concrete Composites, Vol. 21 No. 2, pp.117-121.

Bentz, D. P., Garboczi, E. J., Haecker, C. J., Jensen, O. M. 1999. Effects of cement particle size distribution on performance properties of Portland cement-based materials. Cement and Concrete Research, Vol. 29 No. 10, pp. 1663-1671.

Bentz, D. P., Peltz, M. A. 2008. Reducing Thermal and Autogenous Shrinkage Contributions to Early-Age Cracking. ACI Materials Journal, Vol. 105, No. 4, pp. 414-420.

Bentz, D. P., Irassar, E. F., Bucher, B. E., Weiss, W. J. 2009(I). Limestone Fillers to Conserve Cement (in Low w/cm Concretes). Part I: An Analysis Based on Powers' Model. Concrete International, Vol. 31, No. 11, pp. 41-46.

Bentz, D. P., Irassar, E. F., Bucher, B. E., Weiss, W. J. 2009(II). Limestone Fillers to Conserve Cement (in Low w/cm Concretes). Part II: Durability issues and the effects of limestone fineness on mixtures. Concrete International, Vol. 31 No. 12, pp. 35-39.

Bigas, J. P. and Gallias, J. L. 2002. Effect of fine mineral additions on granular packing of cement mixtures. Magazine of Concrete Research, Vol. 54, No. 3, pp. 155-164.

Bigas, J. P. and Gallias, J. L. 2003. Single-drop agglomeration of fine mineral admixtures for concrete and water requirement of pastes. Powder Technology, Vol. 130, No. 1-3, pp. 110-115.

Binns T., 2003. Pumped concrete. Advanced Concrete Technology, Processes. John Newman (ed), Elsevier Ltd pp. 15/1-15/33.

Bobrowski, C. S., Wilson J. L. and Daugherty K. E. 1977. Limestone substitutes for gypsum as a cement ingredient. Rock Products, Vol. 8, No.2 pp.64-67

Bonavetti, V., Donza, H., Rahhal V. and Irassar, E. 2000. Influence of initial curing on the properties of concrete containing limestone blended cement. Cement and Concrete Research, Vol.30, No.5, pp.703-708

Bonavetti, V., Donza, H., Menéndez, G., Cabrera, O., Irassar, E., F. 2003. Limestone filler cement in low w/c concrete: A rational use of energy. Cement and Concrete Research, Vol. 33, No. 6, pp. 865-871

Breton, D., Carles-Gibergues, A., Grandet, J. 1993. Contribution to the formation mechanism of the transition zone between rock-cement paste. Cement and concrete research, Vol. 23, No.2, pp. 335-346.

Breugel, K. van. 1997. Simulation of hydration and formation of structure in hardening cement based materials. Ph.D. Thesis, Delft University of Technology, Delft, The Netherlands.

Brouwers, H. J. H. and Radix, H. J. 2005. Self-compacting concrete: the role of the particle size distribution. In: First International Symposium on Design, Performance and Use of Self-Consolidating Concrete SCC'2005 - China, 26 - 28 May 2005, Changsha, Hunan, China

Brown P. and Doerr, A. 2000. Chemical changes in concrete due to the ingress of aggressive species. Cement and Concrete Research, Vol. 30, No.3, pp. 411-418.

Brown, P. and Hooton, R. D. 2002. Ettringite and thaumasite formation in laboratory concretes prepared using sulfate-resisting cements. Cement & Concrete Composites, Vol. 24, No. 3-4, pp.361-370.

BY 50 Betoninormit 2004. (Finnish concrete code), Suomen Betoniyhdistys r.y.

Cembureau, 2012.
http://www.cembureau.be/sites/default/files/documents/World%20cement% 20production- by%20region%202011.pdf (last viewed on 24.5.2013)

Chatterji, S. and Jeffery, J. W., 1967. Further evidence relating to the new hypothesis of sulphate expansion. Magazine of Concrete Research, Vol. 19 No. 60, pp.185-189

Clark L. A (Chairman). 1999. The thaumasite form of sulfate attack: risks, diagnosis, remedial works and guidance on new construction: report of the Thaumasite Expert Group, Department of the Environment, Transport and the Regions, London, UK.

Crammond, N. J. and Halliwell, M. A. 1997. Assessment of the conditions required for the thaumasite form of sulfate attack, in: K.L. Scrivener, J.F. Young (Eds.), Mechanisms of Chemical Degradation of Cement- Based Systems, E&FN Spon, London, pp. 193- 200.

Cyr M., Lawrence P., Ringot E. 2005. Mineral admixtures in mortars: Quantification of the physical effects of inert materials on short-term hydration. Cement and Concrete Research, Vol. 35, No. 4, pp. 719-730.

Cyr M., Lawrence P., Ringot E. 2006. Efficiency of mineral admixtures in mortars: Quantification of the physical and chemical effects of fine admixtures in relation with compressive strength. Cement and Concrete Research, Vol. 36, No. 2, pp. 264-277.

Daimon, M. and Roy, D. M. 1979. Rheological properties of cement mixes II: Zeta potential and potential and preliminary viscosity studies. Cement and concrete research, Vol.9, No.1, pp.103-110.

Daniels, A. 1949. Calcite concrete - a new type of concrete. Betong, Vol. 33, No.1, pp.1-14.

Danielsen, S. W., Wallevik, O. 1989. Tilslag og fersk betongs egenskaper - statusrapport ("Aggregates and properties of fresh concrete - state-of-the-art"), Materialutvikling Høyfast betong, delrapport 1.1, 75 pp. In Norwegian.

Detwiler R. J. and Mehta, P. K. 1989. Chemical and physical effects of silica fume on mechanical behaviour of concrete. ACI Materials Journal. Vol. 86, No. 6, pp. 609-614.

Ellerbrock, H. G., Sprung, S. and Kuhlmann, K. 1985. Effect of interground additives on the properties of cement. Zement - Kalk - Gips, Vol 38, No. 10 pp. 586-588.

Erlin, B. and Stark, D. C., 1966. Identification and occurrence of thaumasite in concrete. Highway research record No.113 pp. 108-113.

Ezziane, K., Kadri, E. H., Hallal, A. and Duval, R. 2010. Effect of mineral additives on the setting of blended cement by the maturity method. Materials and Structures, Vol.43, No.3, pp.393-401.

Fagerlund, G. 2009. Chemically bound water as a measure of degree of hydration. Method and potential errors. Report TVBM-3150. Lund University. Sweden.

Farran, J. 1956. Contribution Mineralogique a L'etude de L'adherence Entre les Constiuants Hydrates des Ciments et les Materiaux Enrobe. Revue des Materiaux de Construction, No. 490-91, pp. 155-172.

Feng, N. Q., Li, G. Z. and Zang, X. W., 1990. High-strength and flowing concrete with a zeolitic mineral admixture. Cement, Concrete and Aggregates. Vol. 12, No. 2, pp. 61-69.

Fennis, S. A. A. M., 2011. Design of ecological concrete by particle packing optimization. Ph.D. Thesis. Delft University of Technology. The Netherlands.

Féret R. 1892. Sur la compacité des mortiers hydrauliques. Annale des Ponts et Chaussées Vol. 4 pp. 5-161.

Fiskaa, O., Hansen, H. and Moum, J., 1971. Concrete in alum shale. Norwegian Geotechnical Institute, Publication no. 86, Oslo 32p. (In Norwegian with an English summary).

Flatt, R. J., Houst, Y. F., Bowen, P. and Hofmann, H. 2000. Electrosteric repulsion induced by superplasticizers between cement particles - an overlooked mechanism? 6th CANMET/ACI International Conference on Superplasticizers and Other Chemical Admixtures in Concrete.

Hansen, P. Freiesleben and Pedersen J., 1977. Maturity Computer for Controlled Curing and Hardening of Concrete. Nordisk Betong, 1, pp. 19-34.

Fuller, W. B., Thompson, S. E. 1907. The laws of proportioning concrete. Transactions, American Society of Civil Engineers, Vol. 59, pp. 67-143.

Funk Sr. J. E., Dinger D. R., Funk Jr. J. E., 1980. Coal Grinding and Particle Size Distribution Studies for Coal-Water Slurries at High Solids Content. Tech. Rept., Empire State Electric Energy Research Corp., Syracuse, N.

Furnas, C. C. 1928. The relation between specific volume, voids, and size composition in systems of broken solids of mixed sizes. Report of Investigation Serial No. 2894, Department of Commerce, Bureau of Mines.

Furnas, C. C. 1931. Grading Aggregates - I - Mathematical Relations for Beds of Broken Solids of Maximum Density. Industrial and Engineering Chemistry. Vol. 23, No. 9 pp. 1052-1058.

Gallias, J. L., Kara-Ali R. and Bigas, J. P. 2000. The effect of fine mineral admixtures on water requirement of cement pastes. Cement and Concrete Research, Vol. 30 No. 10, pp. 1543-1549.

Goldman, A., Bentur, A., 1992. Effects of pozzolanic and non-reactive microfillers on the transition zone in high strength concretes. Proceedings of International Conference Interfaces in Cementitious Composites, RILEM, Toulouse, France, pp. 53-61.

Goldman, A., Bentur, A., 1993. The influence of microfillers on enhancement of concrete strength. Cement and Concrete Research, Vol. 23, No.4, pp. 962-972.

Goltermann, P., Johansen, V. and Palbol, L. 1997. Packing of aggregate: an alternative tool to determine the optimal aggregate mix. ACI Materials Journal, Vol. 94, No.5 pp. 435-443.

Greene, K. T. 1960. Early hydration reactions of Portland cement. Proceedings of the fourth International Symposium on Chemistry of Cements, Washington, pp. 359-386.

Gutteridge, W. A., Dalziel, J. A. 1990. Filler cement: The effect of the secondary component on the hydration of Portland cement: Part I. A fine non-hydraulic filler. Cement and Concrete Research, Vol. 20, No. 5, pp. 778-782.

Hartshorn, S. A., Swamy, R. N. and Sharp, J. H. 2001. Engineering properties and structural implications of Portland limestone cement mortar exposed to magnesium sulphate attack. Advances in Cement Research, Vol. 13, No. 1, pp.31-46.

Heikala, M., El-Didamonyb, H., and Morsyc, M. S. 2000. Limestone-filled pozzolanic cement. Cement and Concrete Research. Vol. 30, No. 11, pp.1827-1834.

Hewlett, P. (editor) 1998. Lea's Chemistry of Cement and Concrete (Fourth Edition).

Hoshino, M. 1988. Difference of the W/C ratio, porosity and microscopical aspect between the upper boundary paste and the lower boundary paste of the aggregate in concrete. Materials and Structures, Vol. 21, No.5, pp. 336-340.

Hunger, M., Brouwers, H. J. H. 2009. Flow analysis of water-powder mixtures: Application to specific surface area and shape factor. Cement and Concrete Composites, Vol. 31, No. 1, pp. 39-59.

Interational Energy Agency, 2009. Cement Technology Roadmap 2009, Carbon emissions reductions up to 2050.

Irassar, E. F., Bonavetti, V. L., Trezza, M. A. and González, M. A. 2005. Thaumasite formation in limestone filler cements exposed to sodium sulphate solution at 20 °C. Cement and Concrete Composites, Vol.27, No. 1, pp. 77-84.

Jensen, O. M., Hansen, P. F. 2001. Water-entrained cement-based materials I. Principles and theoretical background. Cement and Concrete research, Vol. 31, No. 4, pp. 647-654.

Johansen, K., Meland, I., Lindgård, J., Wallevik, O., Skjeggerud, K., Lindevall, G. and Hauck, C. 1992 Effekt av ulike fillertyper i sementbasert materialer (Effects of different fillers on cement based materials), Materialutvikling Høyfast Betong, delrapport 3.7., In Norwegian

Johansson A. and Tuutti K. 1976. Pumpbetong och betongpumpning. CBI forskning 10:76 Stockholm. (In Swedish)

Jones, M. R., Zheng, L. and Newlands, M. D. 2003. Estimation of the filler content required to minimise voids ratio in concrete. Magazine of Concrete Research, Vol. 55, No. 2, pp.193-202

Jones, M. R., Zheng, L. and Newlands, M. D. 2002. Comparison of particle packing models for proportioning concrete constituents for minimum voids ratio. Materials and Structures, Vol. 35, No.5, pp. 301-309.

Katz, A. and Baum, H. 2006. Effect of High Levels of Fines Content on Concrete Properties. ACI Materials Journal, Vol. 103, No. 6, pp. 474- 482.

Kjellsen, K., Lagerblad, B. 1995. Influence of natural minerals in the filler fraction on hydration and properties of mortars. CBI Report/ CBI Rapporter 3:95, 41 pp.

Kronlöf, A. 1997. Filler effect of inert mineral powder in concrete. Technical Research Centre of Finland, Publication 322.

Kwan, A. K. H. and Mora, C. F. 2001 Effects of various shape parameters on packing of aggregate particles. Magazine of Concrete Research, Vol. 53 No.2, pp. 91-100.

Lagerblad, B., Vogt, C. 2004. Ultrafine particles to save cement and improve concrete properties. CBI Report/ CBI Rapporter, 2004:1, 40 pp.

Larbi, J. A. 1993. Microstructure of the interfacial transition zone around aggregate particles in concrete. Cement and Concrete Research, Vol. 19, No. 2, pp. 161-172.

Larrard, F. de, 1989. Ultrafine particles for the making of very high strength concretes. Cement and Concrete Research, Vol. 19, No. 2, pp. 161-172.

Larrard F. de, Sedran, T. 1994, Optimization of ultra-high-performance concrete by the use of a packing model. Cement and Concrete Research, Vol. 24, No. 6, pp. 997-1009.

Larrard, F., de, 1999. Concrete Mixture Proportioning. E. & F. Spon, London

Lawrence, P., Cyr M., Ringot E. 2003. Mineral admixtures in mortars: Effect of inert materials on short-term hydration. Cement and Concrete Research, Vol. 33, No.12, pp. 1939-1947.

Lawrence, P., Cyr, M., Ringot, E. 2005. Mineral admixtures in mortars: Effect of type, amount and fineness of fine admixtures on compressive strength. Cement and Concrete Research, Vol. 35, No.6, pp. 1092-1105.

Malhotra, V. M., 1999. Role of supplementary cementing materials in reducing greenhouse gas emissions. Infrastructure regeneration and rehabilitation improving the quality of life through better construction : a vision for the next millennium : (Sheffield, 28 June - 2 July 1999).

Mannonen, R. 1996. Effects of addition time of sulphonated naphthalene-based superplasticizer on the properties of concrete. Dissertation. Report, Helsinki University of Technology, Faculty of Civil Engineering and Surveying, Concrete Technology, 1235-5925; 7

Marquardt, I. 2002. Ein Mischungskonzept für selbstverdichtenden Beton auf der Basis der Volumenkenngrößen und Wasseransprüche der Ausgangsstoffe. Dissertation. Rostocker Berichte, Heft 7, Universität Rostock. A short summary in English: Marquardt, Diederichs, Vala, 2003. Determination of the Optimum Water Content of SCC Mixes. DUSCC: Self-Consolidating Concrete-Notes from the First North American Conference. Editors: S. Shah, J. Daczko, J. Lingscheit. pp.81-87.

Maso, J. C. 1980. The bond between aggregates and hydrated cement pastes. Proceedings of the 7th International Congress on the Chemistry of cement, Paris, pp. 3-15.

Matthews, J. D. 1994. Performance of limestone filler cement concrete. Euro-Cements - Impact of ENV 197 on Concrete Construction, Ed. R. K. Dhir and M. R. Jones, E&FN Spon, London, pp. 113-147.

Mehta, P. K. 1987. Studies on the mechanisms by which condensed silica fume improves the properties of concrete. Proceedings International Workshop on Condensed Silica Fume in Concrete, CANMET, Ottawa, pp. 1-17.

Mehta, P. K. 1994. Rice husk ash: A unique supplementary cementing material. Advances in Concrete Technology, CANMET, Malhotra, V.M., ed., 2nd. edition, p. 407.

Miller, K. T., Melant, R. M., Zukoski, C. F. 1996. Comparison of the compressive yield response of aggregated suspensions: Pressure filtration, Centrifugation, and osmotic consolidation. Journal of the American Ceramic Society, Vol. 79, No. 10, pp. 2545-2556.

Mills, R. H. 1966. Factors influencing cessation of hydration in water-cured cement pastes. Special report No. 90, Highway Research Board, Washington D.C. pp. 406-424.

Monteiro, P. J. M., Mehta, P. K. 1986. Improvement of the aggregate-cement paste transition zone by grain refinement of hydration products. Proceedings of the 8th International Congress on the Chemistry of Cement Rio de Janeiro. pp. 433-437.

Moosberg, H. 2000. Utilisation of chemically inert or puzzolanic particles to modify concrete properties and save cement. Licentiate thesis, Luleå University of Technology, Sweden, p. 41.

Moosberg-Bustnes, H. 2003. Fine particulate by-products from mineral and metallurgical industries as filler in cement-based materials, Doctoral thesis, Luleå University of Technology Sweden, p. 97.

Negro, A., Abbiati, G. and Cussino, L. 1986. On the use of limestone to control cement setting. 8th 8th International Congress on the Chemistry of Cement Vol. 3, pp. 109-113.

Nehdi, M. 1996. Optimization of high strength limestone filler cement mortars. Cement and Concrete Research, Vol. 26, No.6, pp.883-893.

Nehdi, M. 1998. Microfiller effect on rheology, microstructure and mechanical properties of high-performance concrete. PhD thesis, University of British Columbia, Canada p. 186

Nehdi, M. Mindess, S. and Aïtcin, P. C. 1998. Rheology of High-Performance Concrete: Effect of Ultrafine Particles. Cement and Concrete Research. Vol. 28, No .5, pp. 687-697.

Nehdi, M. 2000. Why some carbonate fillers cause rapid increases of viscosity in dispersed cement-based materials. Cement and Concrete Research, Vol. 30, No. 10, pp.1663-1669.

Neto C. and Campiteli V., 1990. The influence of limestone additions on the rheological properties and water retention value of Portland cement slurries, Carbonate Additions to Cement, STP 1064, ASTM, Philadelphia. P. Klieger, R.D. Hooton, Editors , pp. 24-29.

Neville, A. M., 1995 Properties of concrete. 4th ed. Harlow : Longman.

Nykänen, J. 1973. Pumptransport av betong. Nordisk Betong G-1973. (In Swedish)

Okamura, H., Ozawa, K., 1995. Mix-design for Self-Compacting Concrete, Concrete Library, JSCE, No. 25, pp.107-120.

Ollivier, J. P., Grandet, J. 1982. Processus de formation de l'aure'ole de transition, Liaion pates de ciment materiaux associes, Coll. Int., pp. a14-a22.

Pera, J., Husson, S. and Guilhot, B. 1999. Influence of finely ground limestone on cement hydration. Cement and Concrete Composites, Vol. 21, No.2, pp.99-105.

Ping, X., Beaudoin, J. J. and Brousseau, R. 1991. Effect of aggregate size on transition zone properties at the portland cement paste interface. Cement and Concrete Research, Vol. 21, No. 6, pp. 999-1005.

Poijärvi, H. 1966. Kiviaineksen hienojakoisimman osan vaikutuksista betonin ominaisuuksiin. / On the effects of the finest part of aggregate on the properties of concrete. State Institute for Technical Research, Publication 110. (In Finnish).

Portland-Zementwerke Heidelberg, A.-G., 1972. Increasing sulfate resistance of Portland cement. German Patent 1646910, 31 May, 3 pp.

Powers, T. C., Brownyard, T.L. 1947. Studies of the Physical Properties of Hardened Portland Cement Paste. Journal of the American Concrete Institute, Oct. 1946-April 1947, Proceedings Vol. 43 (published in multiple parts). Published also in Research Laboratories of The Portland Cement Association Bulletin 22, Chicago 1948.

Puntke, W. 2002. Wasseranspruch von feinen Kornhaufwerken, Beton (5/02), pp. 242-248. (in German).

Ramachandran, V. S. and Zhang, C. 1986. Dependence of Fineness of Calcium Carbonate on the Hydration Behaviour of Tricalcium Silicate. Durability of Building Materials, Vol. 4 pp. 45-66.

Ramachandran, V. S. 1988. Thermal analysis of cement components hydrated in the presence of calcium carbonate. Thermochimica Acta, 127, 385-394.

Ramachandran,V. S., Malhotra, V.M., Jolicoeur, C. and Spiratos, N. 1998. Superplasticizers: Properties and Applications in Concrete. CANMET, Canada

Ramachandran, V. S. 2001. Concrete admixtures handbook: properties, science, and technology / edited by V.S. Ramachandran., Norwich (NY): Knovel.

RILEM TC 119-TCE. 1997. TCE1:Adiabatic and semi-adiabatic calorimetry to determine the temperature increase in concrete due to hydration heat of the cement. Materials and Structures, Vol. 30, No.8. pp. 451-464.

Rosenberg, A. M., Gaidis, J. M. 1989, A New mineral admixture for high-strength concrete, Concrete International, Vol. 11, No. 4, pp.31-36.

Schindler, A. and Folliard, K. 2003. Influence of supplementary cementing materials on the heat of hydration of concrete. Proceedings of the Ninth Conference on Advances in Cement and Concrete, Copper Mountain, Colorado, August 10-14, pp. 17-26.

Schmidt, M., 1992. Cement with interground additives - capabilities and environmental relief, part 1 Zement-Kalk-Gips, Vol. 45, No. 2, pp. 64 - 69.

Schmidt, M., Harr, K. and Boeing, R. 1993. Blended cement according to ENV 197 and experiences in Germany. Cement, Concrete, and Aggregates, ASTM, Vol. 15, No. 2, pp. 156 - 164.

Scrivener, K. L., Pratt, P. L. 1986. A preliminary study of the microstructure of the cement/sand bond in materials. Proceedings of the 8th International Congress on the

Chemistry of Cements, Rio de Janeiro, Vol. III, p. 466-471

Scrivener, K. L., Pratt, P. L. 1987. The charachterisation and quantification of cement and concretes microstructures, In: Proceedings of the First International Rilem Congress Vol 1 Pore structure and Materials Properties, Versailles, France, pp. 61-68.

Scrivener, K. L., Crumbie, A. K. Laugesen, P. 2004. Interfacial Transition Zone (ITZ) Between Cement Paste and Aggregate in Concrete. Interface Science 12, pp. 411-421.

Scrivener, K. L. 2004. Backscattered electron imaging of cementitious microstructures: understanding and quantification, Cement & Concrete Composites Vol. 26, No. 8, pp. 935-945.

Sedran, T., de Larrard F., Hourst, F. and Contamines, C. 1996. Mix design of self-compacting concrete. In: Bartos PJM et al (eds) Proceedings of the international RILEM conference on production methods and workability of concrete. Paisley, Scotland, pp. 439-450.

Sellevold, E. J., Bager, D. H., Klitgaard-Jensen, E. K., and Knudsen, T., 1982. Silica Fume Cement Pastes: Hydration and Pore Structure, Report BMI 82.610, Trondheim, Norwegian Institute of Technology, pp. 19-50.

Sellevold, E. L., 1987, The function of condensed silica fume in high strength concrete, Symposium on utilisation of HSC, Trondheim, Norway, June, pp.39-50.

Stumm, W., 1992, Chemistry of the Solid –Water Interface; Processes at the Mineral-Water and Particle-Water Interface in Natural Systems, Wiley, New York.

Stutzman, P. E., 1996. Guide for X-Ray Powder Diffraction Analysis of Portland Cement and Clinker, National Institute of Standards and Technology Internal Report 5755.

SFS-EN 13286-2 Sitomattomat ja hydraulisesti sidotut seokset. Osa 2: Vertailutiiviyden ja vesipitoisuuden määritysmenetelmä. Proctor-tiivistys. Unbound and hydraulically bound mixtures. Part 2: Test methods for the determination of the laboratory reference density and water content. Proctor compaction

SFS-EN 196-3 Sementin testausmenetelmät. Osa 3: Sitomisajan ja tilavuuden pysyvyyden määritys. Methods of testing cement. Part 3: Determination of setting times and soundness.

SFS-EN 12350-5 Tuoreen betonin testaus. Osa 5: Leviämä.

SFS-EN 12350-7 Tuoreen betonin testaus. Osa 7: Ilmamäärä. Painemenetelmät.

SFS-EN 196-1 Methods of testing cement. Part 1: Determination of strength.

SFS-EN 12390-3 Testing hardened concrete. Part 3: Compressive strength of test specimens.

Sims, I. and Huntley, S. A., 2004. The thaumasite form of sulfate attack-breaking the rules. Cement & Concrete Composites, Vol. 26, No.7, pp. 837-844.

SINTEF 1994. Konstruksjoner og betong. Kvalitetskring. Betong. Bestemmelse av kapillær sughastighet og porøsitet. Trondheim.

Soroka, I. and Stern N. 1976. Effect of calcareous fillers on sulfate resistance of Portland cement. Ceramic bulletin. Vol. 55, No. 6, pp.594-595.

Soroka, I. and Stern, N. 1976. Calcareous fillers and the compressive strength of Portland cement. Cement and Concrete Research Vol. 6, No. 3, pp. 367-376.

Soroka, I. and Setter, N. 1977.The effect of fillers on strength of cement mortars. Cement and Concrete Research, Vol. 7, No. 4, pp. 449-456.

Sprung, S., and Siebel, E. 1991. Assessment of the Suitability of Limestone for producing Portland Limestone Cement, Zement-Kalk-Gips, Vol. 44, No. 1, pp. 1-11.

Stovall, T., de Larrard, F., Build, M. 1986, Linear Packing Density Model of Grain Mixtures. Powder Technology, Vol. 48, No.1, pp. 1-12.

Sugamata, T., Edamatsu, Y. and Ouchi, M. 2001. Distinction between particle-dispersion and particle-repulsion effects of superplasticizers on the viscosity of fresh mortar. Proceedings of the Second International Symposium on self-Compacting Concrete, Tokyo, Japan, pp. 213- 220.

Tattersall, G. H. and Banfill, P. F. G. 1983. The rheology of fresh concrete, Pitman Advanced Publishing Program, London.

Taylor, H. F. W., 1997. Cement chemistry. 2nd ed. Thomas Telford, London.

Torres, S. M., Sharp, J. H., Swamy, R. N., Lynsdale, C. J. and Huntley, S. A. 2002. Long term durability of Portland limestone cement mortars exposed to magnesium sulfate attack. 1st International Conference on Thaumasite in Cementitious Materials BRE. Watford, UK.

Toufar, W., Born, M., Klose, E. 1976. Beitrag zur Optimierung der Packungsdichte polydisperser körniger Systeme. Freiberger Forschungsheft 558 pp. 29-44.

Tsivilis, S., Tsantilas, J., Kakali, G., Chaniotakis, E. and Sakellariou, A. 2003. The permeability of Portland limestone cement concrete. Cement and Concrete Research, Vol. 33 No. 9, pp. 1465-1471.

Uysal, M., Yilmaz, K. and Ipek, M. 2012. The effect of mineral admixtures on mechanical properties, chloride ion permeability and impermeability of self-compacting concrete. Construction and Building Materials, Vol. 27, No. 1, pp. 263-270.

Valtion teknillinen tutkimuslaitos, 1970. Betoniteknillisiä koetusohjeita. 3, Runkoaineen koetus, eineosien koetus betonikokein, betonimassan, kovettuneen betonin ja eräiden betonituotteiden koetus. Tiedonanto / Valtion teknillinen tutkimuslaitos, betoniteknillinen laboratorio; 3. (In Finnish)

Vuk, T., Gabrovšekb, R. and Kaučičb, V. 2002. The influence of mineral admixtures on sulfate resistance of limestone cement pastes aged in cold $MgSO_4$ solution. Cement and Concrete Research, Vol. 32, No. 6, pp. 943-948.

Wong, H. H. C. and Kwan, A. K. H. 2008 (I). Packing density of cementitious materials: part 1—measurement using a wet packing method. Materials and Structures Vol. 41, No. 4 pp.689-701.

Wong, H. H. C. and Kwan, A. K. H. 2008 (II). Rheology of cement paste: Role of excess water to solid surface area ratio. Journal of Materials in Civil Engineering Vol. 20, No.2, pp. 189-197.

Yoshioka, K., Sakai, E., Daimon, M. and Kitahara, A. 1997. Role of Steric Hindrance in the Performance of Superplasticizers for Concrete. Journal of the American Ceramic Society. No. 80, No. 10 pp. 2667-2671.

Zimbelmann, R. 1985. A contribution to the problem of cement-aggregate bond. Cement and Concrete Research, Vol. 15, No.5, pp. 801-808.

Appendix 1. Mix design and test results of concretes

Name	Cement [kg/m^3]	MP [kg/m^3]	Type of powder	Water [kg/m^3]	W/C ratio	Aggregate [kg/m^3]	SP [kg/m^3]	SP [%]	Air [%]	Total ≤0.125mm [kg/m^3]	Flow [mm]	fm	Slump [mm]	Compressive strength 1d [MPa]	Compressive strength 7d [MPa]	Compressive strength 28d [MPa]	Compressive strength 91d [MPa]
R1	265	0	-	185	0.698	1952	1.00	0.38	2.4	364.01	200	0.00	30	0.0	26.9	32.3	38.3
R2	265	0	-	185	0.698	1952	1.15	0.43	2.9	364.01	200	0.00	30	8.2	27.4	33.7	38.9
R3	265	0	-	195	0.736	1925	1.15	0.43	1.9	364.01	200	0.00	110	0.0	23.5	28.7	33.7
R4	265	0	-	185	0.698	1951	1.40	0.53	2.7	364.01	200	0.00	40	9.8	26.8	30.3	35.1
R5	265	0	-	180	0.679	1965	1.40	0.53	2.8	364.01	200	0.00	10	0.0	23.0	27.5	33.9
C25L7	250	175	Limest.	175	0.698	1814	2.00	0.47	2.6	494.56	325	1.64	90	11.3	30.8	36.3	42.8
C25L6	250	145	Limest.	171	0.684	1856	1.60	0.41	3.2	469.10	275	0.89	60	11.6	30.5	36.9	43.7
C26L60	262	152	Limest.	158	0.601	1872	2.00	0.48	2.4	489.95	370	2.42	130	12.0	32.8	40.3	44.9
C26L3	265	80	Limest.	170	0.642	1910	2.00	0.58	1.9	411.37	300	1.25	60	12.1	31.9	38.3	44.4
C26L45	265	119	Limest.	169	0.640	1874	1.82	0.47	3.2	453.25	300	1.25	120	16.3	32.7	39.3	45.7
C26L61	265	153	Limest.	169	0.640	1839	1.96	0.47	2.8	492.94	300	1.25	120	19.4	33.0	38.2	45.5
C26L62	265	159	Limest.	185	0.698	1791	1.60	0.33	2.0	493.25	435	3.73	-	10.5	29.0	34.4	40.2
C26N60	265	159	Q. Nilsiä	185	0.698	1791	1.60	0.38	2.4	493.97	415	3.31	-	11.2	29.2	34.3	40.4
C26K6	265	159	Q. Kemiö	185	0.698	1791	1.85	0.44	2.3	493.96	435	3.73	-	9.2	29.7	35.7	41.0
C26L63	265	159	Limest.	185	0.698	1791	1.75	0.38	2.6	493.96	470	4.52	-	9.4	29.8	35.6	40.5
C26N61	265	159	Q. Nilsiä	185	0.698	1790	2.00	0.47	1.5	493.96	525	5.89	-	10.5	31.1	36.7	42.1
C26EHK6	265	159	Q. EHK	185	0.698	1791	1.60	0.43	1.8	492.78	575	7.27	-	9.9	29.0	35.1	44.3
C26L65	265	159	Limest.	185	0.698	1790	2.00	0.47	0.9	492.76	510	8.46	-	10.0	28.3	34.2	41.9
C26L35	265	95	Limest.	185	0.698	1857	1.20	0.33	1.7	428.75	430	3.62	-	9.0	28.0	34.3	42.1
C26K4	265	95	Q. Kemiö	185	0.698	1857	1.20	0.33	2.4	428.75	470	4.52	-	9.0	29.8	35.8	42.3
C26EHK3	265	80	Q. EHK	185	0.698	1871	1.60	0.46	1.1	390.59	505	5.38	-	9.5	29.5	35.9	41.7
C26L8F0	265	205	Limest.	185	0.698	1744	1.90	0.40	2.3	476.43	400	3.00	-	10.8	30.3	36.2	41.9
C26L66	265	165	Limest.	185	0.698	1784	2.00	0.47	2.5	503.32	455	4.18	-	10.9	30.2	36.7	41.7
C26L80	265	215	Limest.	185	0.698	1733	2.25	0.47	1.6	546.54	540	6.29	-	12.0	32.2	38.2	43.4
C26L95	265	250	Limest.	185	0.698	1698	2.35	0.46	2.6	580.85	455	4.18	-	11.5	32.2	37.7	42.0
C26L31	265	80	Limest.	185	0.698	1869	2.00	0.58	1.3	411.89	430	3.62	140	8.4	26.7	33.6	40.1
C26L32	265	80	Limest.	185	0.698	1873	0.70	0.20	3.6	412.23	300	1.25	50	8.4	26.7	32.0	39.7
C26L33	265	80	Limest.	190	0.717	1859	0.90	0.26	2.1	412.61	445	3.95	-	9.1	26.5	31.3	41.0

Name	Cement [kg/m^3]	MP [kg/m^3]	Type of powder	Water [kg/m^3]	W/C ratio	Aggregate [kg/m^3]	SP [kg/m^3]	SP [%]	Air [%]	Total ≤0,125mm [kg/m^3]	Flow [mm]	Γm	Slump [mm]	Compressive strength 1d [MPa]	Compressive strength 7d [MPa]	Compressive strength 28d [MPa]	Compressive strength 91d [MPa]
C26L50	265	135	Limest.	185	0.698	1815	1.80	0.45	0.9	468.76	550	6.56	-	9.7	29.8	33.9	40.6
C26L70	265	186	Limest.	185	0.698	1764	1.80	0.40	1.7	527.41	555	6.70	-	10.4	29.3	35.4	42.0
C26L81	265	212	Limest.	185	0.698	1737	1.80	0.38	1.7	553.38	565	6.98	-	10.0	30.0	35.2	41.4
C26L100	265	265	Limest.	185	0.698	1681	2.90	0.55	2.0	594.71	510	5.50	-	8.7	27.8	33.9	39.0
C26L67	265	159	Limest.	185	0.698	1790	2.00	0.47	1.7	498.69	490	5.00	-	9.0	26.6	33.6	38.9
C26L68	265	159	Limest.	185	0.698	1790	2.00	0.47	1.7	493.96	490	5.00	-	11.7	29.2	35.9	40.6
C26L69	265	159	Limest.	185	0.698	1790	2.00	0.47	1.2	493.96	520	5.76	-	10.9	28.8	36.1	42.0
C26L71	265	159	Limest.	185	0.698	1790	2.00	0.47	1.0	493.96	500	5.25	-	11.0	30.3	36.4	41.9
R6	300	0	-	195	0.650	1894	1.50	0.50	2.5	388.54	405	3.10	-	0.0	24.9	30.6	36.3
R7	300	0	-	182	0.607	1930	0.90	0.30	1.3	387.82	350	2.06	60	11.6	33.8	41.1	47.2
C30L30	300	90	Limest.	190	0.633	1817	1.70	0.44	0.8	457.61	605	8.15	-	12.0	33.7	40.9	48.7
C30L40	300	125	Limest.	175	0.583	1822	1.63	0.38	3.2	496.25	390	2.80	140	19.9	37.4	43.9	51.2
C28L20	283	57	Limest.	190	0.670	1865	1.40	0.41	3.4	420.75	390	2.80	-	11.9	24.1	31.9	43.8
C28L21	283	57	Limest.	200	0.706	1838	1.40	0.41	2.6	420.64	455	4.18	-	11.8	24.3	29.4	35.8
C28K2	283	57	Q. Kemiö	200	0.706	1838	1.40	0.41	2.8	418.94	465	4.41	-	0.0	27.1	32.4	39.4
C28L22	283	57	Limest.	177	0.623	1900	1.40	0.41	4.1	419.39	320	1.56	100	10.0	30.4	36.2	43.6
C28L23	283	57	Limest.	185	0.652	1878	1.40	0.41	3.9	419.05	395	2.90	-	7.7	28.3	33.5	39.4
C28L24	283	57	Limest.	190	0.670	1865	1.40	0.41	3.0	419.05	425	3.52	-	0.0	27.3	33.5	38.5
C28L35	283	100	Limest.	180	0.634	1849	1.20	0.31	7.0	451.61	440	3.84	-	9.8	27.3	31.4	40.3
C28L30	285	85.5	Limest.	190	0.667	1835	1.45	0.39	2.6	456.95	465	4.41	-	0.0	27.7	34.2	40.3
C29L30	293	88	Limest.	185	0.631	1838	1.60	0.42	1.9	448.62	480	4.76	-	12.1	33.3	39.4	46.8
C29L31	293	88	Limest.	185	0.631	1839	1.50	0.39	6.3	448.62	615	8.46	-	9.7	27.1	31.0	39.7
C29L35	293	103	Limest.	185	0.631	1823	1.80	0.45	1.1	464.77	550	6.56	-	12.5	34.4	40.7	49.9
C29N30	293	88	Q. Nilsiä	185	0.631	1839	1.50	0.39	1.1	448.62	580	7.41	-	11.6	34.5	40.6	48.9
C29L45	293	130	Limest.	182	0.621	1803	1.88	0.44	2.7	490.55	485	4.88	-	16.1	35.5	40.9	48.0
C29L32	293	98	Limest.	183	0.625	1834	1.60	0.41	1.4	459.76	555	6.70	-	11.9	33.9	42.4	49.1
C29N31	293	98	Q. Nilsiä	183	0.625	1834	1.60	0.41	1.6	459.76	555	6.70	-	11.8	34.9	42.7	44.1
C29K30	293	98	Q. Kemiö	183	0.625	1834	1.60	0.41	1.3	459.76	525	5.89	-	13.0	37.2	43.7	45.3

Appendix 1. Mix design and test results of concretes

Name	Cement [kg/m^3]	MP [kg/m^3]	Type of powder	Water [kg/m^3]	W/C ratio	Aggregate [kg/m^3]	SP [kg/m^3]	SP [%]	Air [%]	Total ≤0,125mm [kg/m^3]	Flow [mm]	Γm	Slump [mm]	Compressive strength 1d [MPa]	Compressive strength 7d [MPa]	Compressive strength 28d [MPa]	Compressive strength 91d [MPa]
C29EHK	293	98	Q. EHK	183	0.625	1834	1.60	0.41	1.3	464.9	575	7.27	-	13.5	37.1	45.6	51.2
C29L46	293	130	Limest.	182	0.621	1803	1.88	0.44	2.7	490.55	445	3.95	-	16.1	32.3	39.1	44.5
C29L40	295	110	Limest.	185	0.627	1815	1.54	0.38	1.9	479.80	440	3.84	-	15.1	34.2	40.3	47.2
C29L41	295	100	Limest.	185	0.627	1825	1.58	0.40	2.8	477.62	380	2.61	-	14.5	31.9	37.5	44.6
C29L42	295	110	Limest.	185	0.627	1814	1.75	0.43	1.8	487.21	570	7.12	-	13.6	34.0	40.7	46.2
R8	340	0	-	200	0.588	1846	1.40	0.41	3.8	420.84	425	3.52	-	8.8	31.2	37.6	43.7
R9	322	0	-	202	0.627	1858	0.85	0.26	1.0	409.52	440	3.84	100	9.2	30.2	36.4	43.5
R10	322	0	-	202	0.627	1858	1.00	0.31	0.9	399.13	465	4.41	-	10.8	32.3	40.2	44.8
R11	322	0	-	202	0.627	1858	1.00	0.31	0.9	407.50	505	5.38	-	0.0	33.5	40.8	47.2
R12	338	0	-	208	0.615	1828	1.00	0.30	1.8	421.21	440	3.84	90	8.6	31.0	37.3	43.5
R13	340	0	-	200	0.588	1845	1.87	0.55	1.3	420.84	535	6.16	-	15.8	37.1	42.5	49.9
R14	340	0	-	215	0.632	1806	1.40	0.41	1.6	407.23	490	5.00	-	8.5	28.3	34.2	44.6
R15	340	0	-	215	0.630	1806	1.39	0.41	8.1	407.12	630	8.92	-	9.1	26.7	32.1	41.2
C34L2	340	68	Limest.	200	0.588	1776	2.20	0.54	0.8	486.41	615	8.46	-	14.0	38.9	46.3	53.0
C34EHK	340	34	Q. EHK	200	0.588	1810	2.05	0.55	0.9	455.16	580	7.41	-	11.4	36.4	44.7	50.9
C32L30a	322	100	Limest.	195	0.606	1773	2.00	0.47	7.3	495.33	650	9.56	-	10.3	28.6	37.3	45.6
C32L30	322	100	Limest.	195	0.606	1773	2.00	0.47	0.7	491.38	595	7.85	-	14.1	38.2	44.6	51.5
C32L31	322	100	Limest.	190	0.590	1787	1.95	0.46	1.3	491.43	525	5.89	-	14.9	38.1	44.8	51.1
C32L21	340	100	Limest.	200	0.588	1743	2.42	0.55	1	510.44	610	8.3	-	12.5	38.1	46.5	51.5
RR	293	0	-	183	0.625	1933	1.30	0.44	1.7	371.46	330	1.7	50	9.5	30.4	39.2	44.2

Appendix 2. Calculation of parameter H_p and H_v.

Calculation of parameter H_p is defined as follows.

$$H_p = \sum_j h_j = \sum_j \sum_i a_{ij} p_{ij}$$

in which

a_{ij} is the share of the dry material -class *i* in granular class *j* as defined by sieve sizes and satisfies

$$\sum_i a_{ij} = 1$$

for all *j*.

p_{ij} is the passing value of the dry material -class *i* in granular class *j* by weight as retained on each of a specified series of sieves.

Dry material consists of all aggregate, fillers, powders and binders.

Parameter H_v is calculated as H_p but instead of using weights, the results are presented as volume ratios.

Appendix 3. Mix design and test results of concretes used in testing of hydration processes and hydration products

Name	Cement [kg/m^3]	MP [kg/m^3]	Type of powder	Water [kg/m^3]	SP [%]	Air [%]	Total ≤0,125mm [kg/m^3]	Flow [mm]	Slump [mm]	Compressive strength 1d [MPa]	Compressive strength 7d [MPa]	Compressive strength 28d [MPa]
B0	270	0	-	185	0.489	3.6	344.23	340	30	7.3	23.1	30.7
B10	270	27	Limestone	185	0.489	3.2	370.29	400	150	7.9	24.9	34.1
B20	270	54	Limestone	185	0.489	3.0	396.34	430	170	8.1	25.6	34.0
B30	270	81	Limestone	185	0.489	3.0	422.39	440	190	8.0	25.3	33.7
B40	270	108	Limestone	185	0.489	3.0	448.34	410	150	7.8	25.1	33.9
BQ10	270	27	Quartz N	185	0.489	3.0	369.07	380	100	7.9	25.0	34.3
BQ20	270	54	Quartz N	185	0.489	2.9	393.91	440	170	8.0	25.8	34.8
BQ30	270	81	Quartz N	185	0.489	2.6	418.75	440	190	8.5	25.9	33.9
BQ40	270	108	Quartz N	185	0.489	2.7	443.59	420	190	7.9	25.7	33.9

Appendix 4. TGA and TGA derivative curves of cement pastes

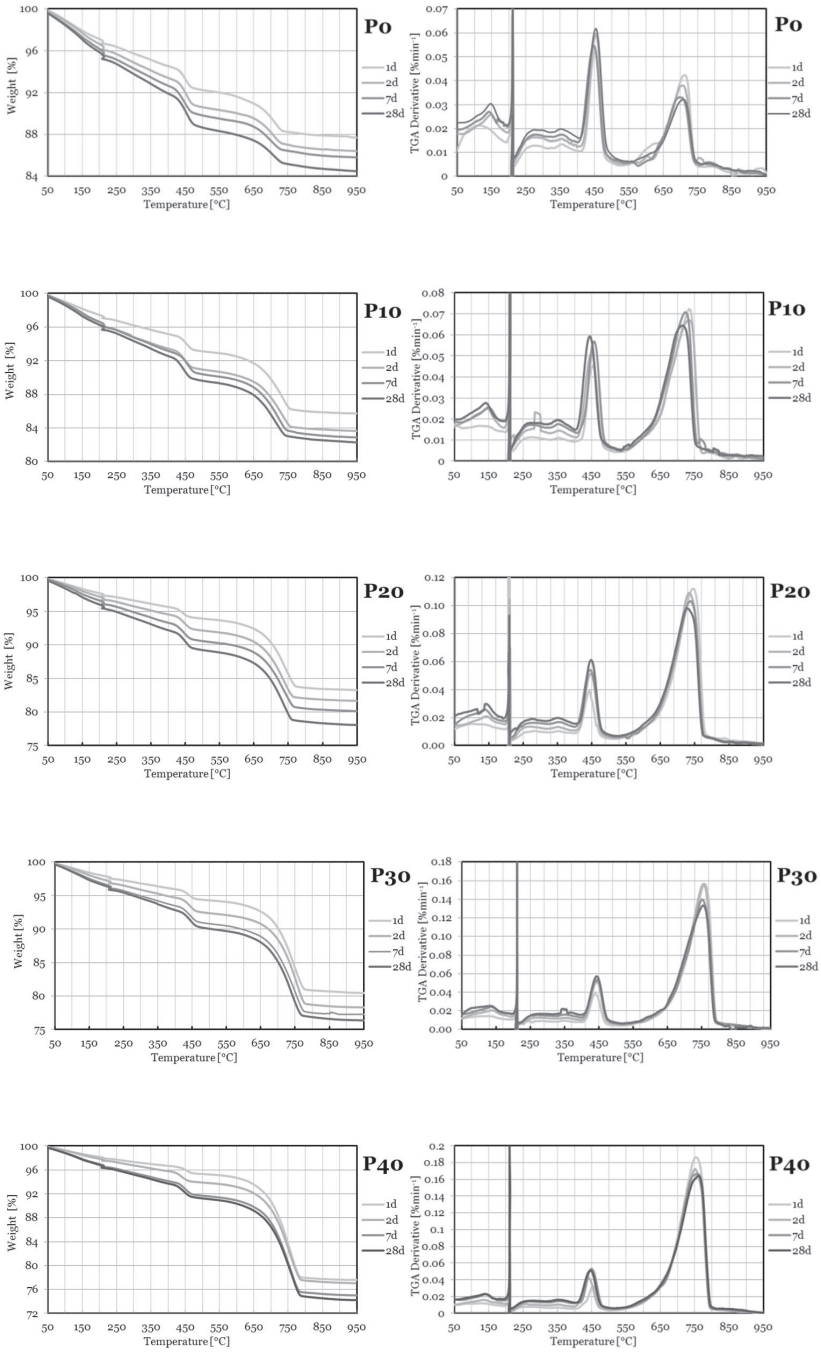

Appendix 4. TGA and TGA derivative curves of cement pastes

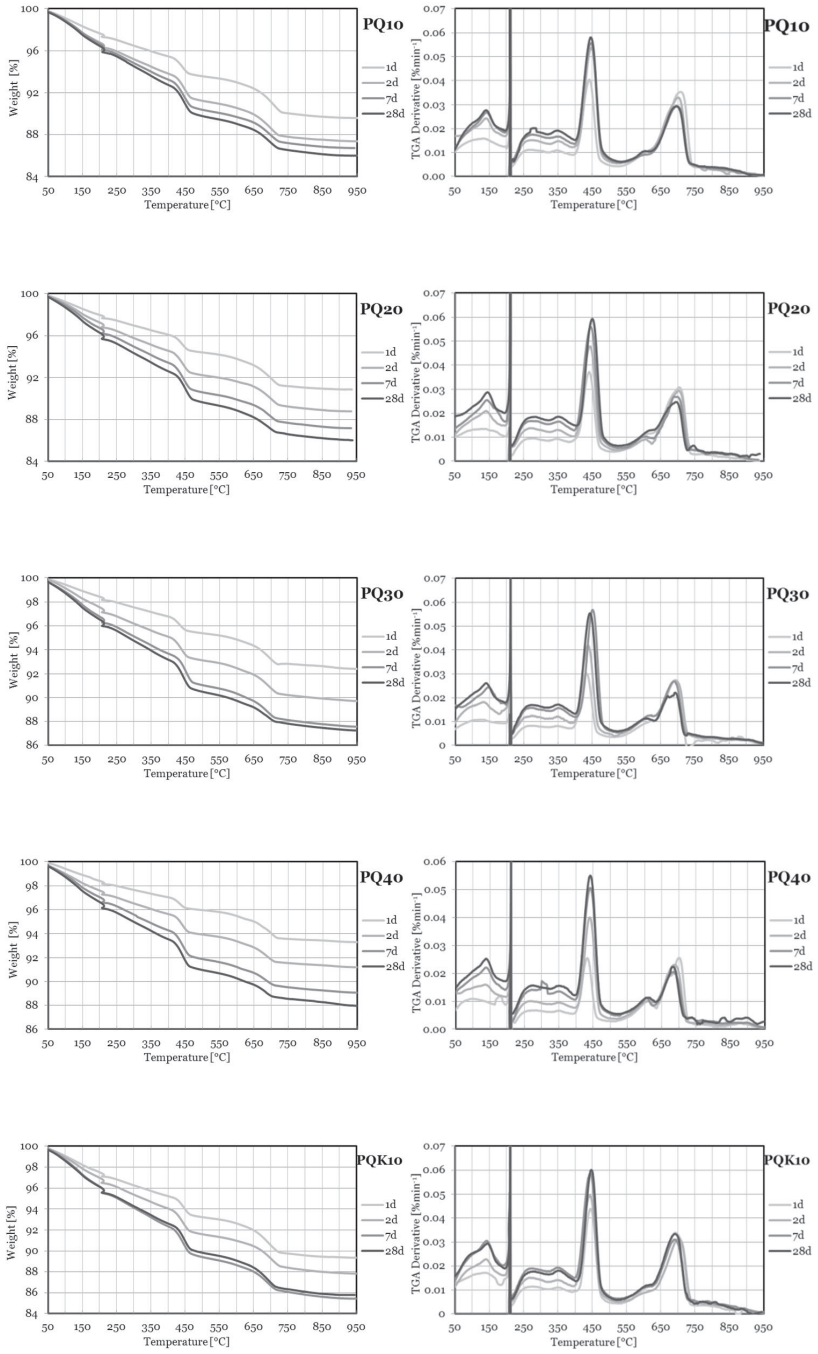

Appendix 4. TGA and TGA derivative curves of cement pastes

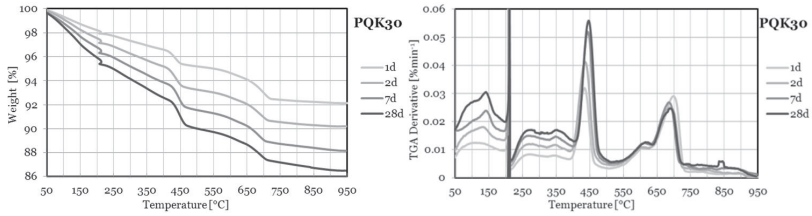

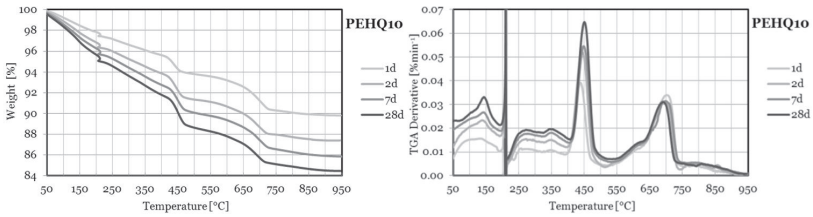

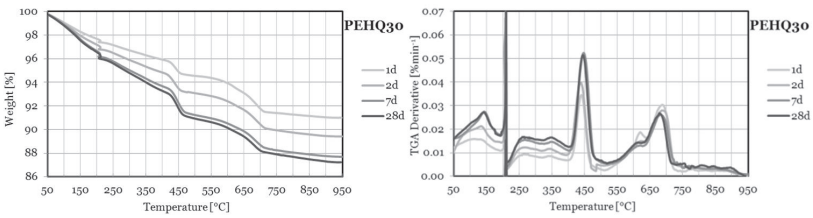

Appendix 5. XRD patterns

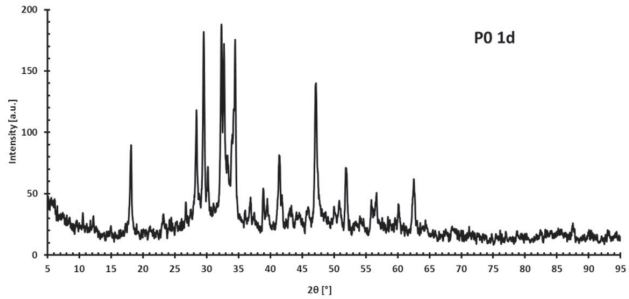

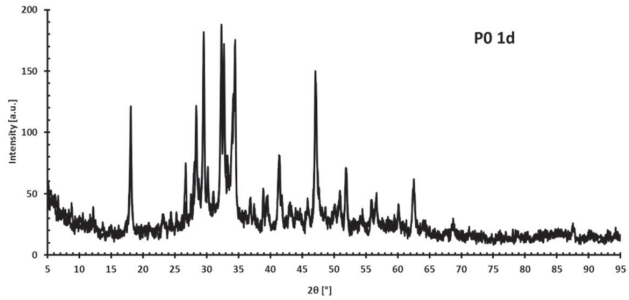

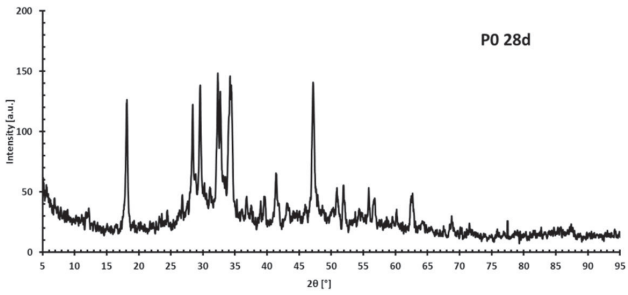

Appendix 5. XRD patterns

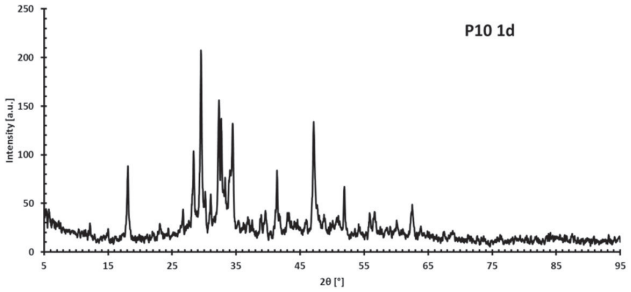

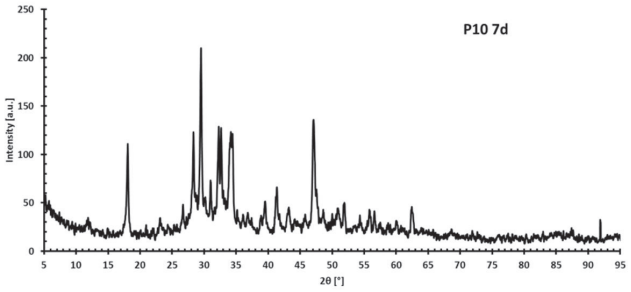

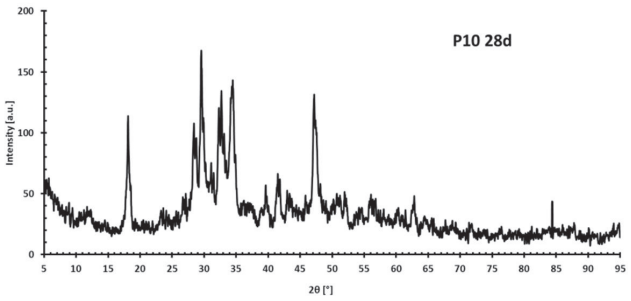

Appendix 5. XRD patterns

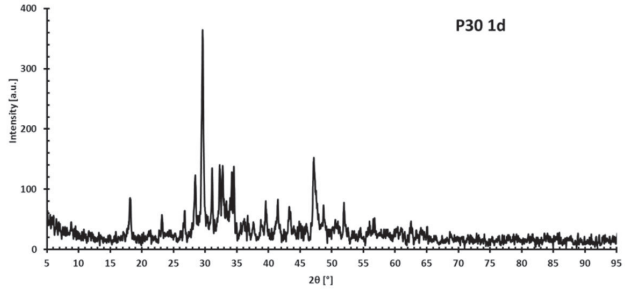

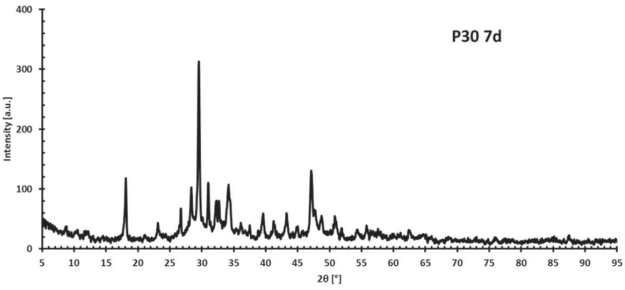

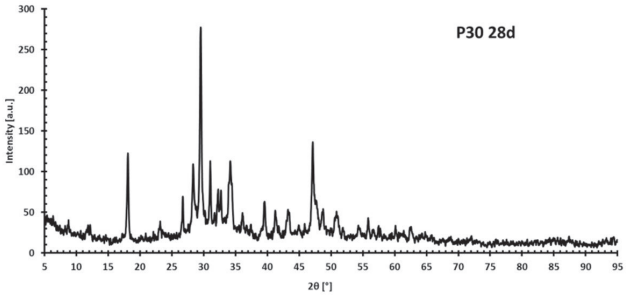

Appendix 5. XRD patterns

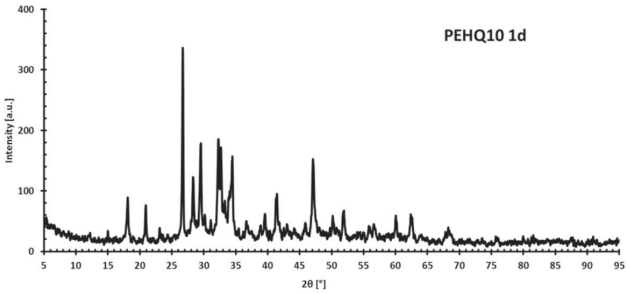

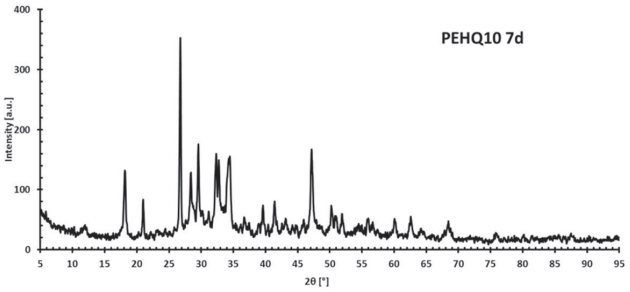

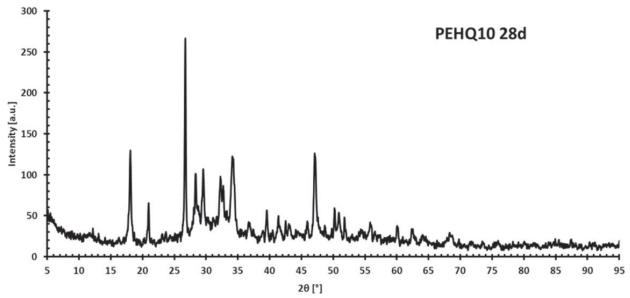

Appendix 5. XRD patterns

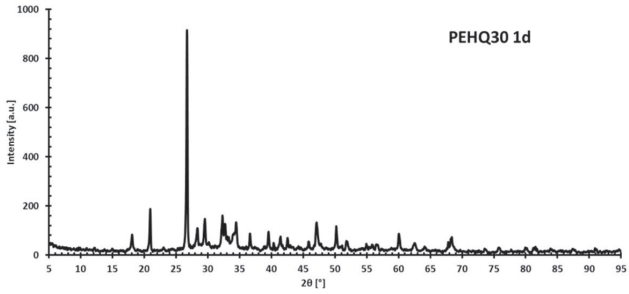

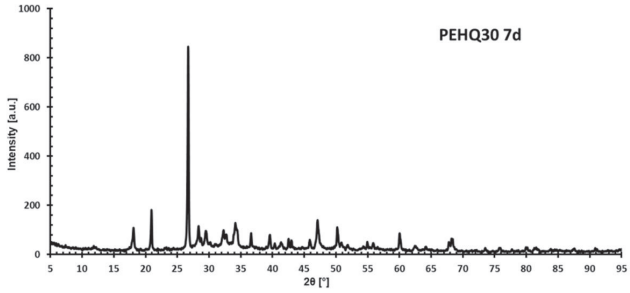

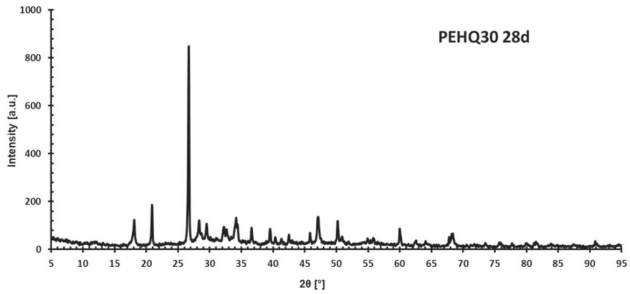

Appendix 5. XRD patterns

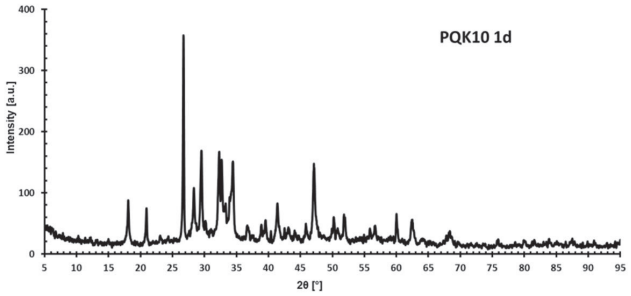

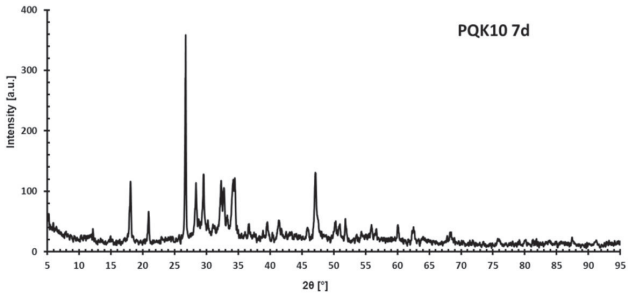

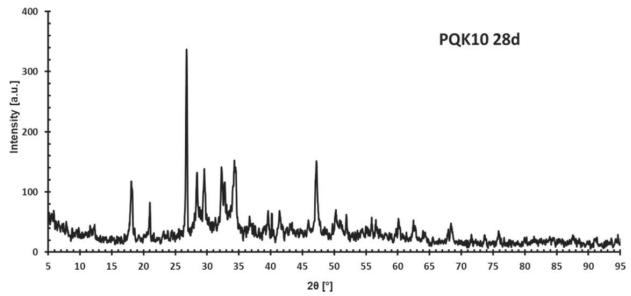

Appendix 5. XRD patterns

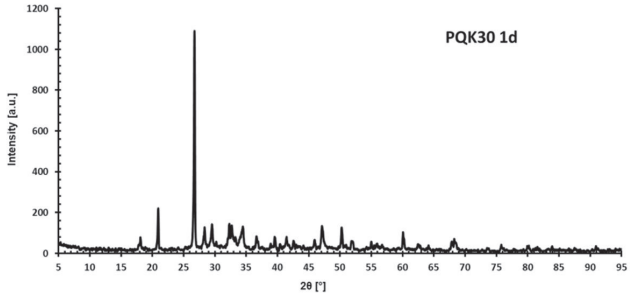

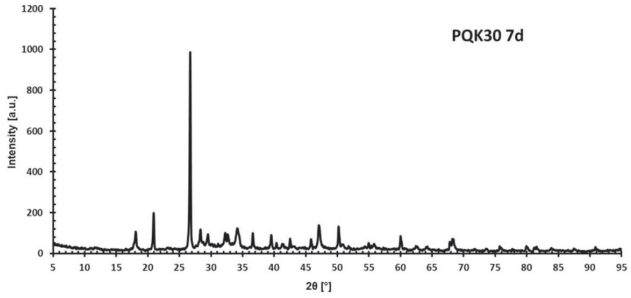

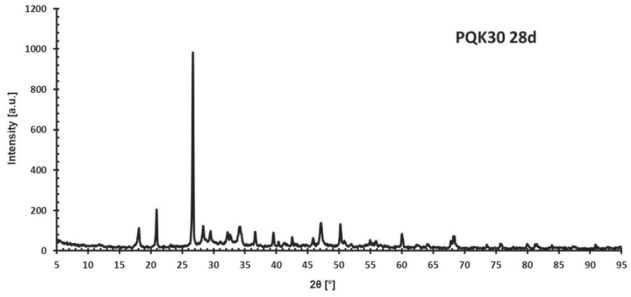

Appendix 5. XRD patterns

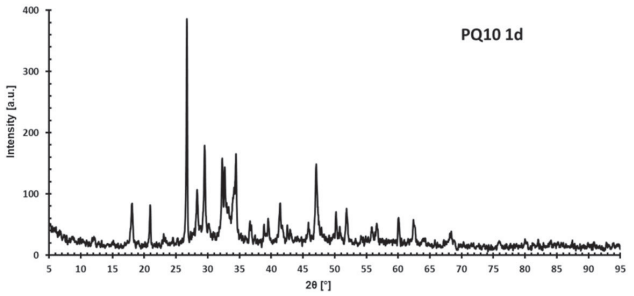

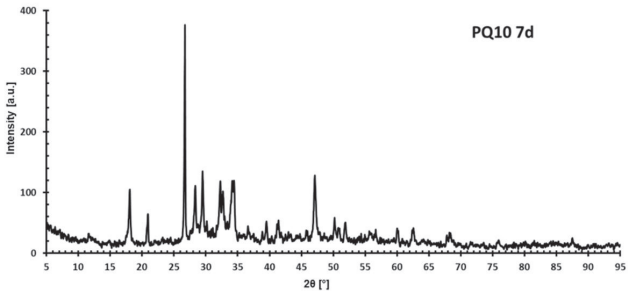

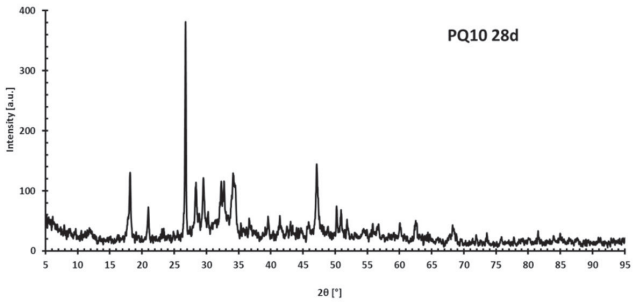

Appendix 5. XRD patterns

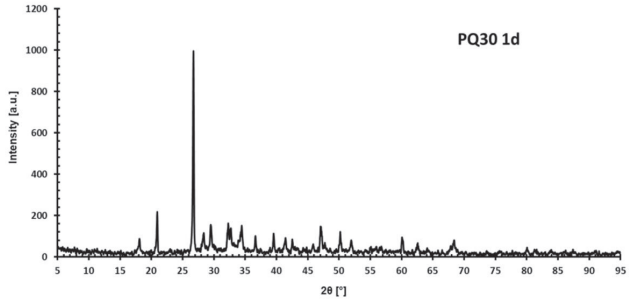

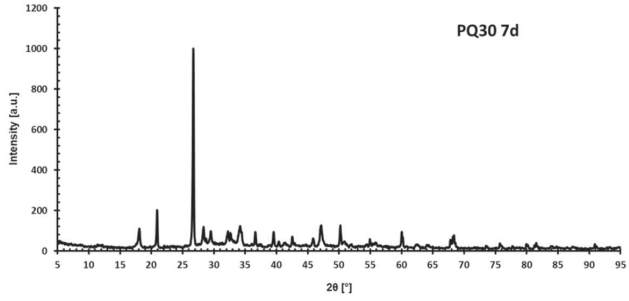

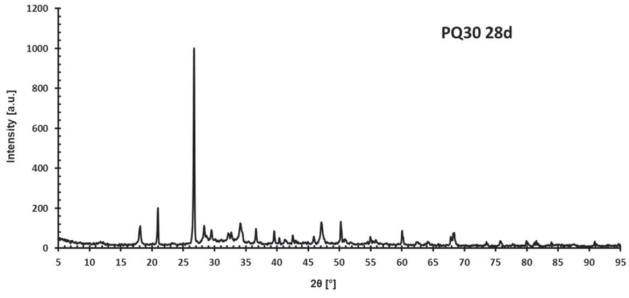

Appendix 6. EVALUATION OF PUMPABILITY

Currently, the pumpability of concrete mixes is considered so important that basic concrete mixes have to possess this property. Currently, there are no standardised test methods that could be used to determine the pumpability of concrete in laboratory conditions. However, most of the concrete used in construction sites is transported by pumping, so the need for a laboratory pumpability test is understandable and the powder concrete mixes that are developed should possess adequate pumpability properties.

Pumpability testing relies mainly on on-site experiments, where it is possible to use a real concrete pump. According to some sources, workability (mainly slump value), is a good guideline for pumpable concrete. For example, according to the ACI standards (ACI 1996), slump values from 2 to 6 in. (5 to 15 cm), are the most suitable for pumping. In mixtures with a higher slump value, aggregates will segregate from mortar and paste. However, concretes with slump values exceeding 6 in. (15 cm) obtained with the use of superplasticisers are usually pumped without difficulty.

The recommendations for proportioning pumpable concrete are, in general, concentrated on optimal gradations of aggregates, water requirements, and cement and admixture recommendations. In the literature, the aim of optimal gradation is usually focused on the larger (above the # 0.125-mm or # 0.25-mm sieve) aggregate particles and the quantity of fines is considered to be fulfilled by the amount of cement. In proportioning pumpable concrete, there are usually no upper limits on the amount of fines (in this case, particles smaller than 0.125 mm) since fines are thought to consist mainly of cement. Therefore, for economic reasons excessive amounts of fines have not been a realistic problem. Usually, the limit values (Nykänen 1973, Johansson and Tuutti 1976) are outdated because of the improved quality of modern superplasticisers.

In this study, in order to measure the workability and to estimate the pumpability of the concretes, a modified MO consistency test (Valtion teknillinen tutkimuslaitos, 1970) was introduced. The MO test is an old test used to measure the consistency of concrete in Finland and some other Nordic countries. The test is neither valid nor used any more, but since it produces a similar thrust motion in a tube as in the actual pumping of the concrete, the test was introduced to measure the workability and to evaluate the pumpability of the concretes.

The test apparatus, presented in Figure 105, consisted of a cylinder with a diameter of 100 mm and a height of 400 mm with a tray section under it, which was filled with concrete and then dropped onto its pedestal until the concrete had flown out of it to such an extent that a hint of light could be seen at the opposite end of the cylinder. The amount of drops needed was expressed as the MO number. The test was repeated 45 minutes after the addition of water into the mix in order to verify the change in the consistency of the concrete after a period of time.

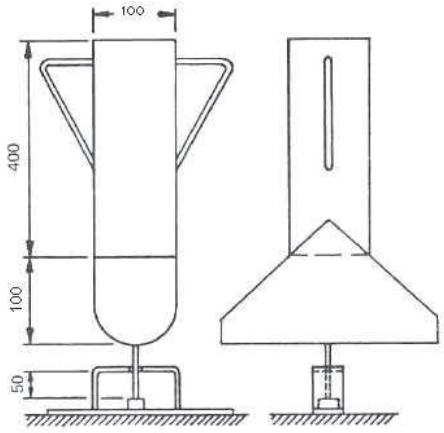

Figure 105. Modified MO apparatus for the testing of the pumpability of concrete.

In order to compare and establish the MO results, to substantiate boundaries for the pumpability of the mineral powder concretes and to assure good pumpability, three concrete mixes were chosen for a pumpability test in which the concretes were pumped through a real concrete pump. The aim of the pumpability tests was not to measure the differences in pumpability between concretes with or without mineral powders, but to assess whether mineral powder concretes were suitable for pumping in general.

Since ordinary Portland cement concrete is, for the most part, known to be pumpable and the object was to find out whether substantial amounts of added fines would hinder the pumping of mineral powder concretes, only concretes with varying amounts of mineral powders were selected for the pumping test. The chosen mixes were selected according to the results obtained from laboratory compositions made prior to the pumping tests. The concretes were made at a precast concrete factory at Nurmijärvi, in Finland, and the test procedures and the concrete pumping were performed outdoors, where the ambient temperature was approximately +5 °C.

For the estimation of pumpability in the laboratory, it was hoped that the modified MO test would be at least moderately suitable for the purpose. As anticipated for most of the concretes, a good result in the flow table test resulted in a small number of drop values in the MO test. On average, the concrete mixes that reached flow table results of 500 mm or more had MO consistencies of 0. The concrete mixes that contained greater amounts of fines began to present the characteristics of self-compacting concretes. This meant that, for example, in the MO test, concrete flowed through the vertical cylinder and out from the apparatus gutter without any drop values of the test equipment. However, these concretes cannot be considered self-compacting.

The MO test and the flow table test results are only an estimation of the pumpability of the concrete and do not guarantee the good behaviour of a concrete mix in a real pumping situation. The main properties that influence the pumpability of concretes, besides consistency, are the amount and type of fines (cement, fillers) the grading of the aggregate, the shape of the aggregate, air content, temperature and admixtures (Nykänen 1973, Binns 2003). The three mixes which had proved to be applicable in the laboratory tests were selected for the pumping test because of their different characteristics.

- Composition I was a workable mix with a lower mineral powder content (< 100kg/m^3) and with a flow table result in the laboratory of 470 mm, but had required a few drops in the MO apparatus.
- Composition II contained a higher amount of mineral powder than Composition I but was a workable mix with a flow table result of 575 mm and an MO consistency of 0 drops.
- Composition III had the highest mineral powder content, of 212 kg/m^3, and water/(cement+MP) ratio, of 0.39. In the laboratory, the mix was workable with a flow table result of 565 mm and an MO consistency of 0 drops but was notably more adhesive than the other two compositions.

The mix design for the concretes was the same as in the laboratory compositions, i.e. the gradation, as well as the amounts of mineral powder and cement, were the same as in the laboratory mixes. The cement used was a sulphate-resisting cement, CEM I 42.5 N, used in normal factory production, and it had an almost identical gradation curve to the previously used CEM II/A-M 42.5 N, but with a slightly smaller water requirement. The aggregates, natural filler, cement and water were fed into the mix automatically; therefore, some deviations in the amounts of the planned and actual material quantities were found. This is also the reason why the pumped mixes had slightly different flow, MO test and compressive strength values compared to the laboratory mixes made prior to the pumping tests. The mineral

powder and superplasticisers were pre-weighed and hand-fed into the concrete mixes. No additional pumping aids were used. shows the mix proportions and the differences between the planned and realised mix amounts.

Table 27. Mix proportions of the concretes used in pumpability tests.

Planned amounts [kg/m^3]	I	II	II
# 8-16	573	523	504
# 0-8	1192	1174	1130,5
# 0-1	92	92	103
CEM I 42,5 N	264	264	265
Measured amounts [kg/m^3]			
# 8-16	576,5	528,5	504
# 0-8	1196,5	1184,5	1122,5
# 0-1	94	90	103,5
CEM I 42,5 N	258	269,5	266
Mineral powder [kg/m^3]	94,7	159	212,2
Total water [kg/m^3]	181,12	184,2	184,6
Superplasticizer [kg/m^3]	1,2	1,6	1,9

In addition to pumping, the effects of transportation on the consistency of the concrete were also investigated. Therefore, the workability tests were performed before and after transport and after the pumping itself. The time spans between the tests were around 5, 15 and 25 minutes, respectively. All of the test results are presented in . After pumping, the concrete was examined visually to ensure that it had maintained its homogeneity and had resisted segregation.

Table 28. Test results of the actual pumpability tests with concrete pumps.

I	Before transport	After transport	After pumping
Flow [mm]	485	475	475
MO consistency	24	31	0
Concrete temperature [°C]	13	13,1	13
II			
Flow [mm]	580	535	560
MO consistency	0	0	0
Concrete temperature [°C]	14,6	14,2	14,2
III			
Flow [mm]	560	510	485
MO consistency	0	0	0
Concrete temperature [°C]	16,9	14,9	15,8

All three test concretes were pumpable but because of the mix differences of the concretes with regard to the large amounts of fines, concrete III started to stiffen faster in comparison to the two other test concretes. This is caused by the effect of the large amount of fines on the cement setting time (Soroka and Stern 1976(II), Heikala et al. 2000). Therefore, the third concrete mix would not have been pumpable after a longer period of time (over 25 minutes). The transportation and the pumping did not seem to have negative effects on the properties of the concrete; on the contrary, the workability of the first two concretes improved after pumping.

Since all of the test concretes were pumpable, it could be concluded that the use of mineral powders did not hinder their pumpability. However, according to the pumpability tests that were conducted, the amount of fines most likely should not exceed 480 kg/m^3 and the water/(cement+MP) ratios should not be notably below 0.40 for pumpable concretes.

Aalto-DD 182/2013

ISBN 978-952-60-5423-0
ISBN 978-952-60-5424-7 (pdf)
ISSN-L 1799-4934
ISSN 1799-4934
ISSN 1799-4942 (pdf)

Aalto University
School of Engineering
Department of Civil and Structural Engineering
www.aalto.fi

BUSINESS +
ECONOMY

ART +
DESIGN +
ARCHITECTURE

SCIENCE +
TECHNOLOGY

CROSSOVER

**DOCTORAL
DISSERTATIONS**